STRUCTURE-FUNCTION ANALYSES OF PROSTAGLANDIN E$_2$ RECEPTOR

SUBTYPES 1 AND 3

By

JASON DUANE DOWNEY

Dissertation

Submitted to the Faculty of the

Graduate School of Vanderbilt University

in partial fulfillment of the requirements

for the degree of

DOCTOR OF PHILOSOPHY

in

Pharmacology

December, 2012

Nashville, Tennessee

Approved:	Date:
Vsevolod Gurevich, chair	11/06/2012
Richard Breyer, mentor	11/06/2012
Roy Zent	11/06/2012
Lawrence Marnett	11/06/2012
Craig Lindsley	11/06/2012

To my greatest fans and my original mentors,

my parents Eddie and Sandra Downey

ACKNOWLEDGEMENTS

This work would not have been possible without the help and support of an entire village of people. The person that deserves the most commendation is my advisor, Rich Breyer. Rich is probably the most laid-back, genial, and intelligent supervisor I have ever had. Rich has been incredibly flexible with respect to the amount of guidance to give me. At times I needed an almost constant back-and-forth to muddle through some challenges, and he was always there with his door open, his cell phone on, or his email open. I admire Rich for his dedication to his research and his family. I am forever grateful for the immense amount of advice he has given me, from technical writing, to research presentations, high-end beer selections, and film between the years of 1920 and 1990, and everything in between. I know I don't say it as often as I should, but thank you.

I have the most supportive committee I could possibly ask for. As best I can tell, I have had it so easy scheduling committee meetings and I am grateful to my committee for their availability. I would like to thank Dr. Gurevich for advice in the laboratory, guidance through the logistics of graduate school, and the countless letters of recommendation. Dr. Gurevich is my committee chairman and it always seems like I have my post-meeting letter from him before I can get back to my desk. I appreciate it. I would like to thank Dr. Marnett not only for priceless input in my project but also for allowing me to participate in the Interdisciplinary Training in Therapeutic Discovery training program my first two years in the laboratory. This was an invaluable experience that allowed me to learn about every angle of chemical biology and drug development while also financially supporting my research. I would like to thank Dr. Lindsley for

for performing assays, teaching assay theory and execution, and being available for my numerous questions with those aspects of my project.

Lastly, I would like to thank my friends and family. I would have burned out a long time ago if it weren't for the never ending support and shenanigans. Especially, I would like to thank my parents for patiently listening to the scientific nonsense I constantly complain about and having supportive feedback and humor I so needed to pick myself back up.

TABLE OF CONTENTS

Chapter

TABLE OF CONTENTS

TABLE OF CONTENTS

LIST OF TABLES

LIST OF FIGURES

LIST OF FIGURES

LIST OF FIGURES

LIST OF ABBREVIATIONS

17PTPGE$_2$	17-phenyl-ω-trinor PGE$_2$
α_{2A}AR	α_{2A} adrenergic receptor
ACE	angiotensin converting enzyme
ACh	acetylcholine
ACR	albumin-to-creatinine ratio
Ang II	angiotensin II
AQP2	aquaporin 2
ASA	acetylsalicylic acid, Aspirin
AUC	area under the curve
AVP	arginine vasopressin
β_2AR	β_2 adrenergic receptor
BCA	bicinchonic acid
β -gal	β -galactosidase
B$_{max}$	receptor density
BRET	bioluminescence resonance energy transfer
BSA	bovine serum albumin
$[Ca^{2+}]_i$	intracellular calcium
cAMP	cyclic AMP
$[cAMP]_i$	intracellular cyclic AMP
CDCl$_3$	deuterated chloroform
cDNA	complementary DNA

CHO	chinese hamster ovary
CL_H	hepatic clearance
CL_{int}	intrinsic clearance
CL_p	plasma clearance
c_{max}	maximum plasma concentration
COX	cyclooxygenase
cPGES	cytosolic prostaglandin E synthase
CPRG	chlorophenolred- β-D-galactopyranoside
$CRTH_2$	chemoattractant receptor homologous molecule expressed on T_H2 cells
CVLM	caudal ventrolateral medulla
DA	ductus arteriosis
dbcAMP	dibutryl cyclic AMP
DM	diabetes mellitus
DMEM	Dulbecco's modified Eagle medium
DMSO	dimethylsulfoxide
DP	D-prostanoid
EC_{50}	effective concentration at 50 % activity
ECI	extracellular loop 1
ECII	extracellular loop 2
EGFR	epiderminal growth factor receptor
ELSD	evaporative light scattering detector
E_{max}	maximum efficacy
EP	E-prostanoid

ERK	extracellularly-regulated kinase
ESI	electrospray ionization
ESRD	end stage renal disease
EST	expressed sequence tag
F	bioavailability
FBS	fetal bovine serum
FP	F-prostanoid
F_U	fraction unbound
GFR	glomerular filtration rate
GI	gastrointestinal
GPCR	G-protein coupled receptor
GSH	glutathione
GSIS	glucose-stimulated insulin secretion
HA	hemagglutinin
HBSS	Hanks buffered salt solution
HIF-1α	hypoxia inducible factor-1α
HPGD	15-hydroxyprostaglandin dehydrogenase
HPLC	high-performance liquid chromatography
HRP	horseradish peroxidase
IC_{50}	inhibitor concentration at 50 % activity
ICV	intracerebroventricular
IL-1β	interleukin-1β
IP	I-prostanoid

IP$_3$	inositol trisphosphate
IV	intravenous
K$_D$	equilibrium dissociation constant
LCMS	liquid chromatography mass spectrometry
LPS	lipopolysaccharide
MAP	mean arterial pressure
MHz	megahertz
mPGES	microsomal prostaglandin E synthase
mTOR	mammalian target of rapamycin
NMR	nuclear magnetic resonance
^{1}HNMR	proton nuclear magnetic resonance
NSAIDs	non-steroidal anti-inflammatory drugs
NTS	nucleus tractus solitarius
OAT	organic anion transporter
PAPS	phosphoadenosine phosphosulfate
PBS	phosphate-buffered saline
PGA	prostaglandin A
PGD	prostaglandin D
PGE	prostaglandin E
PGF	prostaglandin F
PGG	prostaglandin G
PGH	prostaglandin H
PGI	prostaglandin I, prostacyclin

PGs	prostaglandins
PGT	prostaglandin transporter
PI3K	phosphoinositol-3 kinase
PKA	protein kinase A
PKC	protein kinase C
PLA_2	phospholipase A_2
PLC	phospholipase C
PO	*per os*, by mouth
ppm	parts per million
RAAS	renin-angiotensin-aldosterone system
rfu	relative fluorescence units
RhoGEF	Rho guanine nucleotide exchange factor
ROCK	RhoA kinase
RSNA	renal sympathetic nerve activity
RVLM	rostral ventrolateral medulla
SC	subcutaneous
$t_{1/2}$	half-life of elimination
T1DM	type I diabetes mellitus
T2DM	type II diabetes mellitus
TBS	tris-buffered saline
t_{max}	time to maximum plasma concentration
TXA	thromboxane
UDPGA	UDP-glucuronic acid

UV	ultraviolet
VIP	vasointestinal peptide
V_{ss}	volume of distribution at steady state

CHAPTER I

INTRODUCTION

History of Prostaglandins (PGs) and Non-Steroidal Anti-inflammatory Drugs (NSAIDs)

Willow bark, the prehistoric anti-inflammatory. As is the case for many therapeutics, the story of Aspirin begins with a plant preparation recognized to lower fever and the four symptoms of inflammation: tumor, rubor, calor, dolor; or swelling, redness, heat, and pain. Use of the leaves and bark of the willow trees as treatments for the many symptoms of inflammation likely predates recorded history. Stone tablets document the prescription of willow leaves for inflammation by Assyrian physicians. One of the hundreds of recipes in the ancient Egyptian Ebers papyrus (ca. 1500 B.C.) prescribes cooling substances (e.g., the leaves of a willow tree) to draw out the heat of an inflamed wound[1]. While the ancient Egyptians seemed to have missed the mark with their death-repelling potion (half an onion in beer froth promised "a delightful remedy against death"[2]), history is replete with fever, pain, and inflammation treatments that include the bark or leaves of the willow tree. The bark and leaves of *Salix alba*, as well as a number of other plants, contains the glucoside salicin. When salicin is consumed, the glucoside is cleaved to glucose and salicyl alcohol in the digestive tract. The alcohol is absorbed and oxidized by a cytochrome P450 to salicylic acid, the active anti-inflammatory and anti-pyretic (Figure 1)[3]. Salicin and salicylic acid derive their names from *Salix*, the genus of willow trees.

Salicylates are still used in many over-the-counter topical applications (e.g., wart treatment) and analogues of salicylic acid are common inflammatory bowel disease and ulcerative colitis therapies[4].
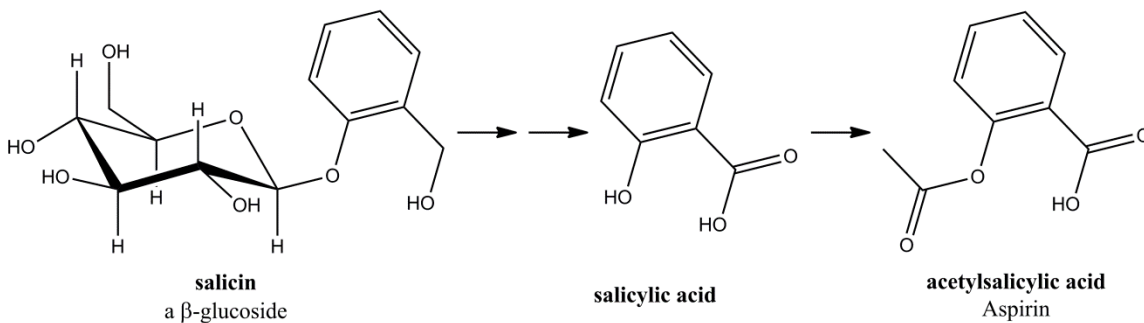
Figure 1 - Salicin, the pharmacological agent of *Salix* bark and leaves; salicylic acid; and acetylsalicylic acid, or Aspirin

Bayer, discovery of Aspirin, and World War I. In 1853, Charles Frederic Gerhardt became the first to synthesize Aspirin by acetylating salicylic acid. In an attempt to alleviate the gastrointestinal (GI) toxicity of salicylic acid by raising the pH of its solution, he "buffered" salicylic acid solutions with sodium and acetyl chloride, acetylating salicylic acid to make acetylsalicylic acid (ASA), or Aspirin. Gerhardt's form of ASA was impure and prone to decomposition and the project lost attention[5]. Felix Hoffman is credited with synthesizing and commercializing ASA in 1897 while working for Bayer. Bayer was concerned by the high propensity for addiction to morphine and Hoffman was studying chemical modifications that would reduce this troubling side effect. Similar to acetylation of salicylic acid, he synthesized diacetylmorphine, trademarked Heroin, so named for the "heroic" feeling it instilled in its users. Aspirin and

Heroin were both registered intellectual property of Bayer. At the conclusion of World War I, Bayer along with most of the booming German chemical industry was forced by the Treaty of Versailles to surrender their intellectual property as reparations. The rights to Bayer's intellectual property were bought by Sterling, and eventually the market exclusivity on Aspirin expired, flooding the market with generics[6]. The molecular target and mechanism of action for Aspirin remained a mystery until the 1970s.

von Euler, prostaglandin, and vesiglandin. Ulf S. von Euler is best known for his Nobel Prize winning research around norepinephrine and its production and storage in the axon terminals of neurons[7]. In 1936, while working from the Karolinska Institute in Sweden, von Euler published his seminal work describing vasodilating and muscle contracting substances isolated from the accessory genital glands of humans[8]. Using a battery of physical chemistry approaches, he characterized the active component of human semen extracts, suspecting his previous discovery Substance P. After purifying and characterizing the active component, von Euler had excluded all previously known hormones and concluded he must be working with some novel substance. Since the active compound was isolated from prostate gland extracts and secretions, he referred to the mystery agent as "prostaglandin." He evaluated its effect on various organ preparations. Intravenous injection of prostaglandin produced a rapid and sustained drop in the blood pressure of anesthetized rabbits. Prostaglandin added to isolated frog heart preparation increased the rate of contraction as well as exaggerating the systolic phase of contraction, which he noted was "similar to that caused by an excess of calcium." Prostaglandin was demonstrated to relax frog hind limb vessels, and constrict the intestines and uteri of

humans and a variety of other animals. von Euler also identified a substance he referred to as "vesiglandin" for its concentration in vesicular gland extracts. Vesiglandin had similar but less potent properties to prostaglandin. "Prostaglandin" in this case was probably a mixture of prostaglandin E_1 (PGE$_1$), prostaglandin E_2 (PGE$_2$), 19-OH-PGE$_1$, and 19-OH-PGE$_2$. "Vesiglandin" likely referred to 19-OH-PGE$_1$[9] (Figure 2). World War II all but stopped research in the field. Sune Bergström led the prostaglandin field when work resumed[10].
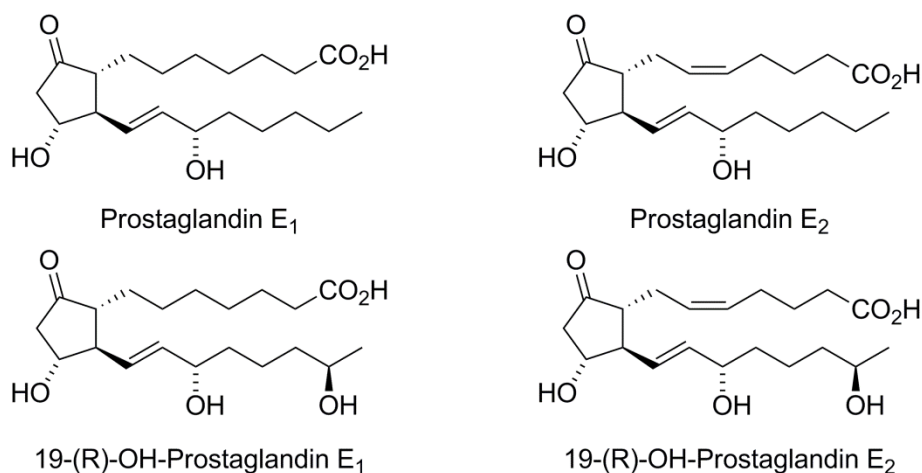
Figure 2 – The components of the mixtures referred to by Ulf von Euler as "prostaglandin" and "vesiglandin"[8].

The "prostaglandin synthetase" postulate and discovery of the prostanoid family. Prostaglandin E (PGE) and prostaglandin F (PGF) derive their names from the original purification of the compounds. Bergström and Sjövall described a prostaglandin in the ether fraction (PGE) of the purification and another in the phosphate fraction (PGF, "phosphate" is *fosfat* in Swedish)[11]. Prostaglandin A (PGA) was formed by dehydration

4

of PGE_2 in acid and prostaglandin B by isomerization of PGA in base[12]. The gaps in the alphabet were filled in with the other prostaglandins (PGD_2, PGG_2, PGH_2, and PGI_2) as they were discovered. In 1960, Sune Bergström published back-to-back papers describing the composition and structure of PGF[13] and PGE[14]. Bergström and van Dorp simultaneously published papers in 1964[15,16] describing the synthesis of PGE_2 starting with radiolabeled arachidonic acid. They attributed this enzymatic activity to a "prostaglandin synthetase," now known as cyclooxygenase (COX). By now it was appreciated that prostanoid synthesis was not restricted to accessory genital glands. Bengt Samuelsson is credited with first proposing and later confirming prostaglandins are synthesized from arachidonic acid by a dioxygenation reaction that yields a cyclic endoperoxide intermediate that is then isomerized by separate enzymes into the different prostanoids (Figure 3)[17,18].
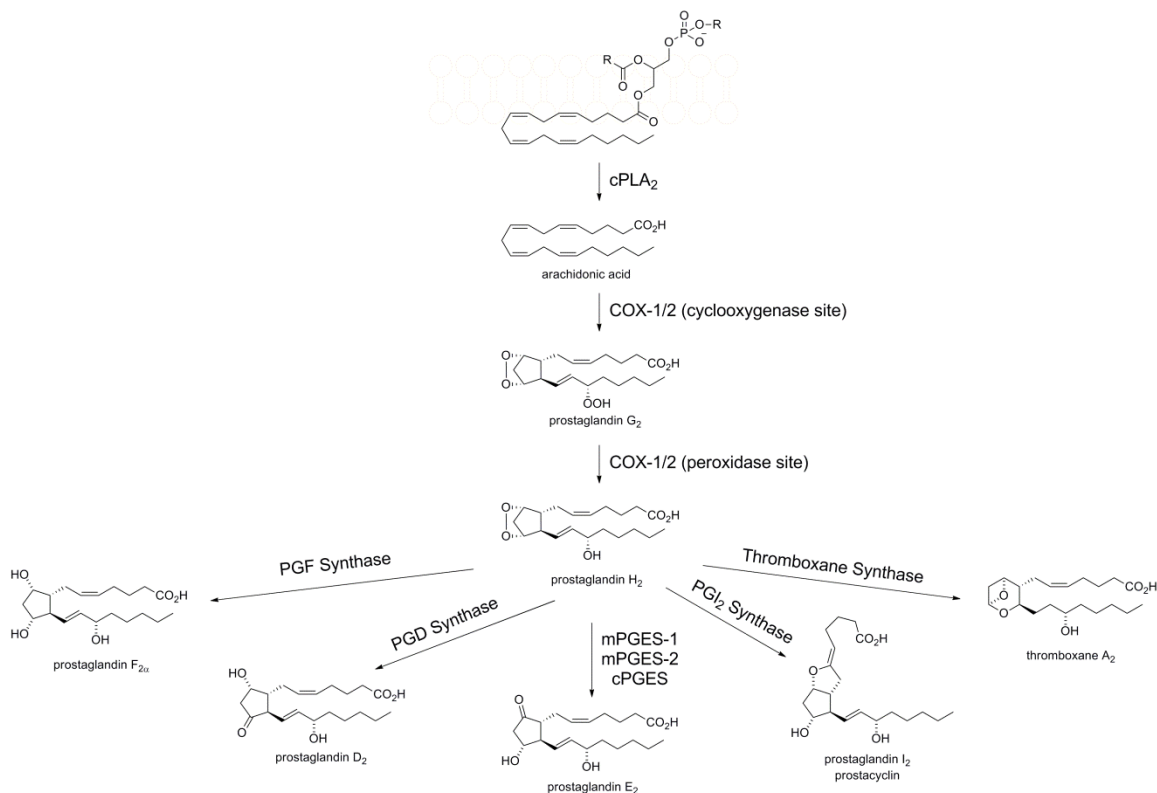
Figure 3 – Biosynthesis of the five principal prostanoids from membrane-derived arachidonic acid

Biosynthesis of prostanoids. Prostanoids are a family of oxidized lipid autacrine and paracrine signaling molecules that are arachidonic acid metabolites of COX (Figure 3). Arachidonic acid is freed from the phospholipid bilayer by phospholipase A_2 (PLA_2). COX catalyzes the dioxygenation of arachidonic acid to form the unstable intermediate prostaglandin G_2 (PGG_2). A second active site on COX catalyzes the reduction of PGG_2 to prostaglandin H_2 (PGH_2). The five tissue-specific synthase catalyze the isomerization of PGH_2 into the five principal prostanoids: prostaglandin $F_{2\alpha}$ ($PGF_{2\alpha}$), prostaglandin D_2 (PGD_2), PGE_2, prostacyclin (PGI_2), and thromboxane A_2 (TXA_2). The molecular targets of prostanoids are G-protein coupled receptors (GPCRs). $PGF_{2\alpha}$ is the endogenous

agonist for the F-prostanoid (FP) receptor, PGD_2 for the D-prostanoid (DP) receptor subtypes 1 (DP1) and 2 (DP2, or CRTH2), PGE_2 for the E-prostanoid (EP) receptor subtypes $1 - 4$ (EP1 $-$ EP4), prostacyclin for the I-prostanoid (IP) receptor, and TXA_2 for the T-prostanoid (TP) receptor.

Sir John Vane and the mechanism of action of "Aspirin-like drugs". While the prostaglandin field was purifying and characterizing the prostanoid family, a number of investigators had noted the formation of these prostanoids was sensitive to Aspirin, indomethacin, or salicylate pretreatment. In 1971, Sir John Vane published a study demonstrating the mechanism by which "Aspirin-like drugs" act[19]. He showed that indomethacin, Aspirin, and salicylate each inhibited $PGF_{2\alpha}$ formation in a dose-dependent manner. He also suggested the mechanism of action of these drugs is what is responsible for the well-known GI toxicity of the class of drugs. His body of work ultimately earned Sir John Vane election as Fellow of the Royal Society in 1974, the Nobel Prize in Physiology or Medicine in 1982, and knighthood from Great Britain in 1984[20].

Side effects of NSAIDs. For as long as salicylates and Aspirin have been marketed therapeutics, their toxicities have been well documented. As will be discussed in some detail below, NSAIDs are known to affect the cardiovascular system, the GI, and even respiration. Salicylates are known to uncouple oxidative phosphorylation thus increasing respiration and, in severe cases, causing hyperventilation. At long-term high doses, they also directly stimulate the respiratory center of the medulla[4]. Ensuing bicarbonate

excretion in the kidney to normalize blood pH is accompanied by sodium and potassium excretion.

Several studies point to a link between chronic NSAID use and increases in blood pressure. In 1994, Anthony Johnson *et al.* published a meta-analysis combining 38 randomized, placebo-controlled clinical studies and 12 randomized, head-to-head clinical studies in which two or more NSAIDs were directly compared. The results showed NSAID use was associated with a 5.0 mmHg increase in supine mean arterial pressure (MAP). The magnitude of effect varied between each NSAID and was worst for piroxicam, perhaps due to its exceptionally long terminal half-life of elimination[21].

Other studies indicate NSAIDs may exacerbate pre-existing hypertension even in the face of pharmacological therapy. In the Johnson meta-analysis, investigators noticed NSAID use reduced the efficacy of different classes of anti-hypertensive therapy, especially antagonizing the effect of β-blocker anti-hypertensives[21]. Another meta-analysis showed that even when controlling for salt intake patients taking some types of NSAIDs for less than 24 hours had a significant increase in MAP[22].

In 1986, Cinquegrani and Liang showed an effect of indomethacin on hydralazine anti-hypertensive therapy in human patients. The exact mechanistic details of how hydralazine functions are not known; however, hydralazine is a direct vasodilator and was a popular anti-hypertensive and heart failure therapeutic in the past. Cinquegrani and Liang found that indomethacin treatment significantly blunted the vasodepressor activity of hydralazine, but that the vessel beds they were studying, the renal and limb vasculature, were not likely to be the site of action. Indomethacin did not augment the amount of catecholamines released in response to hydralazine. Also, a fraction of the

hydralazine vasodepressor activity remains in the face of indomethacin treatment, suggesting there are additional vasodepressor substances or mechanisms aside from prostaglandins[23].

The therapeutic action of other anti-hypertensives can be antagonized by NSAIDs, including diuretics[24-26], β-blockers[25,26], calcium channel blockers[27], and angiotensin converting enzyme (ACE) inhibitors[28-30]. In addition to exacerbating hypertension, a few clinical cases of acute renal toxicity with co-administration of captopril and NSAIDs have been reported[31,32]. NSAIDs can cause acute renal failure in patients with compromised renal function. With reduced renal perfusion, the renin-angiotensin-aldosterone system (RAAS) will stimulate the formation of angiotensin II (Ang II), which constricts the pre- and post-glomerular arterioles. Only in the pre-glomerular arterioles does Ang II stimulate synthesis of vasodilating prostaglandins which act as a local counter-regulator to maintain afferent arteriolar patency, leaving the efferent arteriole constricted, and stabilizing glomerular filtration rate (GFR)[33]. Elimination of this counter-regulator with NSAIDs would be expected to reduce glomerular perfusion and therefore GFR in a patient population whose renal function is already compromised.

In patients with renal insufficiency, flurbiprofen acutely decreased experimental measures of GFR (inulin and creatinine clearance). This effect appeared an hour after the first dose of flurbiprofen and eventually resolved despite continued dosing. The effect of flurbiprofen on sodium excretion was significant and sustained; patients receiving flurbiprofen had 75 % - 85 % less sodium excretion than the placebo controls that reached a peak by four hours and remained through the end of the study. Patients had significantly more urinary sodium excretion after one and four weeks of chronic

flurbiprofen compared to the acute dose of flurbiprofen. Flurbiprofen significantly increased serum potassium but not sodium. As one would expect, sodium retention lead to an increase in body weight for patients taking flurbiprofen, likely from mild edema, and this effect was more pronounced in the out-patient arm of the study where patients were not on a controlled diet. Most significantly, chronic flurbiprofen treatment increased blood pressure by 27 mm Hg systolic / 12 mmHg diastolic and this effect resolved when flurbiprofen was withdrawn, highlighting the net hypotensive role of the prostaglandin family as a whole[34].

The deleterious effects of chronic NSAID use in hypertensive patients may be dose related. Smith *et al*. demonstrated low-dose Aspirin combined with captopril did not exacerbate hypertension and may have beneficial anti-thrombotic effects. ACE inhibitors increase vasodilatory prostaglandins through the build-up of bradykinin, which feed-forward activates PLA_2, the enzyme that catalyzes the rate-limiting step for prostaglandin biosynthesis[28,35,36]. It was hypothesized that if ACE inhibitors also increased the production of platelet TXA_2, then selective blockade of this potent vasoconstrictor and not PGE_2 or PGI_2 should have additional benefit. Patients were randomized to captopril/placebo and captopril/low-dose Aspirin treatment arms after a two week washout period. As expected, captopril/placebo significantly increased circulating thromboxane as well as urinary excretion of PGE_2. Patients in the captopril/low-dose Aspirin arm had suppressed levels of TXA_2, even lower than during the washout period. Blood and urinary PGI_2 concentrations and blood pressures were not different in any treatment arm. While the antihypertensive effects of captopril were not enhanced by

addition of low-dose Aspirin therapy, it stands to reason that attenuation of captopril-augmented TXA_2 synthesis would reduce the risk of thrombotic events[37].

Perhaps the best appreciated side effect of the entire class of NSAIDs is their GI toxicity. These side effects include gastric ulceration, exacerbation of peptic ulcers, and in severe cases gastric hemorrhage[38,39]. The GI toxicity of Aspirin is particularly severe because of the irreversible nature of its inhibition of COX. PGI_2 and PGE_2 prevent acid secretion, increase mucosal blood flow, and increase mucus secretion at the GI epithelium. Inhibition of COX-1 by NSAIDs prevents the formation of these cytoprotective eicosanoids in the gastric epithelium. Therapeutics that can be used to treat conditions of chronic pain without these side effects represent a significant unmet medical need.

Discovery of an inducible isoform of COX and separation of NSAID side effects. A major indication for NSAIDs and pain relievers in general is for the treatment of pain associated with rheumatic diseases, specifically rheumatoid arthritis and osteoarthritis. These diseases are characterized by, among a host of other symptoms, chronic pain. A therapeutic that alleviates this symptom without the dependency and GI toxicity of established remedies would be a boon to arthritis patients. The search for a better tolerated NSAID began anew with the discovery of a novel, inducible isoform of COX, COX-2. In 1989, two independent laboratories studying genes modulated during the cell cycle reported identification of an inducible form of *Gallus gallus* COX from chicken embryo fibroblasts (CEF-147)[40,41] and *Mus musculus* COX from 3T3 cells (TIS-10)[42,43]. These isoforms were first found as one of many transcripts induced by a number of

11

stimuli and were subsequently identified as a novel isoform of COX. Basal expression of COX-2 was low but upregulated in response to cytokines, phorbol esters, and oncogenes. Subsequent to the discovery of COX-2, the dogma became: COX-1 was a constitutively expressed enzyme responsible for normal tissue homeostasis such as the maintenance of GI epithelium; COX-2 had negligible basal expression and could be induced in response to insult, producing the pain and inflammatory phenotypes. The field began to focus on selectively inhibiting the activity of COX-2 and thereby pain and inflammation while leaving COX-1 activity untouched in hopes of sparing the integrity of the gut lining.

With the X-ray crystal structures of COX-1 and COX-2 solved, subtle differences in the architecture of the two enzymes emerged. COX-1 and COX-2 are structurally similar; they both are peripheral membrane proteins that pull their substrate, arachidonic acid, from the phospholipid bilayer through a lobby and deep into the active site of the enzyme where a tyrosine radical catalyzes the cyclooxygenase reaction. Traditional NSAIDs are non-selective because they bind around a gate between the lobby and the active site common to COX-1 and COX-2 and occlude substrate entry to the active site. A few differences in amino acid sequence of the active site form a small, hydrophobic side pocket in the active site that COX-1 lacks [44]. Exploitation of this hydrophobic side pocket is the basis for molecules that are selective for COX-2 versus COX-1. Rofecoxib (Vioxx) and etoricoxib are Merck products. Valdecoxib (Bextra) and celecoxib (Celebrex) are products of Pfizer. A few previously discovered NSAIDs were later appreciated to have COX-2 "preferring" activity; that is, the molecule is not truly selective for inhibition of COX-2 over COX-1, but it more potently inhibits COX-2 than COX-1. Nimesulide,

12

meloxicam, and diclofenac are such NSAIDs that are now known to inhibit COX-2 more potently than COX-1[45].

Coxibs – a cautionary tale. As rofecoxib was being studied against pain and colorectal cancer, it became apparent that long-term administration of rofecoxib was associated with a significant increase in the risk of adverse cardiovascular events[46,47]. Placebo-controlled, randomized clinical trials using three coxibs (celecoxib, rofecoxib, and valdecoxib) all indicated an increased risk of myocardial infarction, stroke, and thrombosis with chronic use of these drugs[47-49]. The design of the rofecoxib studies to compare rofecoxib head-to-head with naproxen rather than placebo is a confounding factor. It is possible naproxen has some cardioprotective properties[50] and comparison of naproxen to rofecoxib would therefore exaggerate any deleterious cardiovascular trends observed for rofecoxib. The cardiovascular phenotype was not exclusive to the purpose-made COX-2 selective inhibitors: COX-2 "preferring" NSAIDs were found to be have a similar cardiovascular risk profile[51]. It seemed the toxicity was mechanistic and the severity of toxicity was proportional to the ratio of inhibition of COX-2 to COX-1.

COX-2 selective inhibitors remain on the market, despite Merck's dramatic and arguably premature withdrawal of rofecoxib from the market. Celecoxib is still on the market and is prescribed for the treatment of pain associated with arthritis. Coxibs have been demonstrated to be one of the most potent classes of chemicals against colorectal cancer[52,53]. Careful consideration of which patients to whom these drugs are prescribed may be a more appropriate course of action for this class than complete removal of the product from the market.

It is now appreciated that the source of the surprise cardiovascular toxicity was an underdeveloped understanding of the roles of the cyclooxygenases in homeostasis and disease. Thrombogenesis is under tight regulation by, among many other things, the balance of the anti-thrombotic action of endothelial COX-2-derived prostacyclin and the pro-thrombotic action of platelet COX-1-derived thromboxane. Selective inhibition of COX-2 removes the counter-regulatory actions of prostacyclin, making the system more pro-thrombotic[54]. One possibility to mitigate this imbalance is co-administration of low-dose Aspirin so as to specifically inhibit TXA_2 production in platelets[55].

Roles of the PGE_2 Signaling Pathway in Disease

Prostaglandins are critical to the normal homeostatic function of a variety of systems and are key mediators of a number of disease processes. Chronic use of Aspirin or salicylates causes severe GI toxicity, highlighting the role of prostaglandins in the maintenance of GI epithelium. Willow tree bark and Aspirin have long been used to reduce symptoms of inflammation and risk of stroke and myocardial infarction, implying involvement of prostaglandins in the pathobiology of inflammation and thrombotic diseases.

With the aid of powerful chemical, pharmacological, and genetic tools prostanoids are now known to be involved in a host of physiological and pathophysiological processes. PGD_2 and PGE_2 are potent mediators of the immune system, demonstrated to be involved in normal and abnormal immune function[56]. Prostacyclin is a potent

vasodilator and anti-thrombotic agent required for normal hemodynamics and regulation of thrombus formation[57-59]. Thromboxane plays a role in hemodynamics, bronchoconstriction, and platelet aggregation[60-63]. PGE_2 has paradoxical actions on blood pressure; depending on how it is administered, PGE_2 is a vasodepressor[64,65] or a vasopressor[66]. More recently, attention has been focused on the role of PGE_2 in the following conditions: pain[67-72], thrombosis[73-76], diabetes mellitus[77-79], hypertension[80-83], patent ductus arteriosis[84-87], cancer[88-91], and salt/water handling[83,92,93]. The connection between PGE_2 and diabetes and hypertension is discussed below.

Diabetes Mellitus. Diabetes mellitus (DM) is a chronic disease characterized by hyperglycemia with insufficient insulin production, type 1 DM (T1DM), or insufficient response to insulin and subsequent overproduction of insulin, type 2 DM (T2DM). Of the patients in the U.S. currently under care for end-stage renal disease (ESRD), DM is the primary cause of 38 % of these cases. DM is the primary cause of 44 % of the more than 100,000 new cases of ESRD in the U.S. each year[94]. The use of NSAIDs to treat diabetes mellitus has been documented as far back as 1876 when Ebstein noticed oral salicylate given to diabetic patients reduced their glucosuria[95]. In 1957, Reid reported treatment of diabetic patients with oral Aspirin reduced blood glucose levels and glucosuria and that this effect reversed when Aspirin was withdrawn[96].

The link between PGs and insulin regulation came from the observation that PGE_1 or PGE_2 modulates the effects of adrenergic stimulation and that α-adrenergic stimulation was known to oppose insulin release[97]. Infusion of PGE_1 into humans and dogs increases circulating glucose levels and blocks glucose-stimulated insulin release (GSIS)[97,98]. This

15

attenuation of insulin release in response to increased circulating glucose is the basis of the hypothesis that PGE_2 plays a role in the pathophysiology of DM. PGE_1 has been shown to increase hepatic glucose release in rats[99,100]. It was hypothesized that tonic synthesis of PGE_2 by pancreatic cells functions as a suppressor of GSIS. When rat pancreatic cells cultured in high glucose were exposed to ibuprofen or salicylate, insulin levels increased with a coincident with a fall in PGE_2 and addition of PGE_1 reversed this effect[101]. In normal human volunteers, infusion of PGE_2 blunted acute GSIS and infusion of salicylate augmented acute GSIS[102]. In patients with type II DM (T2DM), acute GSIS is typically absent. However, in these patients infusion of ASA or salicylate partially restored both the acute and second phase GSIS and improved the acute insulin response to the direct insulin secretagogue arginine[102,103]. Other investigators have found the effect of salicylate on arginine-stimulated insulin release is only observed in diabetic patients, not normal control volunteers[104]. This would suggest a role for prostaglandin signaling in suppressing insulin release *per se* and not necessarily the upstream glucose sensing mechanisms.

Interleukin-1β (IL-1β) is known to upregulate expression of COX-2 and EP3 in pancreatic islets and to suppress insulin secretion through the action of PGE_2[105]. Misoprostol, a synthetic analog of PGE_1, was shown to block GSIS from rat islets in culture and that this effect was sensitive to salicylate and pertussis toxin pretreatment, suggesting the effect was COX-2/PGE_2/EP3-mediated[106].

Long-term DM causes vasculopathies that manifest as diabetic retinopathy, diabetic nephropathy (DN), hypertension, stroke, and myocardial infarction. In mesenteric arteries from a rat model of T2DM, endothelial dysfunction was demonstrated by a deficit in

acetylcholine (ACh)-stimulated, endothelial-dependent dilation of the mesenteric artery. This phenotype was blocked by pretreatment with metformin or with indomethacin, implicating a vasoconstricting prostanoid in the pathophysiology of endothelial dysfunction. Production of TXA_2 and PGE_2 in ACh-stimulated mesenteric arteries was increased in diabetic rats compared to nondiabetic controls. This augmentation of TXA_2 and PGE_2 was completely blocked by chronic metformin treatment[107].

In a rat model of DN, animals were treated with a selective EP1 antagonist or Aspirin for a period of several weeks and evaluated for kidney damage. Diabetic rats had a significant increase in PGE_2 excretion into their urine, implying an increase in local PGE_2 synthesis in the kidney. Aspirin treatment blocked PGE_2 production while the EP1 antagonist had no effect. Protein excretion into the urine, a marker of renal failure, was increased in untreated and Aspirin treatment diabetic rats and absent with EP1 antagonist treatment. This pattern was recapitulated in measures of glomerular hypertrophy by morphometry and glomerulosclerosis by histology[77]. This difference in therapeutic potential between the selective receptor antagonist and pan-prostanoid blockade with Aspirin supports the hypothesis that receptor subtype selective PGE_2 antagonists have a greater therapeutic potential than pan-prostanoid inhibition.

In a genetic screen comparing human patients with T2DM and healthy controls, polymorphisms in *Ptger3* were associated with T2DM, though the study could not conclude whether the polymorphism was activating or inactivating in nature. Previous literature would indicate activation of EP3 suppresses insulin secretion and increases blood glucose, so perhaps these are not inactivating polymorphisms. Using a mouse model of T2DM in which mice are fed a "Western diet" and administered streptozotocin

17

(STZ), the role of the EP3 receptors in glucose regulation in this pathological state was studied. A selective EP3 receptor antagonist acutely lowered blood glucose in "Western diet"-fed, diabetic mice, and this reduction persisted for at least five hours. Twice daily administration of the EP3 antagonist for two weeks dose-dependently lowered blood glucose in "Western diet"-fed, diabetic mice down to the level of nondiabetic controls[108]. The literature suggests EP1 and EP3 are involved in the pathophysiology of diabetic nephropathy, hyperglycemia, insulin release, and insulin insensitivity. Taken together, these studies suggest EP1 and EP3 are involved in the pathophysiology of DM and simultaneous blockade may have benefit beyond individual receptor antagonism alone.

Hypertension. Data regarding NSAID use in hypertensive patients are clear that prostaglandins play some role in at least the pathophysiology of hypertension if not normal physiological hemodynamics. Chronic NSAID use has a dose-dependent hypertensive effect, with daily low-dose users being 55 % more likely to initiate antihypertensive therapy, medium-dose users 64 % more likely, and high-dose users 82 % more likely than similar patients not using NSAIDs[109]. Long-term hypertension is detrimental for the kidney, causing deterioration of kidney function and eventual renal failure. Hypertension is the primary cause of 24 % of the cases for the 500,000 patients in the U.S. currently under care for ESRD. Of the 100,000 new patients diagnosed with ESRD each in the U.S., hypertension is the primary cause of 28 % of these cases[94].

The role of PGE_2 in hypertension has been studied clinically for several years. In an early study, an interaction between PGE_2, renin, and hypertension was investigated. The correlation between urinary PGE_2 excretion and plasma renin activity was direct and

significant, even in the normotensive controls. Indomethacin treatment in normoreninemic hypertensive patients increased body weight, presumably due to mild edema; indeed, urinary sodium excretion was reduced. This volume load likely is the cause of the increase in mean blood pressure. GFR was reduced, contributing to the salt and water retention. Urinary PGE_2 excretion was suppressed as expected, as were plasma renin activity and aldosterone levels[110]. This study supports the hypothesis that downstream targeting of a subset of prostanoid receptors involved in disease (e.g., pain) but sparing receptors involved in homeostatic processes (e.g., salt and water handling) may show therapeutic efficacy with fewer side effects.

Instantaneous arterial pressure is only one facet of cardiovascular disease. Risks of cardiovascular and renal diseases are higher in treated hypertensive patients with the same blood pressure as normotensive controls. Reduction of blood pressure to normotensive levels does not account for the damage already done by the hypertensive insult. In hypertensive patients with cardiovascular or renal comorbidities, suppression of RAAS has been shown to be more protective than normalization of blood pressure *per se*[111,112]. Some pathophysiological action of RAAS exists outside of strictly increasing arterial pressure[113].

High blood pressure, to a point, is not lethal in and of itself. High blood pressure does, however, induce a number of pathological changes in various organs, a phenomenon referred to as "end organ damage." Some of these pathological changes include endothelial dysfunction, atherosclerosis, aortic aneurysm, stroke, vascular dementia, left ventricular hypertrophy, heart failure, renal insufficiency, and renal failure. Chronic hypertension leads to a remodeling of the arteries, making the vessels more rigid

and reducing their ability to dilate. Hypertension causes a number of structural and functional changes to the heart. Arterial pressure is the resistance the left ventricle has to push against to move blood into circulation. As this "afterload" increases, the left heart has to contract harder to eject the same amount of blood through the aortic valve. This stress on the myocardium leads to myocardial hypertrophy and eventually inefficient filling and pumping manifest as reduction in ejection fraction. These structural changes will eventually devolve into overt heart failure. Hypertensive kidney disease can usually be detected by urinary excretion of small amounts of albumin, a protein usually electrostatically excluded from the urine by the glomerular basement membrane. This so-called microalbuminuria is a robust indicator of kidney disease and indicates destruction of some component of the filtration apparatus (i.e., endothelium, glomerular basement membrane, or podocytes). As vascular damage is not limited to the glomerular arterioles, but is systemic, albuminuria is also a predictor of cardiovascular complications in general. Most hypertension complications are treated by RAAS blockade[114]. After several years of hypertensive nephropathy, untreated or undertreated patients progress to overt renal failure, requiring dialysis or transplantation for survival.

Prostaglandin signaling has also been implicated in renovascular hypertension, a disease distinct from essential hypertension in that it is caused by compensatory renal mechanisms secondary to renal artery stenosis. The roles of prostaglandins in renovascular hypertension versus essential hypertension in humans have been compared using Aspirin to block prostanoid synthesis. In patients with unilateral renal arterial stenosis, the ischemic kidney produced significantly more PGE_2 than the contralateral kidney and each was higher than the concentration in aortic plasma. Patients in the

essential hypertension group had no measurable renal arterial stenosis. PGE_2 was produced to similar extents by both kidneys and was higher than aortic PGE_2 concentrations. IV Aspirin treatment significantly attenuated PGE_2 production in all three compartments. Patients with renovascular hypertension receiving Aspirin had a significant attenuation in plasma renin activity and a concomitant reduction in systolic and diastolic blood pressure. Patients with essential hypertension showed a small but significant increase in MAP. This study illustrates the context dependence of the role of prostaglandins in hemodynamics. In the setting of renovascular hypertension, the overproduction of PGE_2 in the ischemic kidney likely augments the release of renin in an effort to raise arterial pressure and increase perfusion. Treatment with Aspirin reduces PGE_2 production and plasma renin activity for the ischemic kidney and lowers MAP by 10 mmHg[115].

Modulation of cardiac function in humans by PGE_1 or PGE_2 has also been studied. Intravenous infusion of PGE_1, an EP and IP agonist, or PGE_2 increased heart rate, cardiac output, and stroke volume in humans. For each of these measures of cardiac function, PGE_1 was much more potent than PGE_2. PGE_1 or PGE_2 each decreased MAP in humans, though by a very small amount. PGE_1 or PGE_2 each reduced forearm vascular resistance, but in this case PGE_2 was more potent. Because of the small reduction of MAP upon infusion of PGE_1 or PGE_2, the increase in stroke volume caused by PGE_1 and PGE_2 is likely a direct inotropic effect and not an indirect effect of reduced afterload on the left heart[116].

Chronic prostaglandin exposure has been explored in dogs. It has long been appreciated that prostaglandins are paracrine and autocrine signaling molecules, not

21

systemic hormones, as they are almost entirely inactivated by a single pass through pulmonary circulation[117]. Indeed, no effect was observed for one week chronic intravenous infusion of PGE_2. However, chronic intrarenal infusion of PGE_2 for one week dramatically increased water intake and urine output with a decrease in urine osmolality and no changes in GFR. Chronic intrarenal PGE_2 infusion caused a transient increase in urinary sodium excretion and no effect on plasma sodium concentration. As hypothesized above for humans with renal artery stenosis, chronic renal artery infusion of PGE_2 increased plasma renin activity and MAP. This study presents further support for the hypothesis that PGE_2 produced by the kidney acts locally to stimulate renin release, ultimately raising blood pressure[118].

Using individual genetic disruptions of the four EP receptor subtypes, investigators studied the effect of PGE_2 on acute hemodynamics and the sexual dimorphisms therein. As observed in humans, acute intravenous infusion of PGE_2 acutely and dose-dependently lowers MAP in wild-type anesthetized mice. In a group of male and female $EP2^{-/-}$ mice, acute PGE_2 infusion resulted in an attenuated but not abrogated decrease in blood pressure, suggesting a second vasodepressor EP receptor. A similar attenuation in PGE_2 vasodepressor activity was observed in a group of male and female $EP4^{-/-}$ mice compared to wild-type controls. When mice are stratified by genotype and not sex, the vasodepressor responses to PGE_2 in $EP1^{-/-}$ or $EP3^{-/-}$ mice were indistinguishable for their wild-type controls[119].

Other investigators have studied the vasoactivity of the EP receptors using a combination of genetic and pharmacological tools. In these studies, when the EP2 receptor was deleted the vasopressor activity of PGE_2 through EP3 was unmasked.

Confirming a vasopressor role for EP1 and EP3, synthetic agonists selective for EP3 and EP1/EP3 induced potent and dose-dependent increase in MAP. An EP4-selective agonist was still able to reduce MAP in $EP2^{-/-}$ mice. From these experiments it can be concluded that under normal conditions, the net action of PGE_2 is to cause a decrease in MAP through EP2. Next, PGE_2 activates EP3 which produces a potent vasopressor activity. Lastly, PGE_2 produces a small but significant vasodepressor activity through EP4 (Figure 4). There appears to be no role for EP1 in the normal homeostatic regulation of blood pressure by PGE_2[120]. These two studies demonstrate the primary homeostatic role for PGE_2 in blood pressure regulation is a vasodepressor action. Pan-inhibition of PGE_2 production with a mPGES-1 inhibitor or a COX inhibitor could be predicted to have a net hypertensive effect as PGE_2 is one of the most abundant prostanoids and is a vasodepressor. These data underscore the importance of selecting a target more distal from PGE_2 in order to separate the pathological actions of PGE_2 from the homeostatic activity of PGE_2.
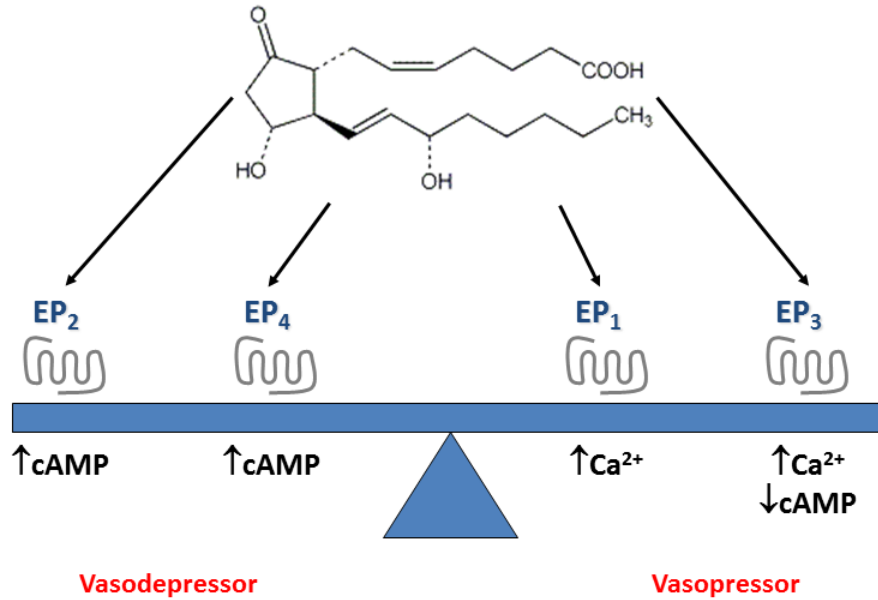
Figure 4 – Diagram of the vasopressor and vasodepressor PGE_2 receptors and their relative contribution to the hemodynamic response to PGE_2.

<u>Other Therapeutic Targets in PGE_2 Pathway</u>

The many side effects of chronic NSAID use illustrates an unmet medical need at the same therapeutic indications as NSAIDs (e.g., pain and thrombosis) but with a better safety profile. COX lies at the top of the biosynthetic pathway for the entire family of prostanoids (Figure 3). The side effects of COX inhibition are derived from inhibiting the synthesis of homeostatic prostanoids while also eliminating the deleterious prostanoid. A

molecular target further down the biosynthetic chain would limit the breadth of affected systems. Enzymes that catalyze the isomerization of PGH_2 to PGE_2 and the catabolism of PGE_2 as well as the prostaglandin transporter and the GPCR targets of PGE_2 are other potential therapeutic targets.

Prostaglandin Synthase (mPGES-1). Human microsomal prostaglandin E synthase-1 (mPGES-1) was first cloned and characterized by Bengt Samuelsson's laboratory in 1999[121]. They reported the enzyme was an inducible membrane-bound protein that required reduced glutathione as a cofactor. mPGES-1 is known to be functionally coupled to COX-2[122], allowing the two to produce large amounts of PGE_2 in response to inflammatory stimuli. Other prostaglandin E synthases have been identified: cytosolic prostaglandin E synthase (cPGES), a constitutively expressed enzyme that couples mainly to COX-1[123]; and mPGES-2, also constitutively expressed and functionally coupled to both COX-1 and COX-2[124,125].

Given the complex hemodynamic effects of PGE_2 in vivo, predicting the effect of mPGES-1 deletion on blood pressure is difficult and turns out to be genetic background-dependent. On the DBA/1 background, mPGES-1$^{-/-}$ mice and wild-type mice had similar baseline blood pressures. Ang II infusion caused similar increases in blood pressure, minimal albuminuria, and no changes in urinary excretion of thromboxane. On the 129/SvEv background, mPGES-1$^{-/-}$ mice had significantly higher basal blood pressures than their wild-type controls. Ang II infusion caused significantly worse hypertension in mPGES-1$^{-/-}$ mice than wild-type controls, worse albuminuria, and had significantly more urinary thromboxane excretion[126]. These data not only indicate a genetic background

25

dependence for the mPGES-1^{-/-} phenotype, but also suggest that in some situations mPGES-1 deletion may shunt excess PGH_2 to other synthetic pathways, thromboxane in this case. The excess thromboxane synthesis likely contributed to the phenotype of the mPGES-1^{-/-} 129 mice.

Using mice on a DBA/1 C57BL/6 mixed background, the involvement of mPGES-1 in Ang II-induced abdominal aortic aneurysm in hyperlipidemic mice was studied. Ang II infusion upregulated COX-2 and mPGES-1 and augmented synthesis of PGE_2. Chronic administration of Ang II in these mice induced aortic aneurysm formation. Mice with these aneurysms were prone to sudden death due to aneurysm rupture. mPGES-1^{-/-} in this setting lowered aneurysm incidence and severity as well as reduced mortality compared to wild-type controls. At no point in the study were blood pressures different between the two genotypes. Again, these investigators saw signs of substrate shunting with deletion of mPGES-1. Urinary excretion of PGD_2 and PGI_2 metabolites was augmented in mice lacking mPGES-1[127]. It would seem the genetic background of the mice may determine which prostanoid the excess PGH_2 is shunted to with mPGES-1 deletion.

15-deoxy-$\Delta^{12,14}$-PGJ$_2$ $IC_{50} < 10$ nM   **MF63**
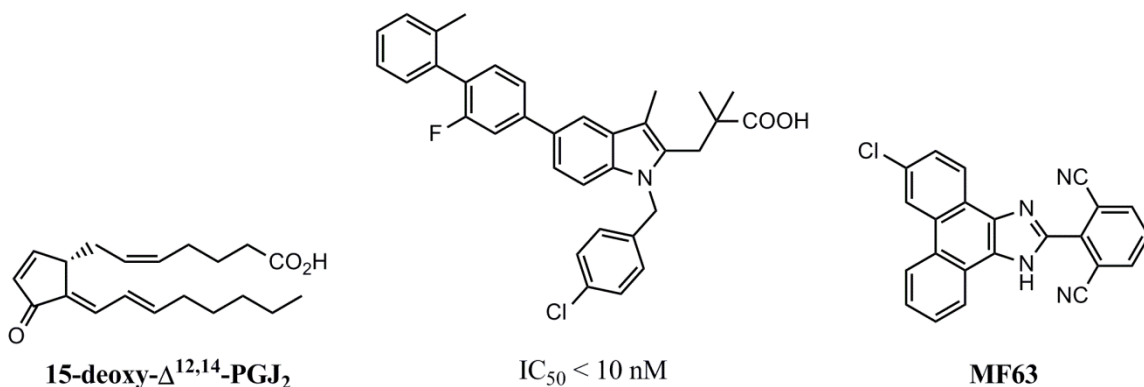
Figure 5 – Inhibitors of mPGES-1

26

Analogues of prostaglandins have been shown to weakly inhibit mPGES-1 (Figure 5). 15-deoxy-$\Delta^{12,14}$-PGJ$_2$ has submicromolar potency at mPGES-1[128]. A known inhibitor of 5-lipoxygenase activating protein, MK-886, also has low micromolar potency at mPGES-1 and analogues based on MK-886 have yielded low nanomolar potency inhibitors[129]. A third compound, from a series of phenanthrenes had low nanomolar potency and displayed analgesia in an animal model of hyperalgesia[130].

Prostaglandin Transporter (PGT). The existence of a selective and active transport process for moving prostaglandins across the plasma membrane was hypothesized based on the observation of differential metabolism of prostanoids by intact pulmonary cells versus lysed pulmonary cells[131,132]. Broken pulmonary cells completely metabolized any prostanoids they came into contact with, whereas intact cells metabolized a subset of prostanoids. A prostaglandin transporter was hypothesized to explain this selectivity, and discovery and characterization of PGT was carried out by Victor Schuster's laboratory[133]. PGT belongs to the family of organic anion transporters (OATs) and indeed shares a considerable amount of secondary structure homology with other OATs. The transporter is composed of a positively-charged anion binding site and a compartment to accommodate the hydrophobic chains that make up the bulk of a prostaglandin's structure. Evidence to support this ultrastructure lies in the ability of an anionic thiol-modifying reagent to inactivate the transporter but not a similar cationic reagent[134], and removal of the carboxylate moiety of PGE$_2$ abolishes affinity of the channel for the substrate[135]. It has been demonstrated that a crucial lysine residue mediates the electrostatic interaction with the carboxyl terminus of PGE$_2$ and that the lysine side chain

must have a positive charge for optimal substrate translocation[136]. A small molecule that inhibits this transporter would be expected to decrease delivery of extracellular prostanoid to the intracellular compartment, reducing its metabolism and increasing its activity.

Compounds that are known to block other OATs also block PGT (Figure 6). Some COX inhibitors have also been found to block PGT[133,137]. More selective inhibitors of PGT have recently been developed[138,139].

bromcresol green   **ibuprofen**

TBGz T34
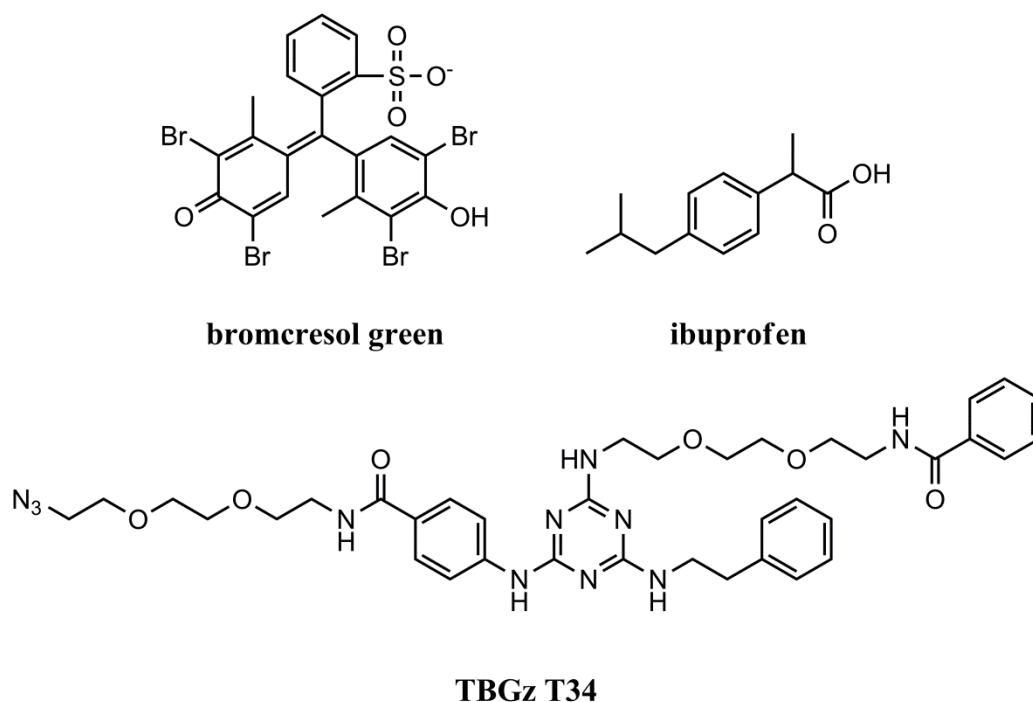
Figure 6 – Inhibitors of the prostaglandin transporter

15-Hydroxyprostaglandin Dehydrogenase (HPGD). HPGD is a NAD-dependent alcohol dehydrogenase that is responsible for the inactivation of prostaglandins in circulation. Anggard and Samuelsson demonstrated the existence of HPGD from guinea pig lung

homogenate in 1964[140]. HPGD is highly expressed in the pulmonary circulation and a single pass through the pulmonary circuit eliminates >90 % of prostaglandins from circulation[117]. Human HPGD was cloned by screening the products of a human lung complementary DNA (cDNA) library against an antibody raised against purified placental HPGD[141]. This enzyme catalyzes the oxidation of the 15-OH common to prostaglandins to a ketone; these compounds are inactive at their GPCRs. Other catabolic enzymes reduce the Δ^{13} double bond or oxidize either the α or ω chain of PGE_2[142].

A few inhibitors of HPGD have been described (Figure 7). Samuelsson's group demonstrated prostaglandins of the B series and a synthetic epimer of PGE_1 inhibited HPGD[131]. Pharmacia developed an inhibitor, Ph CL 28A, with low nanomolar potency[143]. Other inhibitors of HPGD have been identified by high-throughput screen efforts[144].
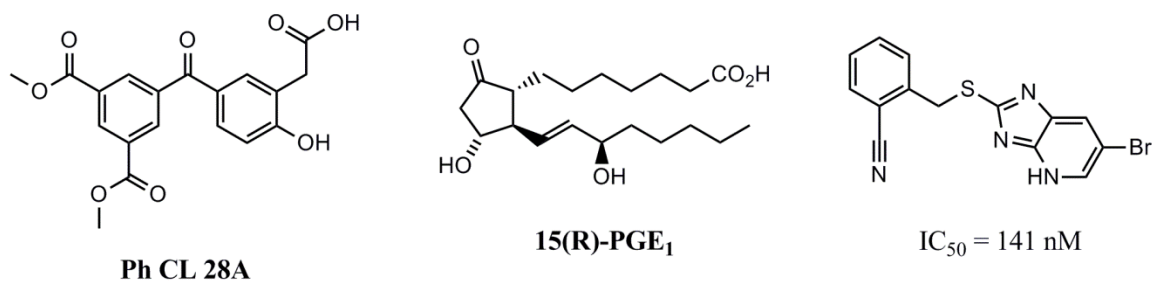
Figure 7 – Inhibitors of HPGD

PGE₂ Receptors. PGE_2 signals through four subtypes of GPCRs, each with distinct downstream signaling cascades (Figure 8). Targeting the GPCRs downstream of PGE_2 synthesis can be expected to have fewer side effects than blocking the activity of the enzymes upstream of the EP receptors. Prostanoids are involved in several homeostatic

processes and evidence of this can be seen in the many side effects of chronic NSAID use. Moreover, the subtypes of PGE_2 receptors have different roles in homeostasis. EP2 and EP4 are known to reduce blood pressure when activated[81]. EP4 has been shown to be cardioprotective against ischemia-reperfusion injury[145]. Positive allosteric modulators of EP2 have been shown to be protective against NMDA-induced excitotoxicity injury[146]. Inhibitors of EP1 are protective against diabetic nephropathy[77] and EP1 genetic deletion has shown beneficial effects in a number of hypertensive models[83]. Blockade of EP3 has been shown to be beneficial in thrombotic diseases[73], ischemic injury due to stroke[147,148], diabetes[108], and morphine withdrawal[149]. Specifically blocking activity through EP1 and EP3 while leaving EP2 and EP4 as well as the other prostanoids untouched could provide enhanced therapeutic benefit beyond blockade of EP1 or EP3 alone.
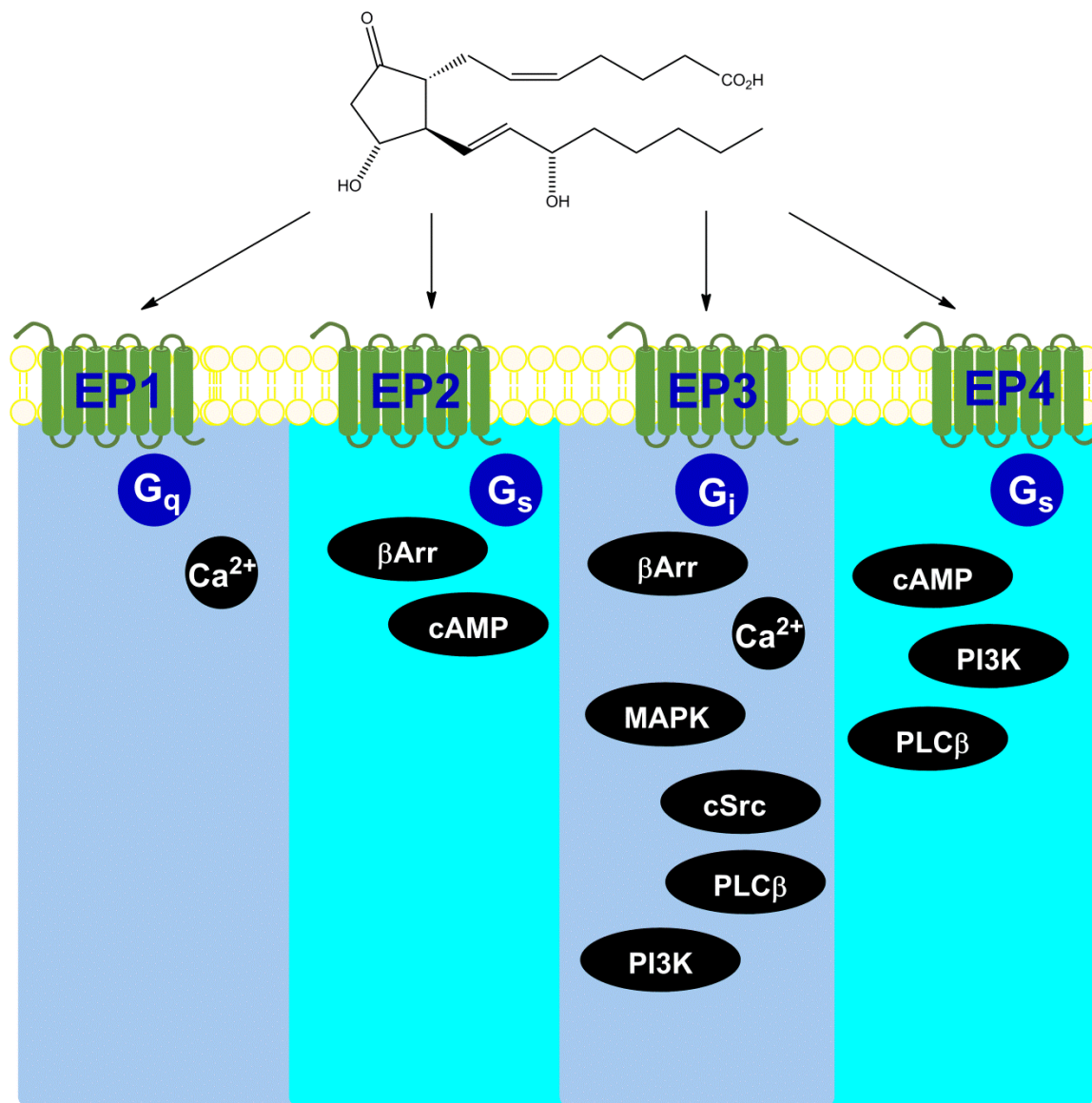
Figure 8 – Signal transduction pathways through which the four subtypes of GPCRs for PGE$_2$ function

E-Prostanoid Receptor Subtype 1 (EP1). The mouse EP1 receptor was first cloned from a mouse kidney cDNA library using a human thromboxane receptor expressed sequence tag (EST)[150]. The clone was found to be similar to the previously identified mouse EP2

and EP3 receptors, but not identical. When heterologously expressed in Chinese Hamster Ovary (CHO) cells, the authors confirmed the receptor bound $[^3H]PGE_2$ with high affinity and had a unique order of affinity for endogenous prostanoids and synthetic prostanoid receptor ligands. The receptor stimulated an increase in intracellular calcium ($[Ca^{2+}]_i$) when PGE_2 was added to mEP1-expressing, Fura-2-loaded CHO cells. The human EP1 receptor was originally cloned out of cDNA library derived from a human erythroleukemia cell line using a human thromboxane receptor EST. The human EP1 receptor also stimulated calcium flux when activated by PGE_2 and displayed ligand affinities characteristic of an EP1 receptor[151].

EP1 is generally accepted to be a G_q-coupled receptor. Mouse EP1-stimulated inositol trisphosphate (IP_3) formation is modest at best. In CHO cells stably expressing mEP1, PGE_2 induced a 20 % increase over baseline in IP_3. When considering the primary sequence of mEP1, consensus sequences for protein kinase A (PKA) and protein kinase C (PKC) phosphorylation have been noted[150]. $[^3H]PGE_2$ binding to mEP1-expressing CHO cell membranes is GTPγS sensitive, with its equilibrium dissociation constant (K_D) increasing from 23 nM to 34 nM with no change in receptor density (B_{max}). This was due to an increase in the off-rate (k_{off}) for $[^3H]PGE_2$ at mEP1 when GTPγS is in the system and receptor-G protein complexes are disrupted. Mouse EP1 is known to increase $[Ca^{2+}]_i$ when activated, demonstrated to be mostly due to calcium influx with a small calcium mobilization contribution. Sulprostone-induced calcium flux was insensitive to phospholipase C (PLC) inhibitor, pertussis toxin, verapamil, or nifedipine pretreatment, calling into question whether this pathway truly is G_q-mediated. The small calcium mobilization response, evident when EP1 is stimulated in the absence of extracellular

32

calcium, was abrogated by PLC inhibition. Sulprostone activation of EP1 stimulated a 40 % increase in IP formation which was dependent on extracellular calcium and was pertussis toxin insensitive. Previous reports have suggested second messenger kinase phosphorylation sites in the mouse EP1 receptor. To investigate an effect of PKA on mEP1 function, investigators measured calcium flux stimulated by sulprostone activation of mEP1 after pretreatment with either forskolin (a direct adenylate cyclase activator) or dbcAMP (dibutyryl-cyclic AMP, a cell-penetrant cAMP mimetic). Neither treatment affected calcium signaling stimulated by mEP1. Pretreatment with phorbol ester (a diacylglycerol mimetic, a direct PKC activator) completely blocked any calcium signaling in response to mEP1 activation, suggesting PKC may phosphorylate mEP1 and that desensitizes mEP1. Pretreatment with phorbol ester for 5 minutes, but not dbcAMP or forskolin pretreatment, reduced specific binding to [^{3}H]PGE$_2$. Binding to control preparations and preparations exposed to dbcAMP or forskolin for five minutes was reduced to the level of phorbol ester-treated preparations when the binding experiments were performed in the presence of GTPγS, suggesting PKC phosphorylation of mEP1 uncouples the receptor for its G-protein. When cells were exposed to phorbol ester for even longer, 24 hours, specific radioligand binding was further reduced as well as production of mEP1 mRNA[152].

It is now appreciated that EP1 can couple to other pathways. Recently, a study reported the human EP1 receptor can couple to G$_i$ proteins[153]. Activation of EP1 caused a pertussis toxin sensitive increase in the expression of hypoxia-inducible factor-1α (HIF-1α) which was found to involve the PI3K (phosphoinositol 3 kinase)/Akt/mammalian target of rapamycin (mTOR) pathway. Evidence also exists for EP1 modulating the

function of other receptors by forming heterodimers. Activation of EP1 in the airway did not constrict mouse trachea. EP1 did blunt the vasodilatory action of β_2AR, but not of forskolin, suggesting an interaction upstream of G_s-adenylate cyclase interaction. Investigators showed EP1 and β_2AR colocalized by bioluminescent resonance energy transfer (BRET) assays and that in cell membrane $[^{35}S]GTP\gamma S$ binding assays the presence and activation of EP1 uncoupled β_2AR from its G protein[154].

Using genetic deletion of EP1 in mice, several roles of EP1 in physiology and disease have been explored. In one study, investigators evaluated a role of EP1 in pain perception and blood pressure regulation. Using intraperitoneal injection of one of two different irritants as a model for pain, a writhing response was compared between wild-type and EP1$^{-/-}$ mice. EP1$^{-/-}$ mice had a significantly reduced stretch response to both noxious stimuli, and this reduction was equal in magnitude to piroxicam, a positive control. This may suggest piroxicam acts to block the formation of PGE_2 as a ligand for the EP1 receptor in nociception. As in previous studies, plasma renin activity was measured in mice of each genotype, stratified as well by sex. A genotype-specific effect was only observed for male mice: male EP1$^{-/-}$ mice had higher plasma renin activity than male wild-type controls and female EP1$^{-/-}$ mice had indistinguishable plasma renin activity from female wild-type controls. EP1$^{-/-}$ mice had significantly lower baseline systolic blood pressure on a "normal"-salt diet, possibly explaining the increase in plasma renin activity seen in the male EP1$^{-/-}$ mice. When the mice were placed on a low-salt diet, the EP1$^{-/-}$ but not wild-type mice had a significant reduction in systolic blood pressure, suggesting some defect in salt-handling in the absence of the EP1 receptor[155].

Other studies have shown an attenuation of Ang II-driven hypertension in EP1$^{-/-}$ mice and blood pressure normalization in spontaneous hypertensive rats treated with an EP1 antagonist[80]. In a mouse model of cerebrovascular dysfunction, chronic Ang II administration reduced cerebral blood flow. Genetic deletion or pharmacological blockade of either COX-1 or EP1 attenuated this phenotype, suggesting a role for EP1 in the cerebral ischemia associated with cerebrovascular dysfunction[156].
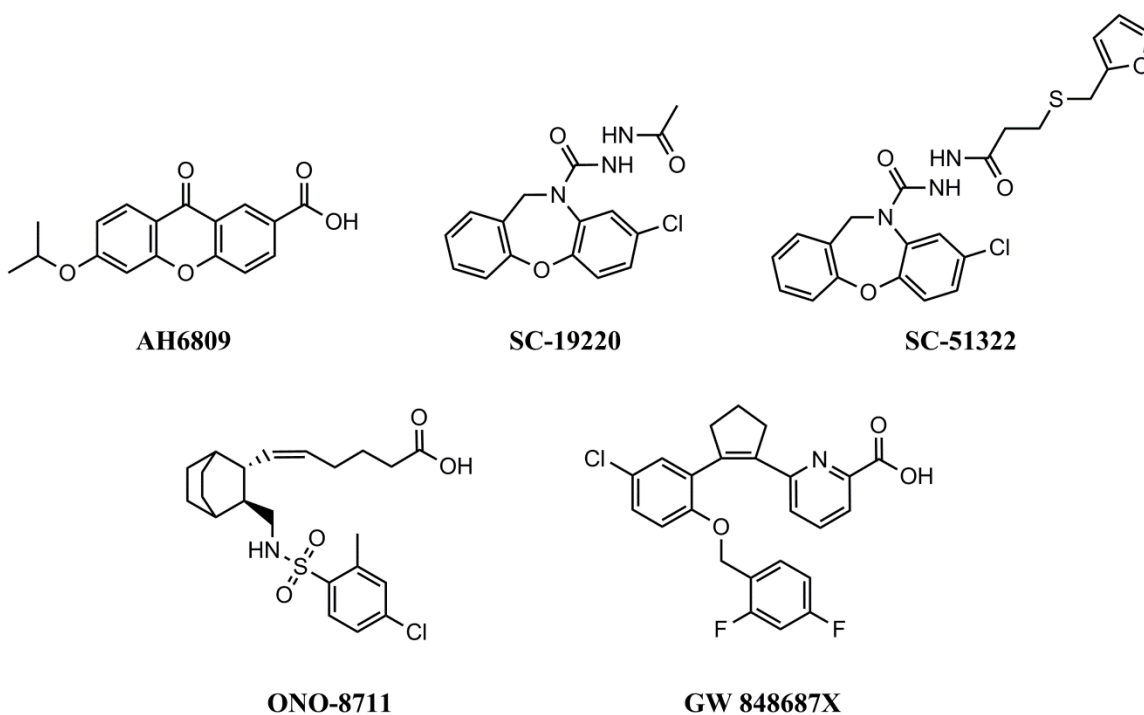
Figure 9 – Antagonists of the EP1 receptor

EP1 is a therapeutic target for various types of pain. SC-19220[157], SC-51322[158,159], and AH6809[160] comprise a set of first generation EP1 antagonists with poor selectivity and affinity. Ono Pharmaceuticals developed ONO-8711 (Figure 9) that has been shown analgesic properties in animal models of inflammatory[161] and post-operative pain[162,163].

GlaxoSmithKline has published several papers on their pursuit of an antagonist of EP1 for pain indications[164-170].

E-Prostanoid Receptor Subtype 2 (EP2). The first EP2 receptors to be cloned for mouse and human were not the EP2 receptor at all! Cloning and characterization of an imposter mouse EP2 receptor isolated from a mouse mastocytoma cDNA library using a mouse EP3 EST was described in 1993[171]. A different group then used an EST from this mouse "EP2" receptor to clone a human EP2 receptor from a lung cDNA library[172]. These new receptors were pharmacologically consistent with an EP2 receptor, except that neither was responsive to the EP2 agonist butaprost[171,172]. In an independent laboratory, John Regan published in 1994 the cloning of a different human EP2 receptor from a human placental cDNA library. This receptor was the true human EP2 receptor and as such possessed all of the pharmacological hallmarks of an EP2 receptor. These investigators posited the previously identified human and mouse EP2 receptors may be misidentified EP4 receptors[173]. The investigators from the mouse study later published the reassignment of their cloned receptor as the mouse EP4 receptor[174].

The EP2 receptor is a G_s-coupled receptor with lower affinity for [^{3}H]PGE$_2$ than EP3 or EP4 (K_D = 13 nM[175]). The EP2 receptor forms signaling complexes with β-arrestin. In a mouse study of papilloma development, investigators determined a G-protein independent signaling cascade through EP2: β-arrestin1 carries active Src to EP2, Src phosphorylates and activates the epidermal growth factor receptor (EGFR), and EGFR then activates H-Ras, ERK1/2, and Akt signaling cascades[176]. Due to a lack of EP2-

selective antagonists, in vivo function of EP2 has been studied using genetic deletions of the receptor gene *Ptger2*.

The most obvious phenotype of the EP2$^{-/-}$ mice is a fertility defect. Female EP2$^{-/-}$ became pregnant less frequently than wild-type controls. When EP2$^{-/-}$ mice did become pregnant, their litters were significantly smaller than wild-type controls. The reduction in pregnancy rate is due to a lower rate of fertilization likely caused by a deleterious change in the oviduct microenvironment and not a defect in the timing of ovulation or the ova themselves. Abnormalities in regulation of blood pressure were observed in EP2$^{-/-}$ mice. EP2$^{-/-}$ mice on a normal-salt diet (0.4 % NaCl) had a significantly lower MAP than wild-type controls. This blood pressure deficit could be reduced by putting the mice on a high-salt diet (6 % NaCl). This would suggest some defect in salt handling in EP2$^{-/-}$ mice. A decrease in blood pressure should stimulate a compensatory release of renin. Plasma renin activity was indistinguishable with respect to genotype under each diet, suggesting a deficiency in the signaling that triggers renin release in response to hypotension. This signaling event may be a direct activity of EP2. Chronic PGE$_2$ infusion increases blood pressure due to a direct stimulation of renin release, and renin release can be stimulated by hormones that increase intracellular cAMP ([cAMP]$_i$)[177].

Similarly, investigators have observed a significant reduction in embryo implantation in female EP2$^{-/-}$ mice independent of whether they were mated with male wild-type or EP2$^{-/-}$ mice. The fertility defect was further narrowed to the number of eggs released and subsequently fertilized per ovulation: EP2$^{-/-}$ mice released significantly fewer eggs per ovulation and fewer of these eggs were fertilized when compared to wild-type controls.

As before, abnormalities in blood pressure regulation and salt-handling were also observed in EP2^{-/-} mice. Bolus intravenous injection of an EP2-selective agonist produced an acute and transient decrease in MAP in wild-type mice. This response was completely absent in EP2^{-/-} mice. In EP2^{-/-} mice, the depressor response to PGE_2 is absent and instead a potent, transient vasopressor response to PGE_2 is unmasked. Vasodepressor responses to an EP4 agonist and vasopressor responses to an EP1/EP3 agonist were indistinguishable between wild-type and EP2^{-/-} mice.

Female EP2^{-/-} mice had a higher baseline systolic blood pressure than wild-type female controls. Deletion of EP2 did not affect male baseline systolic blood pressure. When wild-type mice were placed on a high-salt diet no change in blood pressure was observed, due to a compensatory increase in urinary salt output. When EP2^{-/-} mice were moved from a "normal"-salt diet to a high-salt diet, systolic blood pressure increased by 25 - 30 mmHg. This salt-sensitive hypertension again suggests a salt-handing defect in mice lacking the EP2 receptor[178].

Butaprost
pro-drug agonist

ONO-AE1-259
agonist

Positive
Allosteric Modulator
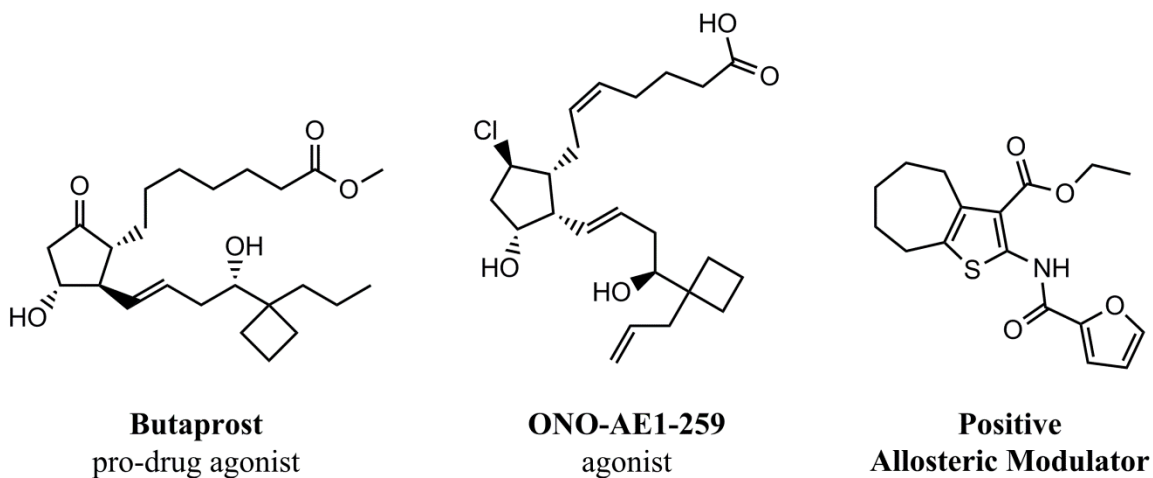
Figure 10 – Agonists and allosteric modulators of the EP2 receptor

AH6809 is the primary EP2 antagonist available, despite its affinity for the EP1 receptor (Figure 10). Butaprost, once known as TR4979, is a select EP2 agonist once the compound is metabolically activated by ester hydrolysis[179]. Next generation EP2 agonists and positive allosteric modulators have been developed. ONO-AE1-259 is a potent and selective EP2 agonist generated by Ono pharmaceuticals using butaprost as a template[180]. Selective, positive allosteric modulators were identified and demonstrated to be neuroprotective in the NMDA-induced excitotoxicity model of cell injury[146].

E-Prostanoid Receptor Subtype 3 (EP3). The mouse EP3 receptor was first cloned from lung cDNA pools using a human thromboxane receptor EST[181]. The mouse EP3 receptor exists as three isoforms differing only in their alternatively spliced C-terminal tails[182,183]. The human ortholog of EP3 was subsequently cloned from human small intestine[184], a human kidney cDNA library[185], a human megakaryocyte cell line[186]. Eight alternative splice variants of hEP3 have been identified[187].

The EP3 receptor exists as a number of different C-terminal splice variants and these differences in C-terminus composition have been shown to affect the receptor desensitization and trafficking as well as to which pathway the receptor couples. For the mouse EP3 receptors, the splice variants are designated mouse EP3α, EP3β, and EP3γ in the order they were discovered. The first mouse EP3 receptor splice variant was identified in 1992 and was shown to have classical $[cAMP]_i$-suppressing G_i activity[181].

The second isoform discovered, mEP3β, was characterized in comparison to mEP3α. In radioligand binding assays, the K_D for mEP3α decreased from 3.0 nM to 1.1 nM when

the binding was performed in the presence of GTPγS. For mEP3β, the K_D increased from

2.8 nM to 5.9 nM. Neither receptor had a decrease in B_{max} when incubated with GTPγS.

Both of these GTPγS-dependent changes in K_D are pertussis toxin sensitive[188]. These data

indicate the association of mEP3β with $G_{αi}$ increases the affinity of the receptor for

[^{3}H]PGE$_2$, as would be predicted by the ternary complex model (Figure 11)[189]. No

change in K_D or B_{max} for mEP3β when incubated with GTPγS suggests the receptor is

only weakly G-protein coupled, if at all. Indeed, Sugimoto *et al*. saw the IC_{50} for mEP3β

against [cAMP]$_i$ accumulation was three orders of magnitude higher than that for mEP3α.

These data demonstrate a difference in G-protein coupling for mouse EP3 receptors with

different C-terminal tails.

$$L + R + G \rightleftharpoons LR + G$$
$$\updownarrow \qquad\qquad\qquad \updownarrow$$
$$L + R^* + G \rightleftharpoons LR^* + G$$
$$\updownarrow \qquad\qquad\qquad \updownarrow$$
$$L + R^*G \rightleftharpoons LR^*G$$
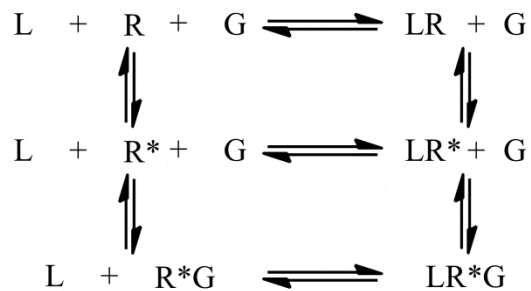
Figure 11 – Ternary Complex Model. L represents a ligand, either an agonist, antagonist, or inverse agonist. R and R* represent an inactive and an active G-protein coupled receptor, respectively. G represents the G-protein to which the receptor couples[189].

The susceptibility of each splice variant to agonist-stimulated receptor desensitization

and internalization was also studied. For mEP3α, 30 minute pre-incubation of mEP3α

expressing CHO cells with PGE$_2$ right-shifted the concentration response curve of PGE$_2$-

stimulated $[cAMP]_i$ suppression. Pre-incubation for 24 hours further right-shifted the concentration response curve and also reduced the maximum efficacy (E_{max}) for the system. Neither pre-treatment for 30 minutes nor for 24 hours affected the concentration response curve of PGE_2 in CHO cells expressing mEP3β. Time- and concentration-dependent internalization from the surface of intact CHO cells was observed for mEP3α and not for mEP3β. Pre-treatment of cells with PGE_2 for 24 hours before membrane harvest reduced the B_{max} for mEP3α by 75 % while mEP3β was unaffected[190]. Taken together these data demonstrate a difference in receptor desensitization and internalization that was dependent on the alternatively spliced C-terminal tails.

Discovery of the third splice variant of mouse EP3, mEP3γ, was reported in 1993[183]. Mouse EP3γ was shown to be G_i-coupled like the other mouse EP3 splice variants. At high concentrations of agonist, mEP3γ also stimulated the accumulation of $[cAMP]_i$. Pertussis toxin treatment reduced the GTPase activity stimulated by mEP3γ activation.

The diversity in downstream signaling from these alternatively spliced receptors was captured well in a study of bovine EP3 receptors. Four isoforms of the EP3 receptor (EP3A − EP3D) were identified from a bovine adrenal medullary cDNA library using a mouse EP3 receptor EST. Surprisingly, the bovine EP3 receptor splice variants were found to stimulate $[cAMP]_i$ accumulation to varying degrees in forskolin-naïve CHO cells in a pertussis toxin-insensitive manner. This suggests the bovine EP3 receptor can couple to G_s proteins in addition to its canonical G_i coupling. The bovine EP3A splice variant did not effectively raise $[cAMP]_i$ but was the splice variant with the highest E_{max} for G_i-mediated $[cAMP]_i$ suppression. EP3A stimulated IP_3 turnover and a small increase in $[Ca^{2+}]_i$, both of which were pertussis toxin-sensitive. The bovine EP3D splice variant

showed modest G_s-coupling and similar G_i activity to EP3A. EP3D also stimulated IP$_3$ turnover and a large increase in $[Ca^{2+}]_i$, neither of which were pertussis toxin sensitive. The net effect of EP3B or EP3C activation seemed to be limited to increasing $[cAMP]_i$ accumulation [191].

The EP3 receptor is known to exhibit a large amount of constitutive activity, depending on the splice variant. In some contexts the activity of mEP3γ can be completely agonist-independent and one might interpret the lack of an agonist-dependent increase in signal as a lack of receptor activity. Without a formally-defined inverse agonist, constitutive activity was not apparent until it was observed that basal $[cAMP]_i$ levels of EP3-transfected cells actually increased when the cells were treated with pertussis toxin[192-194].

EP3 can activate a number of other signaling pathways. One pathway relevant to blood pressure and insulin sensitivity is the RhoA pathway. The EP3 receptor is known to couple to $G_{12/13}$ proteins, which through RhoGEF activate the small GTPase RhoA and its kinase ROCK. ROCK has a number of functions related to the cytoskeleton. In vascular smooth muscle cells, ROCK sensitizes the cell to contraction by inactivating myosin light chain phosphatase[195]. In other countries, ROCK inhibitors are used clinically to treat hypertension and diseases related to vasomotor dysfunction[196-198]. EP3 activation increases $[Ca^{2+}]_i$ as well as sensitizes vascular smooth muscle cells contraction through RhoA/ROCK. It is therefore not surprising that activation of EP3 can be a direct vasoconstrictor, depending on the vascular bed[199-201]. Guinea pig aorta is a robust bioassay of EP3-mediated vasoconstriction, as well as TP-mediated vasoconstriction[200,202]. Robert Jones *et al*. have published studies indicating a critical role

for RhoA/ROCK in transducing the vasoconstrictor response to EP3 receptor activation in guinea pig aorta[200,202].

In other cells, ROCK stimulates the formation of actin stress fibers[203]. In intermedullary collecting duct cells, the diuretic hormone arginine vasopressin (AVP) induces translocation of vesicles of water-permeable aquaporin 2 (AQP2) channels to the cell surface, increasing water excretion into the urine. PGE_2 has long been shown to antagonize this diuretic effect[204,205]. Recently, a mechanism for how PGE_2 antagonizes AVP was proposed. Selective activation of EP3 was shown to suppress AVP-stimulated membrane insertion of AQP2 with a concomitant increase in actin stress fiber formation independent of $[cAMP]_i$ and $[Ca^{2+}]_i$ levels. AVP reduced basal RhoA activation, while EP3 increased RhoA activation over baseline. It was proposed that EP3 caused a reduction in membrane AQP2 by inducing stress fibers that prevented the movement of the AQP2 vesicles to the membrane[206].

Through a similar mechanism, insulin stimulates insertion of GLUT4 vesicles into the membranes of its target tissues. Inactivation of Rho with *Clostridium botulinum* C3 exoenzyme stimulated glucose uptake in cells similar to levels achieved by insulin stimulation[207]. Data exists to suggest a role of PGE_2 in reducing tissue responses to insulin[208,209]. It is therefore possible that in a setting of chronic inflammation, like diabetes mellitus, when PGE_2 would be expected to be high, signaling through EP3 could suppress GLUT4 translocation to the membranes of target tissues by inducing actin stress fiber formation.

Central PGE_2 is known to have a number of EP3-mediated effects: fever[210], activation of sympathetic efferents of the autonomic nervous system[66,211,212] possibly in response to

the baroreflex, and prevention of withdrawal symptoms from drugs of abuse[149,213,214]. Immunostaining of EP3 in the rat central nervous system is extensive[215,216]. Of particular interest is localization of EP3 to the locus coeruleus, the raphe nuclei, several locations lining the ventricles, the tractus solitarius, ganglia of the autonomic nervous system, and dorsal root ganglia.

The locus coeruleus contains noradrenergic neurons that may be involved in sleep[217] and memory[218]. One of the roles of serotinergic raphe neurons is to mediate the analgesic properties of opiates[219]. Some nuclei adjacent to the ventricles of the brain have poorly formed blood-brain barriers. These nuclei sense circulating hormones and cytokines, like IL-1β which augments PGE_2 production in ventricle adjacent nuclei of the hypothalamus, mediating the febrile response to IL-1β[220]. EP3 has been shown to be both pre-synaptic[221] and post-synaptic in localization[216].

EP3 has been described in multiple structures of the baroreflex circuit (Figure 12). The baroreflex is a centrally-mediated vasomotor response. When blood pressure increases, mechanoreceptors in the aortic arch and carotid bodies detect distension of the vessels and stimulate efferents to the nucleus tractus solitarius (NTS). Stimulatory glutamatergic efferents from the NTS stimulate the caudal ventrolateral medulla (CVLM), which trigger inhibitory GABAergic efferents to the rostral ventrolateral medulla (RVLM). The RVLM is the central activator of the sympathetic nervous system. The baroreflex inhibits the RVLM through GABAergic CVLM projections, which also activates vagal efferents. The net effect is to reduce chronotropy and inotropy of the heart, acutely lowering arterial pressure[222].

44
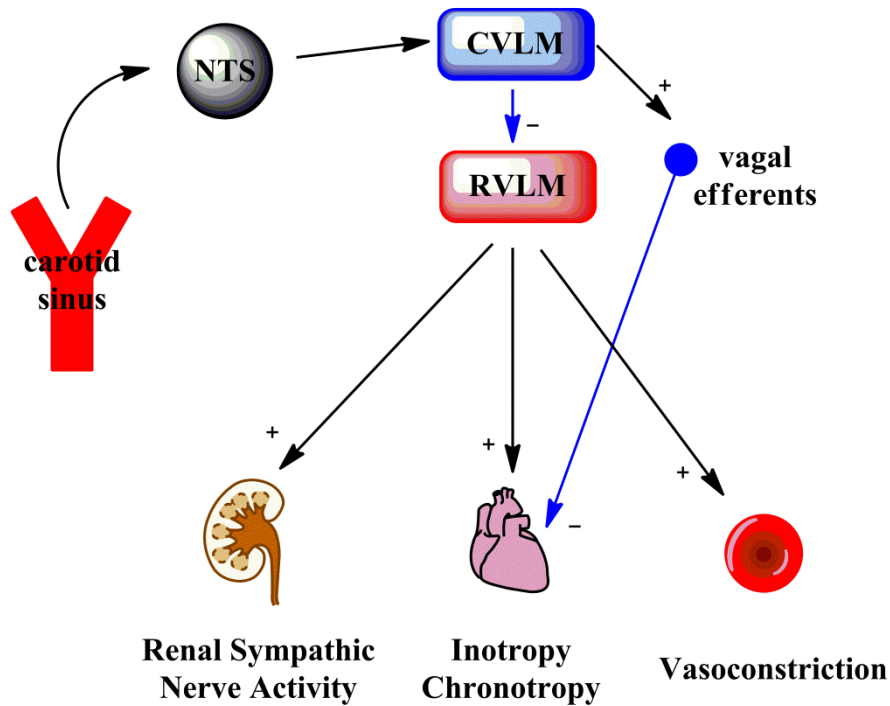
Figure 12 – Baroreflex and basal sympathetic tone are controlled by the central vasomotor center. NTS, nucleus tractus solitarius; CVLM, caudal ventrolateral medulla; RVLM, rostral ventrolateral medulla.

EP3 is hypothesized to either directly or indirectly activate the sympathetic outflows of the RVLM. Intracerebroventricular (ICV) injection of PGE_2 and EP3-selective agonists into rats increased circulating levels of norepinephrine in a dose-dependent manner[211]. Whether EP3 directly stimulates the RVLM or inhibits the CVLM, which then disinhibits the RVLM, cannot be known from these data. In another study, PGE_2 was demonstrated to raise blood pressure, heart rate, and renal sympathetic nerve activity (RSNA) in a dose-dependent manner. These effects were abolished by ganglionic blockers and antagonism of adrenergic receptors, but not an EP1 antagonist. The same sympathomimetic effect was observed with an EP3-selective agonist, but not with EP1-,

EP2-, or EP4-selective agonists[66]. These data support a role for central EP3 receptors in the central regulation of cardiovascular function, especially in the setting of inflammation when PGE$_2$ production would be augmented.

DG-041   ONO-AE3-240   L-798,106
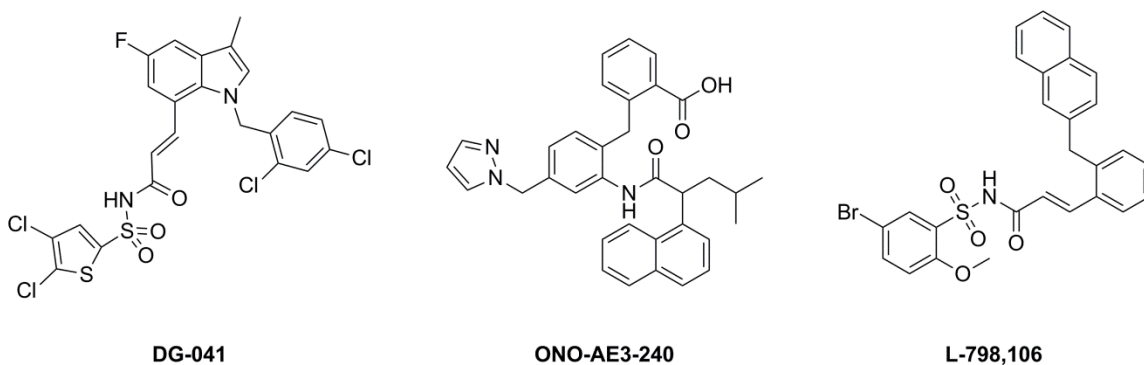
Figure 13 – Antagonists of the EP3 receptor

EP3 receptor antagonists have been developed as therapeutic candidates for thrombotic disorders (Figure 13)[73,76], urinary bladder dysfunction[223], and stroke injury[147]. DG-041 is a high-affinity and selective EP3 antagonist that progressed to Phase II clinical trials as an adjunct therapy to clopidogrel for prevention of thrombotic diseases[73,224-226]. DG-041 was able to block PGE$_2$-stimulated platelet aggregation in vitro and ex vivo without increasing bleeding time in rats, representing a novel class of antiplatelet therapeutics. In a mouse model of acute cerebral infarction, intraperitoneal injection of the EP3 antagonist ONO-AE3-240 significantly reduced infarct size, edema, and neurological dysfunctions to approximately the same levels as genetic deletion of EP3[147].

L-798,106 is another high-affinity, selective antagonist of EP3 that was developed by Merck Frosst[227].

E-Prostanoid Receptor Subtype 4 (EP4). As detailed above, cloning and initial characterization of the mouse[171] and human[172] EP4 receptors were reported in 1993 and 1994, respectively. At the same time, a group at Glaxo published a study in which they pharmacologically identified the EP4 receptor in ovine saphenous vein[228]. Shortly thereafter, John Regan reported cloning the human EP2 receptor[173] and it became clear the originally reported mouse and human EP2 receptors were actually this newly identified EP4 receptor[174].

EP4 is a G_s-coupled receptor with an affinity for $[^3H]PGE_2$ 20 times tighter than EP2 for $[^3H]PGE_2$ ($K_D = 0.59$ nM[175]). Like the EP2 receptor, EP4 has also been shown to signal through G-protein independent β-arrestin mediated signaling complexes. In models of lung and colorectal cancer, signaling of EP4 through β-arrestin1/c-Src transactivation of EGFR has been shown to augment cancer cell migration[229,230]. Functional selectivity of ligands at EP4 for G_s versus G_i/β-arrestin coupled pathways has been reported. PGE_2 potently activated the classical G_s-coupled pathway through EP4; $PGF_{2\alpha}$ and PGE_1-OH preferentially activated the G_i/β-arrestin pathways[231].

Of the four subtypes of PGE_2 receptors, deletion of EP4 has the most striking phenotype. Fetal circulation has a special arterial shunt called the ductus arteriosis (DA) that redirects blood from the fetal pulmonary circuit to the placenta for oxygenation. At and after birth, the DA must constrict shut and be permanently occluded. In about 0.06 % of full-term births and more for premature births, the DA fails to close, a condition

referred to as patent ductus arteriosis, rapidly resulting in arterial pressures reaching the pulmonary circuit, causing pulmonary edema and congestive heart failure. Treatment for patent DA is indomethacin. EP4 deletion on the 129 background was 100 % fatal by the second postnatal day. On mixed backgrounds, EP4 deletion was fatal to almost the entire litter of EP4$^{-/-}$ mice. These mice died of heart failure secondary to patent DA[87,232].

Studies in EP4 knockout mice have been challenging because of their perinatal lethality. Small cohorts can be assembled by breeding mice on a mixed genetic background. EP4, along with EP2, is a vasodepressor receptor. Activation of endothelial EP4 has been shown to induce an eNOS-dependent vasodilation in aortic rings[65]. EP4-selective agonists and antagonists (Figure 14) have confirmed a systemic vasodepressor response to activation EP4[64]. First generation EP4 agonists and antagonists were nonselective and low affinity[233]. Current EP4 ligands have better affinity but lack specificity (Figure 14)[234].
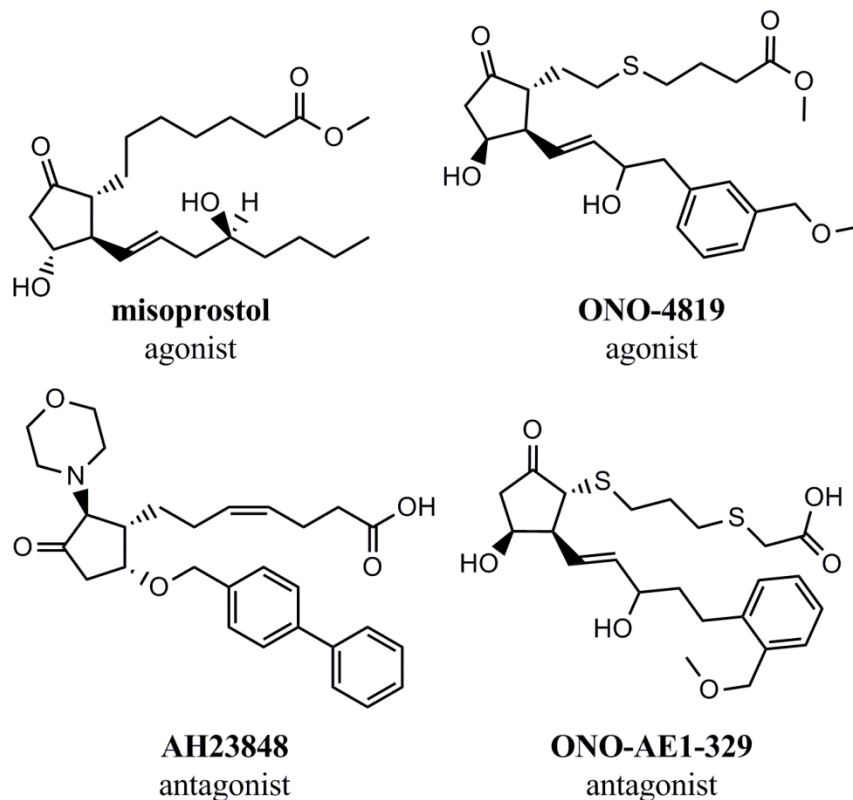
Figure 14 – Agonists and antagonists of the EP4 receptor

Specific Aims

Generate and characterize a mutant of the mouse EP3γ receptor devoid of all cysteine residues for overexpression in E. coli. The three-dimensional architecture of a protein provides a wealth of information concerning a protein functions and how to artificially disrupt or augment those functions[235-237]. Protein structures are inferred using biochemical techniques or solved using a number of low-resolution (atomic force and electron microscopy) and high-resolution (NMR, X-ray crystallography) techniques. High-resolution structural studies of proteins require large amounts of pure protein.

Traditionally, overexpression in *E. coli* is the method of generating large amounts of protein that can then be purified by affinity chromatography. One obvious problem to synthesizing functional GPCRs in *E. coli* is the lack of membrane-bound organelles in the prokaryote which makes proper folding of the GPCR unlikely. While a GPCR is synthesized in eukaryotic cells, an N-terminal signal sequence feeds the first transmembrane domain of the nascent protein through the bilayer of the endoplasmic reticulum, promoting a sequence of events that result in proper folding of the seven-transmembrane domain receptors (Figure 15). When proteins are overexpressed in *E. coli*, they are often driven into insoluble aggregates of misfolded protein called inclusion bodies. However, these inclusion bodies can sometimes be solubilized and the proteins refolded into their native conformations.
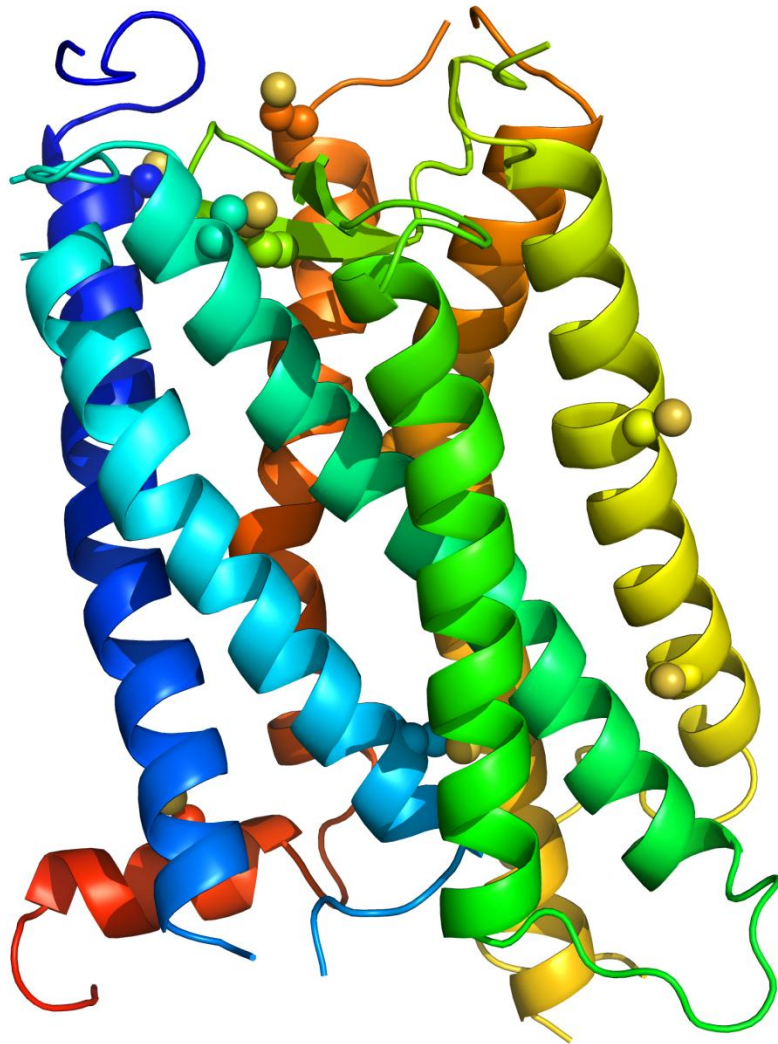
Figure 15 - Model of the three dimensional structure of the mouse EP3γ receptor based on homology to the 2.2 Å crystal structure of bovine rhodopsin (PBD ID 1U19[238]).

When refolding proteins from aggregates, the various cysteine residues of the protein can crosslink, forming covalent disulfide bonds. In many proteins, properly assembled disulfide bonds are absolutely required for natively folded, active protein. In GPCRs, it is well established at least one disulfide bond exists in most if not all Class A GPCRs

between the first and second extracellular loops of the receptor[239-242]. Second and third disulfide bonds occur but are less conserved. Cross-linked, misfolded aggregates can be avoided by determining which cysteine residues are required for native receptor function and mutating the remaining residues[243].

In this Specific Aim (Chapter II), mutants of a hemagglutinin (HA)-tagged mouse EP3γ receptor were generated, each with a different cysteine-to-alanine missense mutation. Retention of native function for each receptor was evaluated using radioligand binding and cell-based signaling assays. In two cases, replacement of a cysteine residue with an alanine abolished radioligand binding and signal transduction through the mutant receptor. To determine whether these deficits were due to a misfolded receptor or failure of the mutant receptor to traffic to the cell surface, surface expression was determined using ELISA against the N-terminal HA tag and intact cell radioligand binding assays.

Synthesize and characterize novel antagonists of the mouse EP1 and EP3 receptors. EP1 and EP3 receptors have been implicated in the pathophysiology of DM and cardiovascular disease. EP1 antagonists have been shown to lower blood pressure in spontaneously hypertensive rats[80] and to prevent the progression of DN in STZ-treated rats[77]. Genetic deletion of EP1 has prevented development of Ang II-dependent hypertension[80,244] and attenuated mortality in the face of chronic Ang II/deoxycorticosterone acetate (DOCA)-driven hypertension[83]. Activation of central EP3 receptors has been shown to increase blood pressure through the sympathetic nervous system[66]. EP3 may augment other vasoconstrictors by increasing calcium sensitivity in smooth muscle cells[200,245]. EP3 may also dampen target tissue sensitivity to insulin[108,209].

EP3 has been implicated in thrombotic diseases[73] and brain injury from stroke[147] and excitotoxicity[148].

In this Specific Aim (Chapter III and IV), a lead compound was identified in the literature[168] that was reported to be a high-affinity antagonist of the human EP1 receptor. The compound had significant off-target affinity for the TP receptor, potentially complicating the interpretation of any in vivo studies in which the compound would be employed. Also, the compound has poor in vivo pharmacokinetics, being rapidly eliminated from circulation. Hypothesizing the lead compound was eliminated by Phase II conjugation reactions at the carboxylate, a small library of amide and *N*-acylsulfonamides based on the lead compound was synthesized. The in vitro pharmacology of these compounds was characterized at the mouse EP1, EP2, EP3, EP4 and TP receptors using radioligand competition binding and calcium mobilization assays (Chapter III). JD-200, a compound previously described to have affinity for both the EP1 and EP3 receptors, and DG-041, a potent and selective antagonist of the EP3 receptor, were synthesized. The in vitro pharmacology of these compounds at mouse EP1 and EP3 receptors was characterized using radioligand competition binding, calcium mobilization, and CRE reporter assays (Chapter IV).

Determine the in vitro and in vivo pharmacokinetic properties of novel antagonists. Drug metabolism and pharmacokinetics assays allowed the study of dosing strategies and potential for drug-drug interactions with novel compounds. With the goal of using these novel EP1 and/or EP3 antagonists in mouse models of diabetes and hypertension, information about how rapidly these compounds are eliminated from circulation, how

they are eliminated, and which routes of administration are optimal for chronic dosing was required. Knowing how a compound distributes in an animal and how it is eliminated can help predict changes in drug exposure when the animal has compromised renal function or large difference in fat mass of a diabetic mouse, for example.

Intrinsic hepatic clearance of compounds with the best selectivity and affinity for EP1 and/or EP3 was determined and the data used to decide for which compounds to determine in vivo pharmacokinetic properties. Plasma protein binding data were also collected for the most selective compounds. Recognizing that the intrinsic clearance of these molecules was high, in vitro metabolite identification assays were also performed to determine whether a compound is being metabolized in several different ways or in a small, manageable set of reactions (Chapter III).

An in vitro metabolite identification experiment for DG-041 was also performed once it was recognized the elimination of DG-041 from the mouse was rapid. These experiments used incubation with mouse liver microsomes with and without glutathione to detect oxidative metabolism at DG-041 and trap potentially reactive metabolites formed in the assay (Chapter IV).

Evaluate the activity of novel antagonists in vivo. In this Specific Aim (Chapters III and IV), compounds were subjected to in vivo assays to determine whether the compounds were functional antagonists of their target receptors in vivo. Acute infusion of sulprostone, 17-phenyl-ω-trinor PGE_2 ($17PTPGE_2$), or phenylephrine are known to transiently increase MAP in anesthetized mice. Using the vasopressor response to sulprostone and $17PTPGE_2$ as a bioassay for EP1 and EP3 activity, the *p-*

chlorophenylsulfonamide analogue of the lead EP1 antagonist was evaluated for antagonism in vivo (Chapter III). Similarly, the ability of pretreatment with DG-041 to block the vasopressor activity of 17PTPGE$_2$ in anesthetized mice was determined (Chapter IV).

CHAPTER II

EVIDENCE FOR THE PRESENCE OF A CRITICAL DISULFIDE BOND IN THE

MOUSE EP3GAMMA RECEPTOR

Introduction

Although the molecular pharmacology of the EP receptors has been studied in detail[152,192,246-248], the structural features of the EP receptors themselves have been incompletely characterized. EP receptors are seven transmembrane domain, Class A GPCRs. A number of cysteine residues are highly conserved within GPCRs, suggesting a critical role for these cysteines in receptor function. Evidence suggests a pair of highly conserved cysteines, one in extracellular loop 1 (ECI) or just after that loop at the start of Helix 3 and one in extracellular loop 2 (ECII), which often form a disulfide bond in the extracellular domain of GPCRs[239,241,242,249]. A covalent bond between two such positions is known to constrain helix topology, promote functional tertiary arrangement, and stabilize the ligand-binding pocket of seven transmembrane domain receptors[242,250].

Intracellular cysteine side-chains can be the targets of enzymatic S-acylation and S-alkylation (isoprenylation) reactions. Cysteine residues in the C-terminal tail of GPCRs often have a molecule of palmitic acid covalently attached via a thioester bond[241,242,251] or an isoprene polymer covalently attached via a thioether bond[252,253]. The lipid moieties are thought to insert into the inner leaflet of the plasma membrane, forming a fourth

intracellular loop. A number of studies have indicated these post-translational modifications are necessary for proper receptor expression[254-256] and function[251,257,258].

The contribution of each of the 13 cysteines present in mEP3γ was evaluated with respect to ligand binding affinity, cell surface expression, and downstream effector coupling of the receptor. While most cysteine-to-alanine mutations were well tolerated, two mutations abrogated detectable radioligand binding and cell signaling and attenuated surface trafficking of the receptor. These cysteines correspond to a pair of conserved cysteines located in ECII and the extracellular end of Helix 3 that are the site of an extracellular disulfide bond in > 90% of the Class A GPCRs. Our results indicate that these conserved cysteine residues are important in enabling efficient surface expression and are also required for the function of surface-expressed EP3 receptor.

<u>Materials and Methods</u>

Materials. HEK293 cells were purchased from ATCC (#CRL-1573, Manassas, VA). PGE_2 and sulprostone were purchased from Cayman Chemical (Ann Arbor, MI). [^{3}H]PGE_2 was purchased from Perkin Elmer (Waltham, MA). Mouse anti-HA mAb, clone 6E2 was purchased from Cell Signaling (Danvers, MA). Horseradish peroxidase (HRP)-conjugated goat anti-mouse antibody was purchased from Jackson ImmunoResearch (West Grove, PA). Indomethacin, sodium butyrate, bovine serum albumin (BSA), and poly-D-lysine were purchased from Sigma Aldrich (St. Louis, MO). Chlorophenolred-ß-D-galactopyranoside (CPRG) was purchased from Roche Applied

Science (Indianapolis, IN). High-glucose, no L-glutamine Dulbecco's Modified Eagle Medium (DMEM), OptiMEM I, and Lipofectamine 2000 were purchased from Invitrogen (Carlsbad, CA). L-glutamine and penicillin/streptomycin were purchased from MediaTech (Manassas, VA). Fetal bovine serum (FBS) was purchased from Atlanta Biologicals (Lawrenceville, GA). HRP substrate kit was purchased from Bio-Rad (Hercules, CA). Bicinchoninic Acid (BCA) Protein Assay kit was purchased from Thermo Scientific (Rockford, Il).

Generation of Mutant HAmEP3γ cDNA. Mutants of mEP3γ were generated as previously described[259]. Mutant HAmEP3γ cDNAs were generated by Mutagenex (Piscataway, NJ) using HA-tagged wild-type mouse EP3 gamma cDNA in pcDNA3 as a template. Wild-type receptor and all mutant receptors contained a single threonine-to-serine variant from published sequence[183] that appears to have no effect on receptor function. Primers used for mutagenesis are listed in Table 1. DNA sequences of mutant receptors were confirmed by Mutagenex and independently at the Vanderbilt DNA Sequencing facility.

Table 1 – Forward and reverse primers used by Mutagenex to produce missense mutations in wild-type mEP3γ plasmid. Lowercase nucleotides indicate the mutagenic sequence.

Mutant	Primer ID	Primer Sequence
C24A	403-1F	5'-AAAGGTCTC GgctGGCTCCGTGTCCGTGG
	403-1R	5'-AAAGGTCTC CCAGCGTCGTCGGTAGTACTT
C68A	403-2F	5'-AAAGGTCTC GgctATTGGCTGGCTGGCGC
	403-2R	5'-AAAGGTCTC ATAGCCAGCAGGAAAGACTTCTT
C107A	403-3F	5'-AAAGGTCTC GgctACCTTCTTCGGGCTAAC
	403-3R	5'-AAAGGTCTC GTAGCCAGACGCCCCGATGG
C184A	403-4F	5'-AAAGGTCTC gctTTCATCAGCACCGGGCCG
	403-4R	5'-AAAGGTCTC GAAAGCCCACGTGCCCGGCCA
C212A	403-5F	5'-AAAGGTCTC gctTTGGGCTTGCTGGCTCTG
	403-5R	5'-AAAGGTCTC CAAAGCGGCGAAGGCGGAGG
C224A	403-6F	5'-AAAGGTCTC CgctAACCTGGCGACCATCAA
	403-6R	5'-AAAGGTCTC TTAGCGGCAAAGGTCACCACCA
C236A	403-7F	5'-AAAGGTCTC GCgcTCGGGCCAAAGCCGC
	403-7R	5'-AAAGGTCTC GAGCGCGGGACACCAGGGCT
C265A	403-8F	5'-AAAGGTCTC GgcTGTGCTGTCCGTCTGTTG
	403-8R	5'-AAAGGTCTC ACAGCCATGATCCCCATGAGCT
C270A	403-9F	5'-AAAGGTCTC TCgcTTGGTCGCCGCTATTGA
	403-9R	5'-AAAGGTCTC AAGCGACGGACAGCACACACA
C291A	403-10F	5'-AAAGGTCTC AgctAAGACACAGATGGGAAAG
	403-10R	5'-AAAGGTCTC TTAGCTTGCTCAACCGACATCTG
C301A	403-11F	5'-AAAGGTCTC GgctAATTCCTTTCTAATTGCAGT
	403-11R	5'-AAAGGTCTC TTAGCCTCCTTCTCCTTTCCCAT
C334A	403-12F	5'-AAAGGTCTC TCgctCAGGTAGCAAACGCTGT
	403-12R	5'-AAAGGTCTC GAGCGAACTTCCGAAGAAGGAT
C343A	403-13F	5'-AAAGGTCTC gctTCTAGTGATGGACAGAAAG
	403-13R	5'-AAAGGTCTC AGAAGCACTGGAGACAGCGTTTG

Cell Culture. HEK293 cells were maintained at 37 °C / 5% CO_2 in complete media (DMEM supplemented with 10% FBS, 2 mM L-glutamine, 100 units/mL penicillin, and 100 μg/mL streptomycin). Cells were cotransfected with 3 μg receptor cDNA plasmid and 3 μg pCRE/lacZ reporter plasmid [260] using Lipofectamine 2000. Six hours after adding DNA-Lipofectamine 2000 complexes, media was replaced with complete media

containing 20 μM indomethacin and 5 mM sodium butyrate. Cells were allowed to recover for 18 to 24 hours before being plated in 96-well plates (5 x 10^4 cells/well) for the reporter assay and 100 mm dishes to prepare membranes. Cells were incubated for an additional 24 to 48 hours, until confluence was reached.

CRE/LacZ Reporter Assay. HEK293 cells in 96-well plates cotransfected with HAmEP3γ receptor plasmid and pCRE/lacZ reporter plasmid were incubated with PGE_2 (1 nM – 1 μM) in Opti-MEM containing 5 mM sodium butyrate and 20 μM indomethacin. After cells were stimulated with agonist for six hours, media was aspirated and cells were washed with phosphate-buffered saline (PBS). Cells were incubated for 10 minutes at room temperature in 25 μL of lysis buffer (10 mM sodium phosphate, 0.2 mM $MgSO_4$, and 10 μM $MnCl_2$, pH 8.0). Assay plates were developed as described[261]. Concentration response curves to PGE_2 were determined by measuring relative enzyme activity as absorbance at 570 nm on Multiskan Ascent plate reader (Thermo Labsystems, Waltham, MA).

Saturation Radioligand Binding. Total cell membranes from HEK293 transfectants used in CRE/LacZ assays described above were prepared as described[262]. Membranes (5 - 10 μg) were incubated with [^{3}H]PGE_2 (0.25 – 8 nM) in 200 μL of binding buffer (25 mM potassium phosphate, 1 mM EDTA, and 10 mM $MgCl_2$, pH 6.2) for 2 hours at 30 ˚C. Nonspecific binding was determined in the presence of the unlabeled sulprostone (5 μM).

Binding reactions were terminated and radioactivity was quantified as previously described[262].

Cell Surface Radioligand Binding. Cells transfected with HAmEP3γ receptor plasmids were plated 18 hours post-transfection at a density of 2×10^5 cells/well in poly-D-lysine coated 24-well plates in media containing 20 μM indomethacin and 5 mM sodium butyrate 24 hours prior to assay. Cells were washed with ice-cold 0.5 % FBS in PBS. Cells were incubated with [^{3}H]PGE$_2$ (5 nM) in the presence and absence of unlabeled sulprostone (5 μM) for 2 hours on ice. Cells were washed twice with ice-cold PBS and lysed with 0.1 M NaOH. Cell surface radioligand binding was quantified by liquid scintillation counting.

Immunodetection of Cell Surface Receptor Expression. Transfected cells were plated in poly-D-lysine-coated 24-well plates at a density of 2×10^5 cells/well in media containing 20 μM indomethacin and 5 mM sodium butyrate 24 hours prior to assay. Cells were washed with PBS and fixed with 250 μL of 3.7 % formalin in Tris-buffered saline (TBS) for 5 minutes at 23 °C and washed with TBS. Cells were blocked with 1 % BSA in TBS for 30 minutes at 23 °C. HA-tagged EP3 receptor was detected by incubation of cells with mouse anti-HA antibody (1:1000 in 1 % BSA) for 1 hour at 23 °C. Cells were washed with TBS and blocked with 1 % BSA in TBS for 15 minutes at 23 °C. HRP-conjugated goat anti-mouse antibody (1:1000 in 1 % BSA) was added to cells for 1 hour at 23 °C. Cells were washed with TBS and developed using HRP substrate kit as prescribed with the exception of using 300 μL of substrate and stop solutions per well.

Figure 1 – Primary sequence of the mouse EP3γ receptor. The location of the 13 cysteines are indicated in shaded residues. The location of a putative disulfide bond is illustrated between ECI and ECII.

C107A or C184A mutations abolish signal transduction through the mouse EP3γ receptor. To determine the functional importance of each cysteine residue of mEP3γ (Figure 1), ligand binding and signaling characteristics were determined for each of 13 cysteine-to-alanine point mutants of HA-tagged wild-type mEP3γ transiently expressed in HEK293 cells. Signal transduction for each mutant was evaluated by a cell-based CRE reporter assay for mEP3γ activation[260,261]. As observed previously for the rabbit EP3 receptor, agonist activation of the mouse EP3 receptor lead to a dose dependent increase

in CRE reporter activity[261]. Each receptor bearing a cysteine-to-alanine mutation (e.g., C24A) was similarly able to transduce an agonist-stimulated reporter signal, with the exception of receptors with mutations at C107 or C184 (Figure 2).
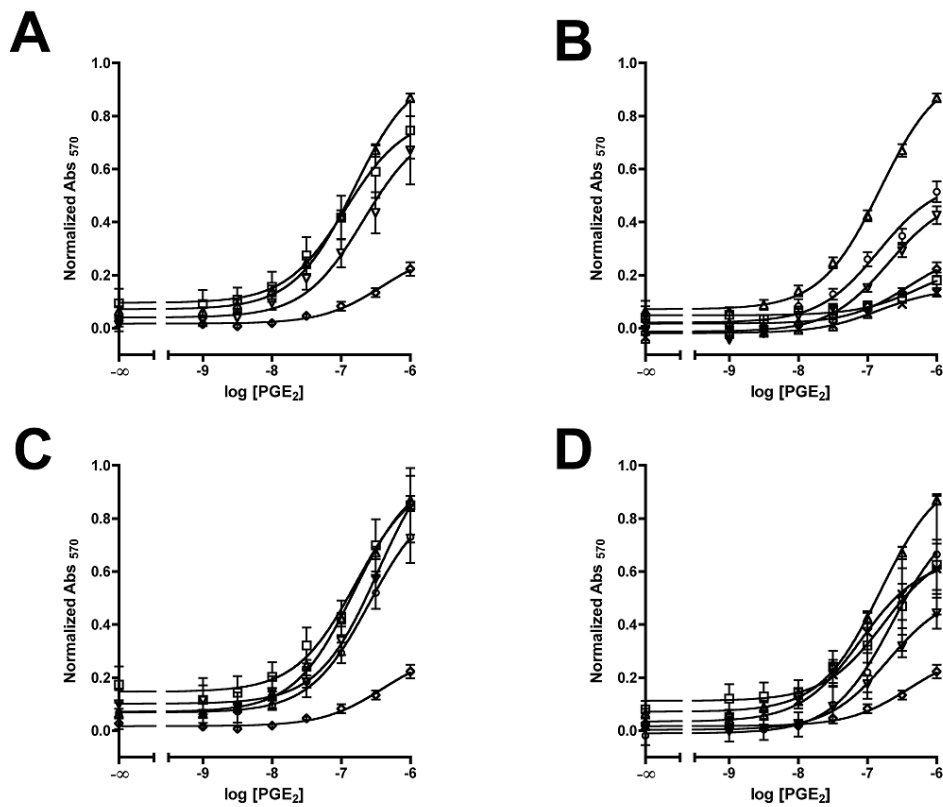
Figure 2 - CRE/LacZ cell signaling assay. HEK293 cells transiently coexpressing the pCRE/LacZ reporter plasmid with either wild-type HA-mEP3γ cDNA, mutant HA-mEP3γ cDNA, or empty pcDNA3 vector. A) Concentration response curves of (△) wild-type, (□) C24A, and (▽) C68A transfected and (◇) pcDNA3 transfected cells to PGE$_2$. B) Concentration response curves of (✕) C107A, (□) C184A, (▽) C212A, and (○) C224A transfected cells to PGE$_2$. C) Concentration response curves of (□) C236A, (▽) C265A, and (○) C270A transfected cells to PGE$_2$. D) Concentration response curves of (□) C291A, (▽) C301A, (○) C334A, and (✕) C343A transfected cells to PGE$_2$. Wild-type and pcDNA3 transfectant concentration response curves from A were replotted in each panel for comparison.

C107A or C184A mutations prevent specific binding of [^{3}H]PGE$_2$ to membranes.
Radioligand binding K_D and B_{max} for wild-type mEP3γ and each mutant receptor were determined from saturation binding isotherms on broken-cell membranes prepared from transiently transfected HEK293 cells. Radioligand binding was undetectable from two mutant receptors, C107A and C184A, suggesting that if expressed these receptors have K_D values at least 50-fold weaker than wild-type, below the limit of detection (Figure 3). Other receptors had no significant decrease in affinity for [^{3}H]PGE$_2$ (Table 2). Although variation of receptor density in these transient transfectants was statistically significant for many of the mutant receptors, only three of the mutants (C68A, C270A, and C301A) displayed dramatically reduced binding levels, indicative of reduced receptor expression.
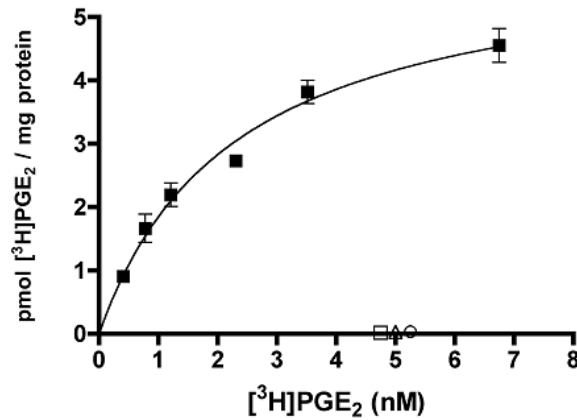
Figure 3 - Saturation radioligand binding curves for membranes prepared from (■) wild-type HA-mEP3γ, mutant HA-mEP3γ, and pcDNA3 transiently-transfected HEK293 cells. Specific binding of 5 nM [^{3}H]PGE$_2$ was undetectable for (○) pcDNA3, (□) C107A, and (△) C184A samples; these symbols are manually displaced horizontally for clarity. Shown are representative data (mean ± SEM) from three separate experiments conducted in triplicate.

Table 2 – Phenotypic analysis of cysteine mutants

Genotype	K_D (nM)	B_{max} (pmol/mg)
Wild-Type	2.6 ± 0.4 (3)	6.9 ± 0.4 (3)
C24A	1.2 ± 0.3 (3) [a]	5.0 ± 0.4 (3) [a]
C68A	0.7 ± 0.3 (4) [a]	0.4 ± 0.1 (4) [c]
C107A	N.D. (3)	N.D. (3)
C184A	N.D. (3)	N.D. (3)
C212A	2.1 ± 0.7 (3)	1.6 ± 0.5 (3) [b]
C224A	1.3 ± 0.5 (3)	1.6 ± 0.7 (3) [a]
C236A	1.7 ± 0.6 (3)	2.4 ± 1.0 (3) [a]
C265A	2.0 ± 0.5 (3)	1.2 ± 0.1 (3) [b]
C270A	0.7 ± 0.1 (3) [a]	0.3 ± 0.1 (4) [c]
C291A	1.9 ± 0.6 (3)	1.2 ± 0.2 (3) [b]
C301A	0.6 ± 0.1 (3) [a]	0.3 ± 0.03 (3) [c]
C334A	1.3 ± 0.4 (3) [a]	1.6 ± 0.7 (3) [a]
C343A	2.0 ± 0.5 (3)	2.7 ± 1.3 (3) [a]

Table 2 – Summarized results from saturation binding isotherm experiments (mean ± SEM) collected for wild-type and mutant HAmEP3γ. [a] $P < 0.05$, [b] $P < 0.001$, and [c] $P < 0.0001$ by two-tailed t-test vs. wild-type. N.D. not detected.

Cell surface presentation of N-terminal HA-labeled C107A or C184A mouse EP3γ receptor was attenuated. To evaluate surface expression of nonfunctional mutant receptors, cell surface ELISAs were performed. The N-terminal HA-tag epitope of mutants C107A and C184A was detected at the cell surface by ELISA, although at significantly attenuated levels as compared to cells expressing HA-tagged wild-type receptor (Figure 4A). Given that a small amount of C107A and C184A receptor proteins could be detected at the cell surface, the ability of the cell surface receptors to bind radioligand was assessed in intact cells. Cell surface radioligand binding was

undetectable however, suggesting that the population of C107A and C184A receptors that were trafficked to the cell surface was unable to bind ligand (Figure 4B).
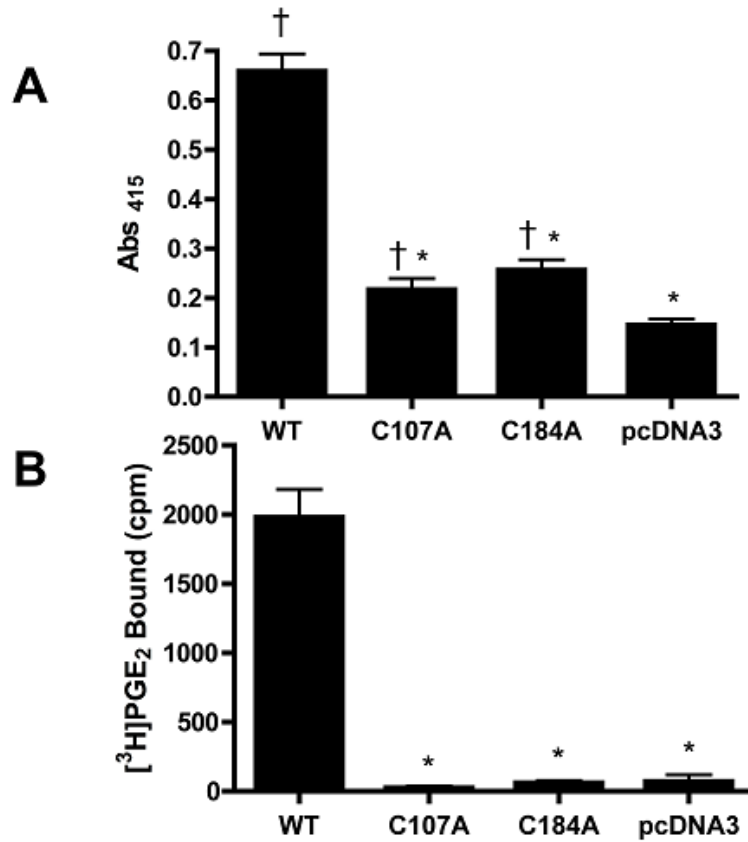
Figure 4 – Surface expression of wild-type and mutant HA-mEP3γ receptors. A) Cell Surface ELISA. Anti-HA detection of N-terminus receptor located in extracellular domain of cell detected by horseradish peroxidase activity and expressed as absorbance at 415 nm (mean ± SEM). Shown are representative data from three separate experiments conducted in triplicate. * $P < 0.001$ vs. WT, † $P < 0.05$ vs. pcDNA3. B) Intact cell radioligand binding. Binding of $[^3H]PGE_2$ to the surface of intact HEK293 cells expressing wild-type and mutant HA-mEP3γ receptors expressed as liquid scintillation counts per minute (mean ± SEM). Shown are representative data from three separate experiments conducted in triplicate. * $P < 0.001$.

Discussion

To facilitate structural studies of integral membrane proteins, our lab and others[243,263,264] have utilized mutant proteins lacking free cysteine residues; a protein lacking the free sulfhydryl groups of cysteine residues is less prone to irreversible aggregation and can be used for site-directed chemical modifications. In this study we characterized the phenotype of individual cysteine-to-alanine mutations of each cysteine residue in the mouse EP3γ receptor. We found that substitutions at 11 of the 13 cysteine residues in mEP3γ were well-tolerated with respect to receptor expression, ligand affinity, and signal transduction as assessed by radioligand binding and cell-based signal transduction assays.

Two cysteine residues at sites that correspond to an extracellular disulfide bond highly conserved among Class A GPCRs were required both for efficient cell surface expression and for the function of that population of the receptor that reaches the cell surface. If the disulfide bond is required and these cysteines do indeed compose a disulfide crosslink, loss of function and efficient trafficking should result from mutating either cysteine of the pair as was observed for C107 and C184 of mEP3γ. It is interesting to note that previous studies on the rabbit ortholog of the mouse EP3 receptor (EP3 77A) showed no dependency for the cysteine residue on the extracellular end of Helix 3 (corresponding to C184 in mEP3γ)[247]. The region of ECII distal to C184 is one of least conserved regions of the entire receptor between mouse and rabbit sequences; this may contribute in part to the interspecific functional differences in the EP3 receptor.

Data presented here show multiple defects in receptors having disulfide bonded cysteines mutated. Cell surface ELISA (Figure 4B) demonstrated that C107A and C184A mutant receptors trafficked to the cell surface in significantly reduced numbers. The highly conserved disulfide bond is likely required to achieve and maintain proper tertiary structure and stability of a GPCR[265]; misfolded receptors may be retained within the cell[266].

The reduced trafficking seen for the C107A and C184A mutant forms of mEP3γ may be due to much of the newly translated receptor failing to fold properly in the endoplasmic reticulum and being targeted for degradation by ER protein folding quality control. Based on experiments with model membrane proteins and cell biological characterization of ER quality control, it has been argued that most mutations that lead to targeting of nascent membrane proteins for degradation are mutations that result in thermodynamic destabilization of those proteins[267]. It is therefore probable the stability of C107A and C184A receptors is decreased with respect to wild-type.

While C107A and C184A mutants have trafficking defects, the remaining receptor that does traffic to the cell surface appears to be nonfunctional. These mutants have detectable cell surface expression as demonstrated by ELISA (Figure 4A); neither displayed detectable radioligand binding in assays of intact cells (Figure 4B) and isolated membranes (Figure 3). Similarly, neither mutant exhibited receptor activation in the CRE reporter assay (Figure 2). This phenotype is consistent with data from other investigators showing a role for GPCR disulfide bonds in ligand binding and receptor-effector coupling[268-270].

Intracellular cysteine residues of GPCRs may be targets of lipid modification. Cysteines in the intracellular C-terminal tail of GPCRs may be palmitoylated or, less frequently, isoprenylated. These lipid modifications can be required for receptor expression[254-256] and function[251,257,258]. However, if mEP3γ is lipid modified, the modification does not appear to be necessary for receptor expression or function. This has also been observed for other GPCRs including the α_{2A} adrenergic receptor (α_{2A}AR), which is palmitoylated, but mutation of the palmitoylation site does not affect ligand binding or effector coupling to α_{2A}AR[271], consistent with the idea that receptor palmitoylation is not required for receptor function.

In the transmembrane environment of the seven-helix bundle, cysteine side chains can participate in hydrogen bonding networks[272,273]. Hwa and colleagues reported deficits in expression of the human prostacyclin receptor when any of three conserved, transmembrane cysteines were mutated to alanines[269]. Similarly, we have found attenuated receptor expression, as evidenced by greater than ten-fold lower B_{max} than wild-type mEP3γ, for three transmembrane cysteines: C68, C270, and C301. Cysteines 68 and 301 are conserved across orthologs of EP3. Cysteine 270 is conserved across the entire superfamily of GPCRs[247]. While the variance in B_{max} may be an artifact of a transiently-transfected system, the reduction in expression of these mutant receptors while maintaining high affinity for [^{3}H]PGE$_2$ could suggest a role for these residues in maintaining the stability of the receptor, potentially by hydrogen bonding interactions. Further experiments are needed to evaluate this hypothesis.

In summary, we have shown through mutagenesis that 11 of 13 of cysteine residues present in mEP3γ are not required for receptor trafficking, ligand binding, or signal

transduction. One pair of cysteines that likely comprise a disulfide bond between ECI and ECII is required for proper function and cell surface expression of the receptor. While future experiments are required to confirm the precise nature of the defect caused by these mutations, these data begin to cast light on some of the structural characteristics of EP receptors.

CHAPTER III

DEVELOPMENT OF AN IN VIVO ACTIVE, DUAL EP1 AND EP3 SELECTIVE

ANTAGONIST BASED ON A NOVEL ACYL SULFONAMIDE BIOISOSTERE

Introduction

Hypertension and diabetes are the primary causes of 62 % of patients with End-Stage Renal Disease (ESRD) and 72 % of patients that develop ESRD each year[94], which requires life-long dialysis or kidney transplantation for survival. Elimination of PGE_2 production with COX inhibitors[46,48], like NSAIDs[109], is not a viable option as highlighted in a number of clinical trials. Recent studies in rodents and humans have suggested a role for the EP1 receptor in mediating at least part of the pathophysiology of DM[77,78,274] and hypertension[66,80,119,275]. EP1 has been prosecuted as a potential therapeutic target for chronic pain[158,276-279]. As such, small molecule, drug-like antagonists of EP1 have been developed. Human prostanoid receptor-targeting molecules are often nonselective[175], owing to the evolution of the EP family of GPCRs to recognize the same endogenous ligand, PGE_2. The molecular pharmacology of these compounds at mouse prostanoid receptors is less well known, often poorly selective, and not always comparable to human pharmacology[280]. In order to study these molecular targets more precisely, we developed EP1 antagonists selective for the mouse receptor to use in mouse models of hypertension and DM.

Materials and Methods

General medicinal chemistry procedures. Standard methods (thin layer chromatography and liquid chromatography-mass spectrometry) were used to monitor the progress of reactions. Products were purified by automated silica gel flash chromatography using the Teledyne Isco CombiFlash Rf system. Reactions performed in a microwave irradiated reactor utilized a Biotage Initiator-60 single mode microwave synthesizer. All nuclear magnetic resonance spectra (NMR) were proton resonance spectra (^{1}H NMR) at 400 megahertz (MHz) taken on a Bruker AMX NMR using deuterated chloroform ($CDCl_3$) as the solvent. Chemical shifts are reported as parts per million (ppm) δ downfield of the trimethylsilane internal standard. Positive ion electrospray ionization (ESI) mass spectra were obtained on an Agilent 1200 liquid chromatography mass spectrometry (LCMS) system with a Kinetex 2.1 x 50 mm C18 column running a gradient of 10 – 95 % (over 1 minute) acetonitrile and 0.1 % trifluoroacetic acid in water with evaporative light scattering detector (ELSD) and ultraviolet (UV) detection at 214 nm and 254 nm. Final products to be used in biological assays were purified by preparative high-performance liquid chromatography (HPLC) using a Gilson 215 preparative HPLC system and a Phenomenex 30 x 50 mm C8 column at room temperature, a gradient of 0.1 % aqueous TFA / acetonitrile = 50 / 50 to 0 / 100 over 5.0 min, a flow rate of 50.0 mL/min, and detection by UV at 220 nm.

*Ethyl 6-(hydroxymethyl)picolinate (**2**).* To a solution of diethyl dipicolinate **1** (5 g, 22.4 mmol) dissolved in ethanol (50 mL) was added sodium borohydride (0.5 g, 13.2 mmol). The mixture was stirred at room temperature for 6 hours. More sodium borohydride (160 mg, 4.2 mmol) was added and the mixture was stirred at room temperature overnight. The mixture was diluted in water (5 mL) and neutralized with glacial acetic acid (1 mL) and the mixture was stirred for 30 minutes. The mixture was extracted with dichloromethane. The organic layers were combined, washed with saturated sodium bicarbonate and water, dried, and evaporated. The product was purified by flash chromatography in ethyl acetate / hexane to yield **2** (1.91 g, 47 %).

*Ethyl 6-((5-chloro-2-hydroxyphenyl)(hydroxy)methyl)picolinate (**5**).* To a solution of **2** (500 mg, 2.76 mmol) in dichloromethane (2 mL) was added dimethylsulfoxide (DMSO; 0.4 mL, 5.5 mmol) and then triethylamine (Et$_3$N; 1.5 mL, 11 mmol) in a 5 mL Biotage microwave reactor vessel. Sulfur trioxide pyridine complex was added (Pyr·SO$_3$; 0.9 g, 5.5 mmol) and the vessel was sealed and heated to 120 °C in a microwave reactor for 15 minutes. When reactions had cooled they were neutralized with 2 M HCl (3 mL). The organic phase was washed with saturated sodium bicarbonate and water, dried, and evaporated. The crude aldehyde **4** was carried to the next step without further purification.

In a clean flask, a solution of *p*-chlorophenol (0.8 g, 6.2 mmol) in dichloromethane (5 mL) under argon was chilled in an ice water bath. A solution of 1 M ethylmagnesium bromide (EtMgBr; 5.5 mL) was added dropwise under argon. When the last of EtMgBr had been added, the solution was moved to room temperature and a solution of the crude

aldehyde in dichloromethane was added. The solution was stirred at room temperature for 2 hours. The reaction was slowly quenched by dropwise addition of 2 M HCl (3 mL) and saturated sodium bicarbonate (3 mL). The organic phase was washed with water and brine, dried, and evaporated. The product was isolated by flash chromatography in ethyl acetate / hexane to yield **5** (448 mg, 54 %) in two steps. MS (ESI, Pos.) m/z 308.2 $(M+H)^+$.

*Ethyl 6-(5-chloro-2-hydroxybenzyl)picolinate (**6**).* A mixture of the diarylmethanol **5** (400 mg, 1.3 mmol) and palladium on carbon (Pd/C; 10 wt% Pd, 40 mg) in ethyl acetate (5 mL) was added to a PAR Hydrogenator vessel. $ZnBr_2$ (10 mg) was added to the vessel followed by dropwise addition of concentrated H_2SO_4 (0.4 mL) and the vessel was purged with argon. The reaction was shaken under 1 atm H_2 overnight. The reaction was filtered through Celite, washed with brine and water, dried, and concentrated. The product was purified by flash chromatography in ethyl acetate / hexane to yield **6** (261 mg, 69 %).

*6-(5-chloro-2-((4-chloro-2-fluorobenzyl)oxy)benzyl)picolinic acid (**7**).* A mixture of the phenol **6** (200 mg, 0.69 mmol), K_2CO_3 (354 mg, 1.37 mmol), and 4-chloro-2-fluorobenzyl bromide (110 μL, 0.70 mmol) was prepared in ethanol (2 mL) in a 5 mL Biotage microwave reactor vessel. The reaction was heated to 120 °C in a microwave reactor for 15 minutes. NaOH (2 M, 10 mL) was added to the reaction and the mixture was refluxed for 1 hour. The reaction was diluted in water, extracted with dichloromethane, washed with brine and water, dried, and concentrated. The crude

74

product was diluted in toluene (5 mL) and water (1 mL). Glacial acetic acid (1 mL) was added dropwise and the reaction was heated to 60 °C and stirred overnight. The cooled organic phase was washed with brine and water, dried, and concentrated. The product was isolated by flash chromatography in ethyl acetate / hexane to yield **7** (192 mg, 68 %) in two steps. ^{1}H NMR (400 MHz, CDCl$_3$) δ 7.99 (d, 1H), 7.90 (d, 1H), 7.44 (m, 2H), 7.20 (m, 4H), 7.01 (d, 1H), 4.88 (s, 2H), 3.32 (s, 2H); MS (ESI, Pos.) m/z 406.0 (M+H)[+].

*6-(5-chloro-2-((4-chloro-2-fluorobenzyl)oxy)benzyl)-N-(cyclopropylmethyl)picolinamide (***8***).* To a solution of acid **7** (10.0 mg, 0.025 mmol), EDC·HCl (5.3 mg, 0.0275 mmol, 1.1 eq), HOBt (6.8 mg, 0.05 mmol, 2 eq), and *N*-methylmorpholine (3.0 μL, 0.0275 mmol, 1.1 eq) in DMF (1.5 mL) was added 1-cyclopropylmethanamine HCl (3.0 mg, 0.0275 mmol, 1.1 eq). The solution was stirred for 18 h at room temperature under argon. The reaction was diluted with water and extracted with EtOAc. The organic layer was washed with NaHCO$_3$, water, and brine, dried over MgSO$_4$, and concentrated in vacuo. The resultant residue was purified by preparative HPLC to yield **8** (1.2 mg, 9.8%). ^{1}H NMR (400 MHz, CDCl$_3$) δ 8.09 (s, 1H), 8.04 (d, 1H), 7.72 (t, 1H), 7.14 (m, 6H), 6.89 (d, 1H), 5.04 (s, 2H), 4.02 (s, 2H), 3.33 (t, 2H), 1.05 (m, 1H), 0.56 (m, 2H), 0.27 (m, 2H); MS (ESI, Pos.) m/z 459.2 (M+H)[+].

*(6-(5-chloro-2-((4-chloro-2-fluorobenzyl)oxy)benzyl)pyridin-2-yl)(pyrrolidin-1-yl)methanone (***9***).* The titled compound was synthesized in the same manner as described for **8** using pyrrolidine instead of cyclopropylmethanamine (1.5 mg, 12 %). ^{1}H NMR

(400 MHz, CDCl$_3$) δ 7.71 (t, 1H), 7.60 (d, 1H), 7.18 (m, 6H), 6.85 (d, 1H), 5.03 (s, 2H), 4.17 (s, 2H), 3.65 (d of t, 4H), 1.88 (d of sext, 4H); MS (ESI, Pos.) m/z 459.2 (M+H)[+].

*6-(5-chloro-2-((4-chloro-2-fluorobenzyl)oxy)benzyl)-N-cyclobutylpicolinamide (**10***). The titled compound was synthesized in the same manner as described for **8** using cyclobutylamine HCl instead of cyclopropylmethanamine (1.5 mg, 12 %). ^{1}H NMR (400 MHz, CDCl$_3$) δ 8.16 (s, 1H), 8.03 (d, 1H), 7.71 (t, 1H), 7.13 (m, 6H), 6.90 (d, 1H), 5.04 (s, 2H), 4.59 (sextuplet, 1H), 4.19 (s, 1H), 2.44 (m, 2H), 2.01 (quintuplet, 2H); MS (ESI, Pos.) m/z 459.2 (M+H)[+].

*6-(5-chloro-2-((4-chloro-2-fluorobenzyl)oxy)benzyl)-N-isobutylpicolinamide (**11***). The titled compound was synthesized in the same manner as described for **8** using isobutylamine instead of cyclopropylmethanamine (1.8 mg, 15 %). ^{1}H NMR (400 MHz, CDCl$_3$) δ 8.10 (s, 1H), 8.04 (d, 1H), 7.72 (t, 1H), 7.19 (m, 6H), 6.88 (d, 1H), 5.03 (s, 2H), 4.17 (s, 2H), 3.29 (t, 2H), 1.88 (m, 1H), 0.97 (d, 6H); MS (ESI, Pos.) m/z 461.2 (M+H)[+].

*N-(sec-butyl)-6-(5-chloro-2-((4-chloro-2-fluorobenzyl)oxy)benzyl)picolinamide (**12***). The titled compound was synthesized in the same manner as described for **8** using sec-butylamine instead of cyclopropylmethanamine (2.1 mg, 17 %). ^{1}H NMR (400 MHz, CDCl$_3$) δ 8.04 (m, 2H), 7.75 (t, 1H), 7.15 (m, 6H), 6.90 (d, 1H), 5.03 (s, 2H), 4.18 (s, 2H), 4.09 (m, 1H), 1.59 (m, 2H), 1.25 (d, 3H), 0.95 (t, 3H); MS (ESI, Pos.) m/z 461.2 (M+H)[+].

76

*N-(tert-butyl)-6-(5-chloro-2-((4-chloro-2-fluorobenzyl)oxy)benzyl)picolinamide (**13**).* The titled compound was synthesized in the same manner as described for **8** using t-butylamine instead of cyclopropylmethanamine (1.7 mg, 14 %). ^{1}H NMR (400 MHz, CDCl$_3$) δ 8.02 (m, 2H), 7.72 (t, 1H), 7.15 (m, 6H), 6.89 (d, 1H), 5.04 (s, 2H), 4.17 (s, 2H), 1.48 (s, 9H); MS (ESI, Pos.) m/z 461.2 (M+H)$^+$.

*6-(5-chloro-2-((4-chloro-2-fluorobenzyl)oxy)benzyl)-N,N-diethylpicolinamide (**14**).* The titled compound was synthesized in the same manner as described for **8** using diethylamine instead of cyclopropylmethanamine (2.0 mg, 16 %). ^{1}H NMR (400 MHz, CDCl$_3$) δ 7.71 (t, 1H), 7.47 (d, 1H), 7.18 (m, 6H), 6.87 (d, 1H), 5.05 (s, 2H), 4.20 (s, 2H), 3.57 (quadruplet, 2H), 3.28 (quintuplet, 2H), 1.29 (t, 3H), 1.09 (t, 3H); MS (ESI, Pos.) m/z 461.2 (M+H)$^+$.

*N-(bicyclo[2.2.1]heptan-2-yl)-6-(5-chloro-2-((4-chloro-2-fluorobenzyl)oxy)benzyl)picolinamide (**15**).* The titled compound was synthesized in the same manner as described for **8** using 2-aminonorborane HCl instead of cyclopropylmethanamine (1.3 mg, 10 %). ^{1}H NMR (400 MHz, CDCl$_3$) δ 8.10 (s, 1H), 8.02 (d, 1H), 7.73 (t, 1H), 7.10 (m, 5H), 6.88 (d, 1H), 5.02 (s, 2H), 4.29 (m, 1H), 4.18 (s, 2H), 2.49 (s, 1H), 2.28 (s, 1H), 2.15 (m, 1H), 1.59 (m, 7H), 0.82 (d, 1H); MS (ESI, Pos.) m/z 499.2 (M+H)$^+$.

*6-(5-chloro-2-((4-chloro-2-fluorobenzyl)oxy)benzyl)picolinamide (**16**).* The titled compound was synthesized in the same manner as described for **8** using ammonia (2.0 M

in ethanol) instead of cyclopropylmethanamine (1.3 mg, 10 %). ^{1}H NMR (400 MHz, CDCl$_3$) δ 8.06 (d, 1H), 7.82 (broad s, 1H), 7.73 (t, 1H), 7.17 (m, 6H), 6.83 (d, 1H), 5.62 (broad s, 1H), 5.03 (s, 2H), 4.17 (s, 2H); MS (ESI, Pos.) m/z 404.9 (M+H)$^+$.

*6-(5-chloro-2-((4-chloro-2-fluorobenzyl)oxy)benzyl)-N-((4-chlorophenyl)sulfonyl)picolinamide (**17**).* To a solution of 28 % aqueous NH$_4$OH (1.0 mL) was added *p*-chlorophenylsulfonyl chloride (10.5 mg, 0.05 mmol, 2 eq) dropwise in CHCl$_3$ (1.0 mL). The solution was stirred for 2 h at room temperature. Solution was diluted with water (5.0 mL) and extracted with DCM (5.0 mL). The organic layer was washed with water and brine, dried under argon, and used in the following reaction without further purification. To a solution of acid **7** (10.0 mg, 0.025 mmol), HATU (13.3 mg, 0.035 mmol, 1.4 eq), and DIPEA (13.1 μL, 0.075 mmol, 3 eq) in DMF (1.0 mL) was added *p*-chlorophenylsulfonamide dropwise in DMF (0.5 mL). Reactions were stirred for 24 hours at room temperature. Reactions were diluted in water and extracted with ethyl acetate. Combined organic layers were washed with brine and water, dried, and concentrated. Crude product was purified by preparative HPLC to yield **17** (1.6 mg, 11 %). ^{1}H NMR (400 MHz, CDCl$_3$) δ 8.12 (d, 2H), 7.98 (d, 1H), 7.74 (t, 1H), 7.55 (d, 2H), 7.17 (m, 6H), 6.94 (d, 1H), 5.07 (s, 2H), 4.18 (s, 1H); MS (ESI, Pos.) m/z 578.7 (M+H)$^+$.

*6-(5-chloro-2-((4-chloro-2-fluorobenzyl)oxy)benzyl)-N-((2,5-dichlorophenyl)sulfonyl)picolinamide (**18**).* The titled compound was synthesized in the same manner as described for **17** using 2,5-dichlorobenzene-sulfonyl chloride instead of *p*-chlorophenylsulfonyl chloride. Yield 2.9 mg, 19 % in two steps. ^{1}H NMR (400 MHz,

CDCl$_3$) δ 8.37 (d, 1H), 7.92 (d, 1H), 7.75 (t, 1H), 7.52 (d of d, 1H), 7.38 (d, 1H), 7.35 (d, 1H), 7.15 (m, 5H), 6.93 (d, 1H), 5.08 (d, 2H), 4.20 (d, 2H); MS (ESI, Pos.) m/z 612.7 (M+H)$^+$.

*6-(5-chloro-2-((4-chloro-2-fluorobenzyl)oxy)benzyl)-N-tosylpicolinamide (*19*).* The titled compound was synthesized in the same manner as described for **17** using tosyl chloride instead of *p*-chlorophenylsulfonyl chloride. Yield 1.3 mg, 9 % in two steps. ^{1}H NMR (400 MHz, CDCl$_3$) δ 8.06 (d, 2H), 7.94 (d, 1H), 7.72 (t, 1H), 7.37 (d, 2H), 7.15 (m, 6H), 6.93 (d, 1H), 5.07 (s, 2H), 4.18 (s, 2H), 2.45 (s, 3H); MS (ESI, Pos.) m/z 558.8 (M+H)$^+$.

*6-(5-chloro-2-((4-chloro-2-fluorobenzyl)oxy)benzyl)-N-(propylsulfonyl)picolinamide (*20*).* The titled compound was synthesized in the same manner as described for **17** using *n*-propylsulfonyl chloride instead of *p*-chlorophenylsulfonyl chloride. Yield 1.1 mg, 9 % in two steps. ^{1}H NMR (400 MHz, CDCl$_3$) δ 7.67 (t, 1H), 7.33 (d, 1H), 7.15 (m, 6H), 6.86 (d, 1H), 5.07 (s, 2H), 4.19 (s, 2H), 3.61 (d of penta, 2H), 1.57 (d, 2H), 1.12 (d, 3H); MS (ESI, Pos.) m/z 510.9 (M+H)$^+$.

*6-(5-chloro-2-((4-chloro-2-fluorobenzyl)oxy)benzyl)-N-((3,4-dichlorophenyl)sulfonyl)picolinamide (*21*).* The titled compound was synthesized in the same manner as described for **17** using 3,4-dichlorophenylsulfonyl chloride instead of *p*-chlorophenylsulfonyl chloride. Yield 2.1 mg, 14 % in two steps. ^{1}H NMR (400 MHz, CDCl$_3$) δ 8.26 (d, 1H) 8.03 (d, 1H), 7.94 (d, 1H), 7.75 (t, 1H), 7.66 (d, 2H), 7.15 (m, 5H), 6.94 (d, 1H), 5.07 (s, 2H), 4.19 (s, 2H); MS (ESI, Pos.) m/z 612.6 (M+H)$^+$.

Cell Culture. HEK293 cells were maintained at 37 ˚C / 5% CO_2 in DMEM supplemented with 10 % FBS, 2 mM L-glutamine, 100 units/mL penicillin, and 100 µg/mL streptomycin. CHOk1 cells were maintained at 37 ˚C / 5% CO_2 in F12k supplemented with 10 % FBS, 100 units/mL penicillin, and 100 µg/mL streptomycin. For cell membrane / receptor preparations, HEK293 cells were transfected with 6 µg receptor cDNA plasmid using Lipofectamine 2000 in DMEM lacking penicillin and streptomycin. Six hours after adding DNA-Lipofectamine 2000 complexes, media was replaced with complete DMEM containing 20 µM indomethacin and 5 mM sodium butyrate. Cells were allowed to recover for 18 to 24 hours before being plated in three to five 100 mm cell culture dishes for membrane harvest. Cells were incubated for an additional 24 to 48 hours, until confluence was reached.

Competition Radioligand Binding. Total cell membranes from HEK293 transfectants described above were prepared as described[262]. Membranes (5 - 10 µg) were incubated with [^{3}H]PGE$_2$ (5 nM for EP2, 2 nM for EP3 and EP4) and a range of unlabeled test compound (1 nM – 10 µM) in 200 µL of binding buffer (25 mM potassium phosphate, 1 mM EDTA, and 10 mM $MgCl_2$, pH 6.2) for 1 hour at 30 ˚C. PGE$_2$ (10 µM) was used as a positive control for receptor binding. Binding reactions were terminated and radioactivity was quantified as previously described[262].

Calcium mobilization assay. CHOk1 cells stably expressing N-terminal HA-tagged mouse EP1 receptor or HEK293 cells stably expressing N-terminal HA-tagged mouse

thromboxane receptor were plated (6 x 10^5 cells / well) in clear-bottom, black-wall 96-well plates in 100 µL complete cell culture media containing 20 µM indomethacin 18 – 24 hours prior to experiment. On the day of the experiment, cell culture media was replaced with 50 µL calcium assay buffer (50 mM HEPES pH 7.4, 2.5 mM probenicid, 100 µM brilliant black, 20 µM indomethacin in Hanks Buffered Salt Solution (HBSS)) containing varying concentrations of test antagonist (1 nM – 100 µM). A 1:1 solution of fluo-4AM and 10 % pluronic acid F-127 was diluted in calcium assay buffer and 50 µL of this solution was added to each well of cells (2 µM final). The fluorophore was allowed 1 hour at 37 °C to load into the cells. Solutions of agonist (17PTPGE$_2$ for mEP1 and U46619 for mTP) were prepared at 2X in calcium assay buffer and aliquoted in V-bottom, 96-well FLEXstation compound plates. Raw fluorescence (rfu)-time curves were collected using the following settings on a FLEXstation in FLEX mode: excitation 494 nm, emission 516 nm, cut off 495 nm, sensitivity 6, addition speed 1. Baseline corrected areas under the curve (AUCs) were calculated for each trace and plotted in the style of Schild[281].

Mouse liver intrinsic clearance assay. The intrinsic clearance (CL$_{int}$) of test compound was studied in mouse hepatic microsomes using substrate depletion methodology, reported as % parent compound remaining. In separate 96-well plates for each time point, triplicate mixtures of 0.1 M potassium phosphate buffer, pH 7.4, 1 µM test compound, 0.5 mg/mL male CD-1 mouse liver microsomes, and 1 mM NADPH (for time points 3, 7, 15, 25, and 45 minutes) or buffer (for 0 min time point) were incubated at 37 °C. At each time point, a plate was quenched by precipitation with 2 volumes of ice-cold solution of

50 ng/mL glyburide internal standard in acetonitrile. The plate was centrifuged at 3000 rpm at 4 °C for 10 minutes. Supernatants were transferred into new 96-well plates and diluted 1:1 with water. Amount of remaining test compound in each sample was determined by HPLC/MS/MS analysis of diluted supernatants. Percent remaining parent compound was calculated by the ratio of amount of test compound at time t to the amount of test compound at time $t = 0$ minutes. In vitro half-life ($t_{1/2}$) is calculated by nonlinear regression of the % Remaining-time data. Calculated CL_{int} (Figure 1) and predicted hepatic clearance (CL_H, Figure 2) were calculated by the following equations:

$$CL_{int} \ (mL \cdot min^{-1} \cdot kg^{-1})$$

$$= \frac{\ln 2}{t_{1/2}} \times \frac{1 \ mL}{0.5 \ mg \ microsome} \times \frac{45 \ mg \ microsome}{1 \ g \ liver} \times \frac{87.5 \ g \ liver}{kg \ mouse}$$

Figure 1 – Formula to calculate an estimate of CL_{int} from $t_{1/2}$ of test compound from in vitro microsomal clearance assays.

$$CL_H \ (mL \cdot min^{-1} \cdot kg^{-1}) = \frac{Q_H \times CL_{int}}{Q_H + CL_{int}}$$

Figure 2 – Formula to calculate a prediction of in vivo CL_H from CL_{int} where Q_H is hepatic blood flow, 90 mL·min⁻¹·kg⁻¹ for a mouse.

In vitro metabolite identification. Solutions of test compound (40 µM), NADPH (2 mM), glutathione (GSH; 2 mM), UDP-glucuronic acid (UDPGA; 2 mM), phosphoadenosine-phosphosulfate (PAPS; 100 µM), MgCl$_2$ (3 mM), and hepatic S9 protein or hepatic microsomal protein (1 mg/mL for microsomes, 5 mg/mL for S9 fractions) in potassium

phosphate buffer (pH 7.4, 0.1 M) were incubated for 1 hour at 37 °C. Reactions to monitor microsome-mediated metabolism only were assembled by replacing GSH/UDPGA/PAPS with more buffer. Reactions to control for metabolism not due to Phase I or Phase II enzymes were assembled by replacing GSH/UDPGA/PAPS and NADPH with more buffer. After 1 hour, reactions were quenched by precipitation with 1 mL of ice-cold acetonitrile. Samples were centrifuged at 3700 rpm at 4 °C for 10 minutes. Samples were incubated on ice for 5 minutes until organic-aqueous phase interface was apparent. An aliquot of the organic phase (750 µL) was transferred to a clean tube, dried at 30 °C under nitrogen, and reconstituted in 85:15 water:acetonitrile (125 µL). A "neat" sample of the test compound was prepared by making a 20 µM solution of compound in 85:15 water:acetonitrile. Samples were analyzed by HPLC/MS.

Plasma protein binding. Protein binding of test compounds to mouse plasma proteins was determined by equilibrium dialysis using single-use RED plates (ThermoFisher Scientific). Triplicate mixtures of mouse plasma (220 µL) and test compound (5 µL, 5 µM final) were prepared in 96-well plates and mixed thoroughly. An aliquot of the plasma-test compound mixture (200 µL) was transferred to one chamber and phosphate buffer (350 µL; 25 mM, pH 7.4) was added to the other chamber. The plate was sealed and incubated with shaking for 4 hours at 37 °C. Aliquots (50 µL) from each chamber were diluted 1:1 with either plasma (for aliquots from the plasma-test compound chamber) or buffer (for aliquots from the phosphate buffer chamber) and transferred to a clean 96-well plate. Analyte was extracted by addition of an ice-cold solution of the internal standard carbamazepine (50 ng/mL) in acetonitrile (100 µL) and the plate was

centrifuged at 4 °C at 3000 rpm for 10 minutes. Supernatants were diluted 1:1 with water and analyzed for amount of test compound remaining bound to plasma by HPLC/MS/MS. Data are reported as the fraction unbound (F_u), calculated as ratio of the concentration of test compound in the buffer chamber to the concentration of test compound in the plasma chamber.

In vivo pharmacokinetics. For EP1A: Sixteen week old male C57B/6J mice, weighing in excess of 30 g, were administered either 1 mg/kg EP1A in 1:1 PEG400:saline (50 µL) intravenously (IV) via tail vein injection or 10 mg/kg EP1A in 1:1 PEG400:saline (100 µL) by mouth (PO) via gavage at time $t = 0$. At time points out to 4 hours (5 min, 15 min, 1, 2, and 4 hours for IV administration; 0.25, 1, 2, and 4 hours for PO administration) serial collections of venous blood (60 µL) by saphenous venesection into EDTA-fortified Microvette capillary tubes were made. Plasma at terminal time points (at 6 hours for IV administration; at 7 hours for PO administration) was similarly isolated from blood collected by cardiac puncture of euthanized mice.

For 1-J: Sixteen week old male C57B/6J mice, weighing in excess of 30 g, were administered either 1 mg/kg 1-J in 1:1 PEG400:saline (50 µL) IV via tail vein injection or 5 mg/kg 1-J in 1:1 PEG400:saline (100 µL) subcutaneously (SC) by intrascapular injection at time $t = 0$. At several time points (5 min, 15 min, 1, 2, and 4 hours for IV administration; 0.25, 0.5, 1, 2, 4, and 8 hours for SC administration) serial collections of venous blood (60 µL) by saphenous venesection into EDTA-fortified Microvette capillary tubes were made. Plasma at terminal time points (at 6 hours for IV

administration; at 24 hours for SC administration) was similarly isolated from blood collected by cardiac puncture of euthanized mice.

Plasma was isolated by centrifugation at room temperature at 5000 rpm for 15 minutes. Plasma was stored at -80 °C until HPLC/MS/MS analysis. Analyte was extracted by precipitation with an ice-cold solution of internal standard in acetonitrile. Mixtures were centrifuged at 3700 rpm at 4 °C for 10 minutes. Samples were incubated on ice for 5 minutes until organic-aqueous phase interface was apparent. An aliquot of the organic phase (750 μL) was transferred to a clean tube, dried at 30 °C under nitrogen, and reconstituted in 85:15 water:acetonitrile (125 μL). Samples were analyzed by HPLC/MS/MS. Test compound plasma concentrations were calculated by comparing the ratio of analyte mass spectrometer response AUC to internal standard mass spectrometer response AUC to a calibration curve of known analyte concentration analyte AUC:standard AUC values.

HPLC/MS and HPLC/MS/MS analysis. For samples collected from intrinsic clearance, plasma protein binding, and in vivo pharmacokinetics experiments, samples were analyzed on a Thermo Electron TSQ Quantum Ultra triple quadrapole mass spectrometer via ESI with two Thermo Electron Accella pumps and a Leap Technologies CTC PAL autosampler. Analytes were separated by gradient elution on a dual column system with two Thermo Hypersil Gold (2.1 x 30 mm, 1.9 μm) columns held at 40 °C. HPLC mobile phase A was 0.1 % formic acid in water and mobile phase B was 0.1 % formic acid in acetonitrile. The gradient started at 10 % B with a 0.2 minute hold; was linearly increased to 95 % B over 0.8 minutes; was held at 95 % B for 0.2 minutes; and returned to 10 % B

over 0.1 minutes. The total gradient run time was 1.3 minutes and the HPLC flow rate was 0.8 mL/min. While pump 1 ran the gradient method, pump 2 equilibrated the alternate column isocratically at 10 % B. Compound optimization, data collection, and processing were performed using Thermo Electron QuickScan software (version 2.3) and Xcalibur (version 2.0.7 SP1).

For samples collected for metabolite identification, an Agilent 1100 HPLC system coupled to a Supelco Discovery C18 column (5 μm, 2.1 x 150 mm) was employed. HPLC mobile phase A was aqueous ammonium formate (pH 4.1, 10 mM) and mobile phase B was acetonitrile. The initial mobile phase was 15 % B and by a linear gradient was transitioned to 80 % B over 20 minutes. The HPLC flow rate was 0.4 mL/min. The HPLC eluate was first passed through an Agilent 1100 diode-array UV detector (single wavelength mode at 254 nm) followed by ESI-assisted introduction into a Finnigan LCQ Deca XPPLUS ion trap mass spectrometer operated in either the positive or the negative ionization mode. Ionization was assisted with sheath and auxiliary gas (ultra-pure nitrogen) set a 60 and 40 psi, respectively. The electrospray voltage was set at 5 kV with the heated ion transfer capillary set at 300 °C and 30 V. Relative collision energies of 25 − 35 % were used when the ion trap mass spectrometer was operated in MS/MS or MSn mode.

Intracarotid blood pressure measurement. Fourteen to seventeen week old male C57B/6J mice were weighed and anesthetized with 120 mg/kg ketamine and 12 mg/kg xylazine and maintained on a 37 °C heating pad throughout the remainder of the experiment. Carotid artery and jugular vein cannulation was performed as previously described[282].

The right jugular vein was accessed by making a 1 cm vertical incision approximately 5 mm from the midline with the caudal end of the incision terminating about 1 mm caudal to the rostral edge of the pectoral muscle. The rostral end of the right jugular vein was ligated with a $6 - 7$ cm piece of wax-coated 4-0 braided silk suture (Syneture SOFSILK, #S-183). A second $6 - 7$ cm piece of suture was placed behind the caudal end of the jugular vein, untied, with the ends pulled taut caudally to prevent backflow of blood from the right atrium. A small incision was made in the ventral side of the vein and 1.1 cm of a Silastic tubing (0.012" internal diameter, Dow Corning #508-001) with a beveled end was advanced caudally into the vein, over the caudal suture, angled slightly toward the right atrium. The caudal suture was tightened over the vein, sealing catheter flow into the vein. Approximately 5 cm of tubing remains outside of the vein and is attached to a saline-filled syringe with a blunt-end 23 gauge needle. About 50 μL of saline was injected into the vein to ensure patency.

A catheter for the artery was prepared as follows. A 5 cm section of PE-10 tubing (polyethylene tubing, 0.011" internal diameter, Becton Dickinson #427400) was slowly stretched to a length of $8 - 9$ cm. A $2 - 3$ mm section of this tubing was fed into a 6 cm piece of Silastic tubing. The other end of the PE-10 tubing was cut with a bevel 9 mm from the Silastic junction.

A 1 cm vertical incision was made with the caudal end terminating about 5 mm rostral from the sternum. The sternomastoid muscle was exposed by blunt dissection of tissue with forceps. The muscle was held aside while the left common carotid artery was isolated and cleaned of connective tissue. Two $6 - 7$ cm sections and one 10 cm section of suture were placed behind the artery. The 10 cm section was used to ligate the rostral

end of the artery and taped down next to the head so as to gently pull the artery taut. One 6 – 7 cm section of suture was used to ligate the caudal end of the artery and the other was tied in a loose knot and temporarily placed on the caudal end of the isolated section of artery. A small incision was made on the ventral face of rostral end of the artery and the lumen of the vessel and cavity were flushed with saline. The catheter was advanced into the artery to the caudal knot. The loose section of suture was tightened over the artery and catheter about 2 mm caudal to the incision in the vessel. The caudal-most knot was untied and the catheter was advanced to the Silastic junction. The caudal-most suture was retied over the vessel and catheter. The rostral most suture was tied over the Silastic portion of the suture to stabilize the apparatus in place. The other end of the Silastic was attached to a syringe filled with 10 % heparin (100 U/mL total) by a blunt-tipped needle and 150 µL of heparin was injected into the artery. The arterial catheter was clamped while being attached to a TXD-310 pressure transducer. Systolic, mean, and diastolic blood pressures as well as heart rate were determined by a Digi-Med Blood Pressure Analyzer 400 (BPA400) operated by a personal computer running DMSI-200 control software. Saline solutions of test compounds (10 µL) were infused through the jugular catheter about 2 hours after subcutaneous injection of 5 mg/kg 1-J in 1:1 PEG400:saline. MAP was recorded over time and the changes in MAP (ΔMAP) in response to vasoactive substances (sulprostone, 17PTPGE$_2$, and phenylephrine) were reported as an average of at least three independent experiments on three different mice.

Animal care and use. All experiments were conducted in accordance with the National Institutes of Health regulations for animal care covered in Principles of Laboratory

Animal Care (National Institutes of Health publication 85-23, revised 1985) and were approved by the Institutional Animal Care and Use Committee.

<center>Results</center>

Synthesis and characterization of the lead acid EP1 antagonist **7**. To develop antagonists selective for the mouse EP1 receptor, we started with compound **7** (Figure 3), synthesized as previously described (Figure 4)[168]. Diethyl dipicolinic acid (**1**) was reduced with $NaBH_4$ to **2**. Parikh-Doering oxidation of **2** with sulfur trioxide-pyridine complex and DMSO produced the unstable aldehyde **3**. 4-chlorophenoxide was then reacted with **3**, followed by neutralization with HCl to form **4**. Reduction of the secondary alcohol of **4** under H_2 and Pd/C with the addition of H_2SO_4 and $ZnBr_2$ gave **5**. Alkylation of **5** with 2-fluoro-4-chlorobenzyl bromide and cleavage of the ester by refluxing with NaOH produced the sodium salt (**6**) of the lead (**7**) which was formed by protonation of **6**. The lead compound was reported to have good affinity for the human EP1 receptor and was stable in microsomes and S9 fractions of several species. However, **7** was previously reported to have a high-affinity interaction with human TP[168]. We evaluated the molecular pharmacology of **7** at the mouse EP receptors as well as the mouse TP receptor.

<center>89</center>
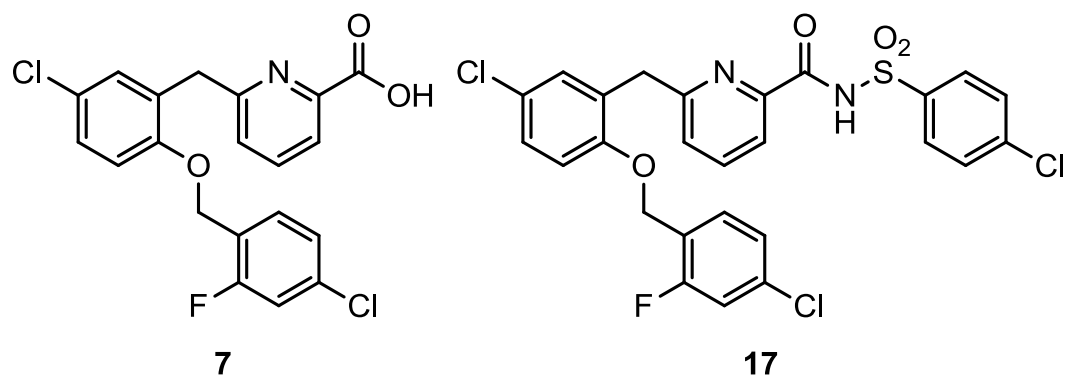
Figure 3 - Lead picolinic acid-based human EP1 antagonist **7**, and 4-chloro-*N*-acylsulfonamide analog **17**
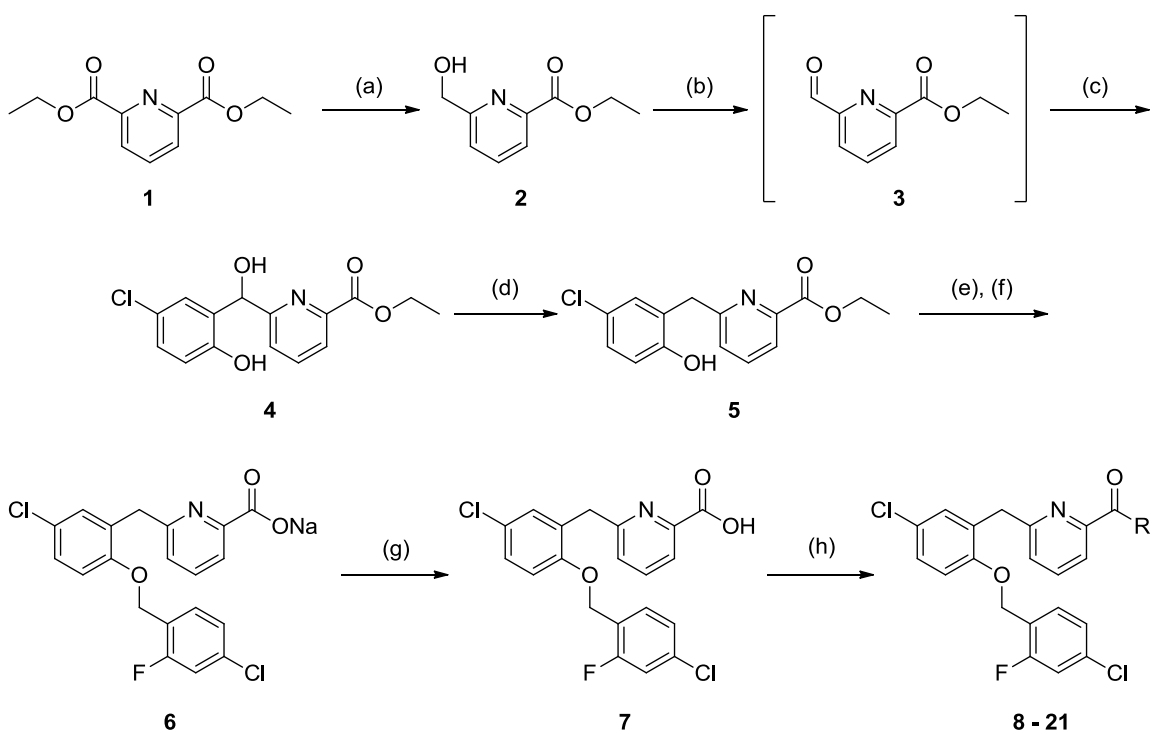
Figure 4 – Synthetic route for lead antagonist **7** and its analogues **8-21**. Reagents: (a) NaBH$_4$, EtOH (47%); (b) Pyr·SO$_3$, DMSO, DCM, (c) 4-chlorophenol, EtMgBr, DCM (54%); (d) H$_2$, Pd/C, H$_2$SO$_4$, ZnBr$_2$, EtOAc (69%); (e) 2-fluoro-4-chlorobenzyl bromide, K$_2$CO$_3$, EtOH, (f) NaOH, reflux, (g) HOAc, PhMe (68%); (h) RNH$_2$, R$_2$NH, or RSO$_2$NH$_2$, EDC·HCl, HOBt, DIPEA, DMF (10% – 20%)

Compound **7** was confirmed to be a functional antagonist of mEP1 in vitro and to have submicromolar affinity for the mouse EP1 receptor by Schild Analysis (Figure 5). **7** had no detectable affinity for mouse EP3 or EP4 receptors by radioligand binding assays. **7** had poor, but detectable affinity at mouse EP2, and suppressed signaling through mouse TP receptor at concentrations 100-fold higher than at the human receptor (Table 1), confirming a weak off-target activity of **7** at mouse TP.

Table 1 - Molecular pharmacology of **7** at mouse EP and TP receptors

mEP1 $pK_D{}^a$	mEP1 K_D (nM)	mEP2 $pK_I{}^b$	mEP3 $pK_I{}^b$	mEP4 $pK_I{}^b$	mTP $pIC_{50}{}^b$
7.32 ± 0.08	47.9	5.76 ± 0.21	<6	<6	6.04 ± 0.18

[a]Value represents mean $\pm$ SEM of at least two independent experiments measured in duplicate.

[b]Values represent mean $\pm$ SEM of at least three independent experiments measured in triplicate.
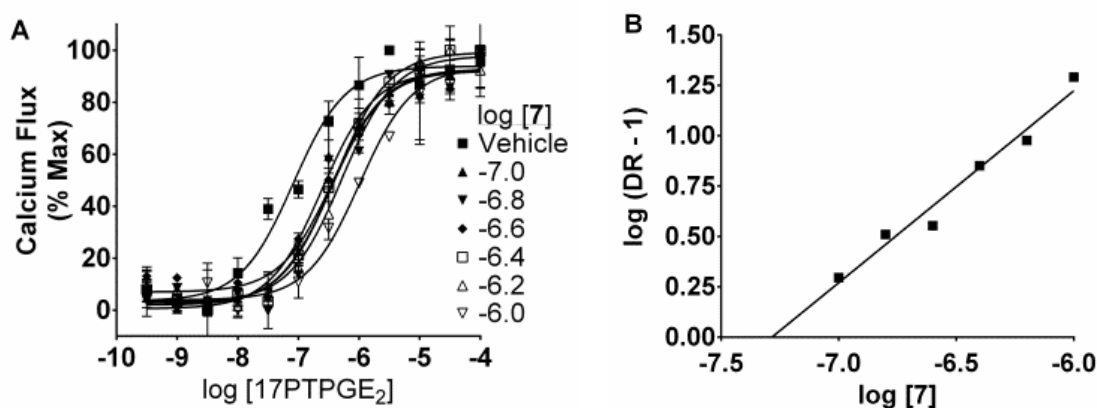
Figure 5 - Concentration response curves (A) and transformed Schild regression (B) for mEP1-expressing CHOk1 cells treated with six concentrations of **7** before being challenged with a range of concentrations of 17PTPGE$_2$ (m = 0.953 $\pm$ 0.085, pK_D = 7.283, r^2 = 0.9689)

Results from in vivo pharmacokinetics experiments (Table 2) revealed compound **7** to possess a moderate systemic plasma clearance (CL_p) and volume of distribution predicted at steady-state (V_{ss}), subsequently displaying a short half-life (> 60 min) in mice receiving a parenteral administration of the EP1 receptor antagonist. We observed a bioavailability (%F) of approximately 14 % following the oral administration (10 mg/kg) of **7** to mice.

Table 2 - Pharmacokinetic parameters for compound **7** following IV (1 mg/kg) or PO (10 mg/kg) dosing

$t_{1/2}$ (min)	CL_p (mL/min/kg)	V_{ss} (L/kg)	F (%)
65 ± 8.2	59.2 ± 6.4	0.90 ± 0.1	13.8 ± 2.1

Synthesis and characterization of bioisosteres of **7**. Recently, Ostenfeld *et al.* have shown that in rats **7** is cleared primarily by glucuronidation and sequestration into the bile[283]. With the goal of inhibiting glucuronidation while improving molecular pharmacology of **7**, a series of carboxylic acid bioisosteres of **7** were pursued. *N*-acylsulfonamides are common carboxylic acid bioisosteres that have been successfully implemented in antagonists of angiotensin II AT1 receptors[284] as well as EP3 receptors[285]. A series of analogues (**8** - **21**) resulting from the amidation of **7** was prepared (Table 3). Each was synthesized by coupling **7** to a series of primary and secondary amines (**8** - **16**) and sulfonamides (**17** – **21**) employing common activators such as EDC·HCl, HOBt, HATU, and DIPEA in DMF (Figure 4).

Table 3 - Molecular pharmacology of amide and acylsulfonamide analogues of **7** at mouse EP and TP receptors

8 - 21
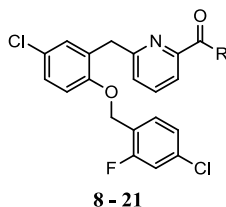
Cmpd	R	mEP1 pK$_D$[a]	mEP1 K$_D$ (nM)	mEP2 pK$_I$[b]	mEP3 pK$_I$[b]	mEP4 pK$_I$[b]	mTP pIC$_{50}$[b]
8	—NH—(cyclopropyl)	6.26 ± 0.02	549	<6	<6	<6	<6
9	—N(pyrrolidine)	4.80 ± 0.05	15800	<6	<6	<6	<6
10	—NH—(cyclobutyl)	6.04 ± 0.06	912	<6	<6	<6	<6
11	—NH—CH(CH$_3$)CH$_2$CH$_3$	6.52 ± 0.36	302	<6	6.67 ± 0.03	<6	<6
12	—NH—CH$_2$CH$_2$CH$_3$	5.86 ± 0.01	1380	<6	<6	<6	<6
13	—NH—C(CH$_3$)$_3$	5.36 ± 0.12	4360	<6	<6	<6	<6
14	—N(azetidine)	6.35 ± 0.34	447	<6	<6	<6	<6
15	—NH—(norbornyl)	5.66 ± 0.13	2190	<6	<6	<6	<6
16	NH$_2$	5.58 ± 0.30	2630	<6	<6	<6	<6
17	—NH—SO$_2$—(4-Cl-phenyl)	7.39 ± 0.39	40.7	<6	6.97 ± 0.22	<6	<6
18	—NH—SO$_2$—(2,5-diCl-phenyl)	7.25 ± 0.32	53.7	<6	6.69 ± 0.13	<6	<6
19	—NH—SO$_2$—(4-methyl-phenyl)	6.67 ± 0.14	214	<6	<6	<6	<6
20	—HN—SO$_2$—CH$_2$CH$_2$CH$_3$	N.D.[c]	N.D.[c]	<6	<6	<6	<6
21	—NH—SO$_2$—(3,4-diCl-phenyl)	6.67 ± 0.16	214	<6	7.18 ± 0.05	<6	<6

[a]Values represent mean ± SEM of at least two independent experiments measured in duplicate.

The molecular pharmacology observed for **8** - **21** was determined at mEP1 - mEP4 and mTP (Table 3). Generally, *N*-acylsulfonamides retained mEP1 affinity higher than that for the amide series (Figure 6). Each analog displayed reduced affinity for mEP2 and mTP. Interestingly, four analogs (**11**, **17**, **18**, and **21**) displayed enhanced affinity for mEP3, a potential therapeutic target for hypertension- and DM-related ESRD. EP3 is of particular interest as it shares signaling pathways and endogenous ligands with EP1 and may represent a compensatory signaling pathway in the event of EP1 blockade[119,192,248,286,287]. These dual-selectivity compounds were confirmed to be functional antagonists of mEP3 by calcium mobilization assays in CHOk1 cells expressing mouse EP3γ receptor (Figure 7).
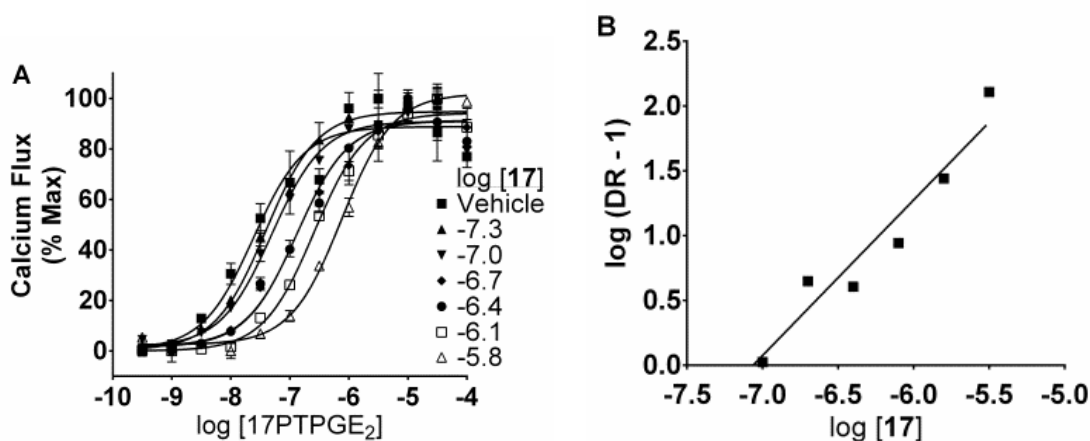
Figure 6 - Concentration response curves (A) and transformed Schild regression (B) for mEP1-expressing CHOk1 cells treated with six concentrations of **17** before being challenged with a range of concentrations of 17PTPGE$_2$ (m = 1.20 ± 0.12, pK$_D$ = 7.063, r^2 = 0.9487)
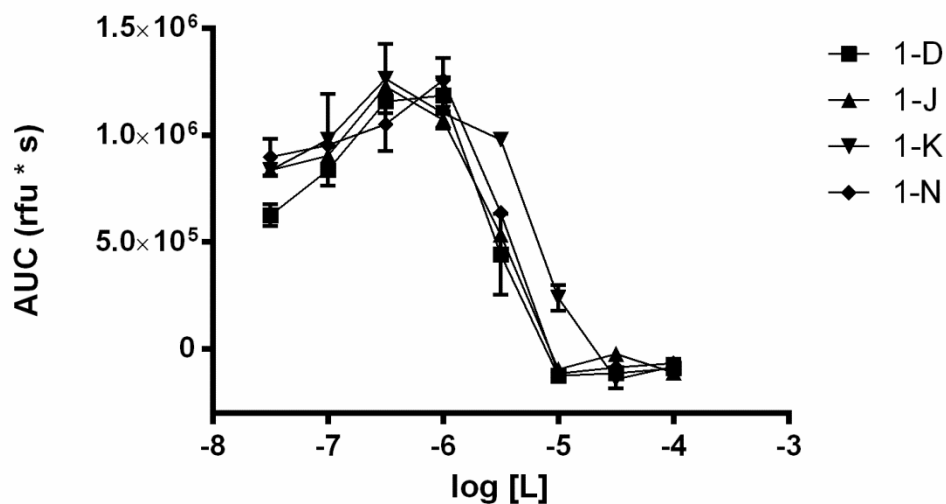
Figure 7 - Calcium mobilization concentration response curves for four EP1/EP3 dual selectivity antagonists challenged with 100 nM sulprostone in mEP3γ-expressing CHOk1 cells.

We subsequently determined Cl_{int} of several potent amide and *N*-acylsulfonamide analogs (Table 4). Results indicated an exceptional instability to metabolism in vitro, displaying estimated predicted CL_{HEP} values that approached the hepatic blood flow in mice (90 mL/min/kg).

Table 4 - Intrinsic clearance of amide and *N*-acylsulfonamide analogs of **7** by mouse liver microsomes

Cmpd	Cl_{int} (mL/min/kg)	CL_{HEP} (mL/min/kg)
7	84.7	43.6
8	11382	89.3
11	9806	89.2
14	7157	88.9
17	2260	86.6
19	5039	88.4
21	2994	87.4

Results from metabolite identification studies in hepatic subcellular fractions indicated extensive biotransformation of the amide **11** and the *N*-acylsulfonamide **17**, including NADPH-independent hydrolysis (i.e., esterases) and NADPH-dependent oxidation (i.e., P450) of these analogs. Figure 8 depicts the metabolism of **17**, including the hydrolysis of the sulfonamide (**M1**), and P450-mediated oxidation of the methylene linker (**M2**) and benzylic oxidation (**M3**). The extent of plasma protein binding in mouse was determined to be extensive for three compounds assessed (F_u: **7** = 0.005, **11** = 0.010, **17** = 0.004).
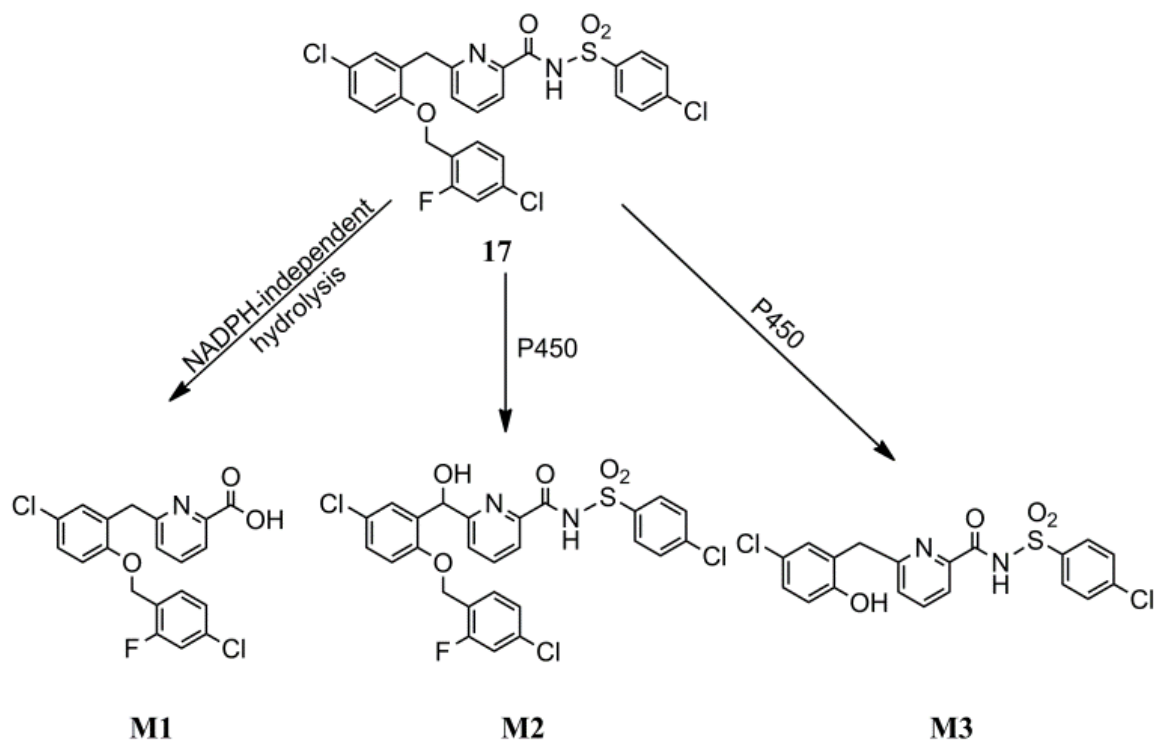
Figure 8 - Metabolism of **17** in hepatic subcellular fractions

Given the molecular pharmacology and in vitro metabolism data, we proceeded to evaluate the in vivo pharmacokinetics of **17**. Mice (n = 3) were subsequently administered a SC dose (5 mg/kg) with intermittent plasma collections to measure systemic levels of **17** (Figure 9). Compound **17** achieved a maximum plasma concentration (C_{max}) of 504 nM ($\pm$ 167) 2 hours (t_{max}) following subcutaneous administration and displayed an AUC of 7508 nM·h.
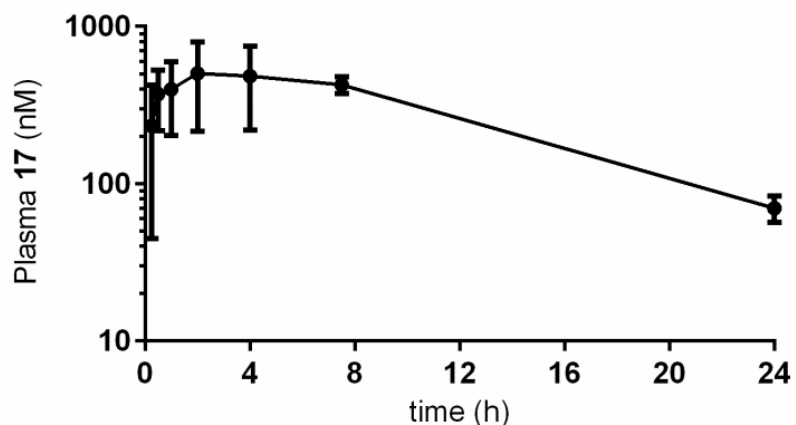
Figure 9 - Plasma concentration-time profile of **17** following SC administration

To evaluate **17** as an antagonist of EP1 and EP3 in vivo, we measured blockade of mEP1 and mEP3 acute vasopressor activity in mice. Left common carotid arteries and right jugular veins of anesthetized mice were cannulated. Direct arterial pressure was measured via carotid catheter. Vasoactive substances were administered via jugular catheter. 17PTPGE$_2$ was used to acutely raise MAP via mEP1 and sulprostone was used for mEP3 (Figure 10). Agonists were administered IV through the jugular catheter 2 h after SC administration of **17**. Pretreatment of mice with 5 mg/kg **17** SC significantly attenuated the pressor activity of an IV bolus of 20 µg/kg 17PTPGE$_2$ (ΔMAP 50.3 ± 5.5 mmHg vs. 27.0 ± 3.6 mmHg). Pretreatment with **17** also significantly suppressed pressor activity of an IV bolus of 10 µg/kg sulprostone (ΔMAP 53.3 ± 2.3 mmHg vs. 32.0 ± 3.5 mmHg). To ensure the observed effect was selective for EP-mediated vasoconstriction, phenylephrine (10 µg/kg) was shown to be unaffected by pretreatment with **17** (Figure 11).
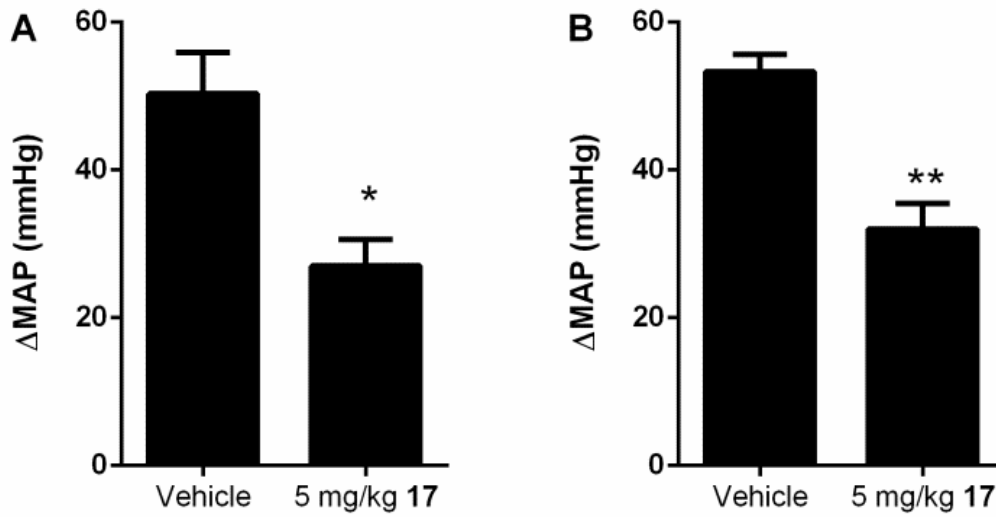
Figure 10 - Change in MAP after IV infusion of (A) 17PTPGE$_2$ (n = 3 each, *P = 0.024 by Student's two-tailed t test) or (B) sulprostone (n = 3 each, **P = 0.007 by Student's two-tailed t test) 2 h after SC injection of 5 mg/kg **17** or vehicle
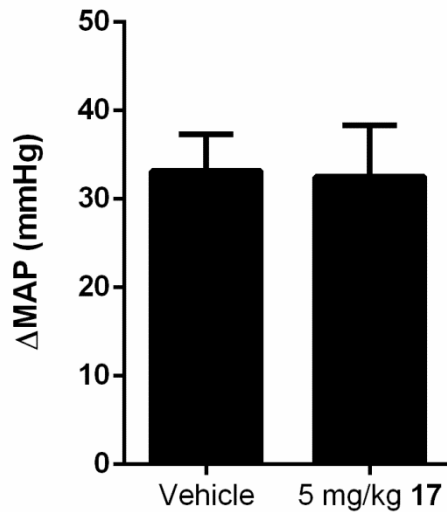
Figure 11 - Change in MAP after IV infusion of 8 µg/kg phenylephrine approximately 2.5 h after SC injection of 5 mg/kg **17** or vehicle

Discussion

In conclusion, we have identified a novel, dual-selectivity antagonist (**17**) of the mouse EP1 and mouse EP3 receptors possessing an acylsulfonamide bioisostere for the prototypical carboxylic acid moiety of EP ligands. **17** was found to have indistinguishable affinity for mEP1 as for mEP3 (mEP1 pK_D vs. mEP3 pK_I, P = 0.40, Student's two-tailed t test). **17** had improved selectively over mEP2 and mTP. **17** was less stable in mouse hepatic microsomes than **7**, due in part to hydrolysis of **17** to **7**, a problem effectively circumvented by SC administration of **17**. Finally, we confirmed **17** is a functional antagonist of mEP1 and mEP3 in vivo by blocking mEP1/mEP3-mediated acute vasopressor activity in anesthetized mice. While the attenuation of pressor activity appears to be incomplete, these results recapitulate experiments performed in mice with genetic disruptions of EP1[80]. Dual selectivity EP1/EP3 antagonists represent a novel class of potential ESRD therapeutics we hypothesize will be more beneficial than blocking either receptor alone.

CHAPTER IV

STRUCTURE-ACTIVITY RELATIONSHIP OF LIGANDS FOR MOUSE EP1 AND

EP3 RECEPTORS

Introduction

In an effort to increase the available tool compounds with which to study the mouse

EP1 and mouse EP3 receptors in vivo, ligands for the human EP1 and human EP3

receptors previously identified in the literature were synthesized. DG-041 is high-affinity,

selective antagonist of human and mouse EP3 receptors that at last report was in Phase II

clinical trials as an adjunct therapy to clopidogrel to treat thrombotic disorders. JD-200 is

a compound previously reported to simultaneously antagonize human EP1 and EP3

receptors. This compound was pursued for its novel pharmacology with the hypothesis

that antagonism of the EP1 and EP3 receptors simultaneously will have additional

therapeutic benefit beyond blockade of either receptor alone. The pharmacology of DG-

041 was studied in vitro, its pharmacokinetics studied in vitro and in vivo, and finally its

ability to block EP-mediated increases in blood pressure was studied. The in vitro

pharmacology of JD-200 was studied, but work with this compound was stopped in

preference of a different molecule (Chapter III, Compound **17**) with a more efficient

synthesis.

<u>Materials and Methods</u>

General medicinal chemistry procedures. Standard methods (thin layer chromatography and liquid chromatography-mass spectrometry) were used to monitor the progress of reactions. Products were purified by automated silica gel flash chromatography using the Teledyne Isco CombiFlash Rf system. Reactions performed in a microwave irradiated reactor utilized a Biotage Initiator-60 single mode microwave synthesizer. All nuclear magnetic resonance spectra (NMR) were proton resonance spectra (^{1}H NMR) at 400 megahertz (MHz) taken on a Bruker AMX NMR using deuterated chloroform ($CDCl_3$) as the solvent. Chemical shifts are reported as parts per million (ppm) δ downfield of the trimethylsilane internal standard. Positive ion electrospray ionization (ESI) mass spectra were obtained on an Agilent 1200 liquid chromatography mass spectrometry (LCMS) system with a Kinetex 2.1 x 50 mm C18 column running a gradient of 10 – 95 % (over 1 minute) acetonitrile and 0.1 % trifluoroacetic acid in water with evaporative light scattering detector (ELSD) and ultraviolet (UV) detection at 214 nm and 254 nm. Final products to be used in biological assays were purified by preparative high-performance liquid chromatography (HPLC) using a Gilson 215 preparative HPLC system and a Phenomenex 30 x 50 mm C8 column at room temperature, a gradient of 0.1 % aqueous TFA / acetonitrile = 50 / 50 to 0 / 100 over 5.0 min, a flow rate of 50.0 mL/min, and detection by UV at 220.

Synthesis of DG-041. DG-041 was synthesized on a fee-for-service basis by the Vanderbilt Institute of Chemical Biology Synthesis Core as previously described[224].

2-nitro-5-(trifluoromethyl)phenol (6). To a solution of 3-trifluoromethylphenol (1 g, 6.2 mmol) in EtOAc was added $NaNO_3$ (1.05 g, 12.4 mmol) and glacial acetic acid (100 μL). The reaction was refluxed overnight. The organic layer was washed with saturated sodium bicarbonate, brine, and water and concentrated. The product was purified by flash chromatography in ethyl acetate / hexane to yield **6** (1.28 g, 71 %).^{1}H NMR (400 MHz, $CDCl_3$) δ 8.27 (d,1 H), 7.49 (s, 1H), 7.27 (d, 1H).

2-(methoxymethoxy)-1-nitro-4-(trifluoromethyl)benzene (7). To a solution of the nitrophenol **6** (1 g, 4.8 mmol) in DCM was added DIPEA (1 mL) and the solution was stirred at room temperature for an hour. Methoxymethyl chloride (3.5 mL) was added to the solution and the reaction was stirred overnight. The organic phase was washed with brine and water and concentrated. The product was purified by flash chromatography in ethyl acetate / hexane to yield **7** (783 mg, 65 %). ^{1}H NMR (400 MHz, $CDCl_3$) δ 7.88 (d,1 H), 7.61 (s, 1H), 7.39 (q, 1H), 5.36 (s, 2H), 3.57 (s, 3H).

2-(methoxymethoxy)-4-(trifluoromethyl)aniline (8). A mixture of the aniline **7** (500 mg, 2.26 mmol) and Pd/C (10 wt% Pd, 50 mg) in methanol was purged with argon and stirred under an atmosphere of H_2 for 1 hour at room temperature. The mixture was filtered over Celite and concentrated. The product was carried to the next step without further purification. ^{1}H NMR (400 MHz, $CDCl_3$) δ 7.27 (s,1 H), 7.13 (d, 1H), 6.76 (d, 1H), 5.25 (s, 2H), 3.53 (s, 3H). MS (ESI, Pos.) m/z 222.1 (M+H)[+].

*Pyridinium 5-methylfuran-2-sulfonate (*14*).* To a solution of 2-methoxyfuran (1 g, 10.2 mmol) in acetonitrile in a 5 mL Biotage microwave reactor vessel was added sulfur trioxide pyridine complex (SO_3·Py; 2.2 g, 14 mmol). The reaction was heated to 120 °C in a microwave reactor for 30 minutes. The reaction was chilled on an ice water bath and the product precipitated. The precipitate was collected by filtration to yield **14** (2.3 g, 88 %).

*5-methoxyfuran-2-sulfonyl chloride (*15*).* To a suspension of sulfonate **14** (2 g, 7.8 mmol) in dichloromethane on ice were added thionyl chloride (1 mL, 14 mmol) and then dimethylformamide under argon. The mixture was brought to room temperature and stirred for 4 hours. The aqueous phase was extracted with dichloromethane and washed with brine and water, dried, and concentrated. Crude **15** (689 mg, 45 %) was carried to the next step without further purification.

N-(2-(methoxymethoxy)-4-(trifluoromethyl)phenyl)-5-methylfuran-2-sulfonamide (**9**). Pyridine (1.5 mL, 18.2 mmol) was added to a solution of the aniline **8** (500 mg, 2.3 mmol) in dichloromethane on ice and under argon. A solution of the sulfonyl chloride **15** (1 g, 5.1 mmol) was added dropwise to the aniline solution. The reaction was allowed to come to room temperature and stir for 6 hours. The reaction diluted in water, extracted with ethyl acetate, washed with 0.5 M HCl, brine, and water, dried, and concentrated. The product was purified by flash chromatography in ethyl acetate / hexane to yield **9** (311 mg, 37 %). ^{1}H NMR (400 MHz, $CDCl_3$) δ 7.62 (d, 1H), 7.45 (s,1 H), 7.34 (s, 1H),

6.27 (s, 1H), 6.09 (s, 1H), 5.23 (s, 2H), 3.49 (s, 3H), 2.33 (s, 3H); MS (ESI, Pos.) m/z 388.1 (M+Na)$^+$.

N-isobutyl-N-(2-(methoxymethoxy)-4-(trifluoromethyl)phenyl)-5-methylfuran-2-

*sulfonamide (***10***).* To a mixture of the sulfonamide **9** (250 mg, 0.68 mmol) and K_2CO_3 (100 mg, 0.72 mmol) in DMF was added methyl iodide (MeI; 100 μL, 1.6 mmol) in an argon-purged 5 mL Biotage microwave reactor vessel. The reaction was heated to 150 °C in a microwave reactor for 15 minutes. The cooled reaction was diluted with water, extracted with ethyl acetate, washed with brine and water, dried, and concentrated. The product was carried to the next step without further purification. MS (ESI, Pos.) m/z 422.2 (M+H)$^+$.

*N-(2-hydroxy-4-(trifluoromethyl)phenyl)-N-isobutyl-5-methylfuran-2-sulfonamide (***11***).* To a solution of the tertiary sulfonamide **10** (250 mg, 0.59 mmol) in MeOH was added 4 M HCl in dioxane (1 mL) at room temperature and the reaction was allowed to stir overnight. The reaction was neutralized with saturated sodium bicarbonate and extracted with ethyl acetate. The organic phases were combined and washed with brine and water, dried, and concentrated. The production was carried to the next step without further purification.

N-(2-((4-cyanobenzyl)oxy)-4-(trifluoromethyl)phenyl)-N-isobutyl-5-methylfuran-2-

*sulfonamide (***12***).* To a suspension of the deprotected sulfonamide **11** (200 mg, 0.53 mmol) and K_2CO_3 (100 mg, 0.72 mmol) in DMF under argon in a 5 mL Biotage

microwave reactor vessel was added 4-bromomethylbenzonitrile (400 mg, 1.06 mmol). The reaction was heated to 150 °C in a microwave reactor for 30 minutes. The cooled reaction was diluted with water, extracted with ethyl acetate, washed with brine and water, dried, and concentrated. The production was purified by flash chromatography in ethyl acetate / hexane to yield **12** (240 mg, 92 %).

N-(2-((4-(1H-tetrazol-5-yl)benzyl)oxy)-4-(trifluoromethyl)phenyl)-N-isobutyl-5-methylfuran-2-sulfonamide, JD-200. To a solution of **12** (200 mg, 0.41 mmol) in DMF in an argon-purged 5 mL Biotage microwave reactor vessel was added tributyltin azide $(Sn(nBu)_3N_3$; 125 µL, 0.45 mmol). The reaction was heated to 100 °C for 15 minutes. Once the reaction had cooled, the solution was poured into saturated sodium bicarbonate and extracted with DCM. The aqueous phase was acidified to pH 1 with HCl. The aqueous phase was extracted with EtOAc. The organic layers were washed with brine and water and concentrated. The product was purified by flash chromatography in ethyl acetate / hexane to yield JD-200 (46 mg, 21 %). MS (ESI, Pos.) m/z 536.1 $(M+H)^+$.

Cell Culture. HEK293 and LVIP2.0Zc cells were maintained at 37 ˚C / 5% CO_2 in DMEM supplemented with 10 % FBS, 2 mM L-glutamine, 100 units/mL penicillin, and 100 µg/mL streptomycin. LVIP2.0Zc cell culture medium also contained 300 µg/mL hygromycin B to maintain integration of vasointestinal peptide (VIP) / *lacZ* reporter plasmid[288]. LVIP2.0Zc cells stably expressing N-terminal HA-tagged mouse EP3γ receptor were generated by transfection of a pcDNA3 plasmid containing receptor cDNA and neomycin résistance cassette. A monoclonal HAmEP3γ-expressing LVIP2.0Zc cell

line was generated by limiting dilution method. Incubating in 500 µg/mL G418 in addition to hygromycin allowed for maintenance of double transformants. For cell membrane / receptor preparations, HEK293 cells were transfected with 6 µg receptor cDNA plasmid using Lipofectamine 2000 in DMEM lacking penicillin and streptomycin. Six hours after adding DNA-Lipofectamine 2000 complexes, media was replaced with complete DMEM containing 20 µM indomethacin and 5 mM sodium butyrate. Cells were allowed to recover for 18 to 24 hours before being plated in three to five 100 mm cell culture dishes for membrane harvest. Cells were incubated for an additional 24 to 48 hours, until confluence was reached. Twenty four hours prior to performing CRE assays, HAmEP3γ-expressing LVIP2.0Zc cells were plated in 96-well plates at a density of 5 x 10^5 cells per well in 100 µL of complete DMEM containing 20 µM indomethacin.

Competition Radioligand Binding. Total cell membranes from HEK293 transfectants described above were prepared as described[262]. Membranes (5 - 10 µg) were incubated with [^{3}H]PGE$_2$ (5 nM) and a range of unlabeled test compound (1 nM – 10 µM) in 200 µL of binding buffer (25 mM potassium phosphate, 1 mM EDTA, and 10 mM MgCl$_2$, pH 6.2) for 1 hour at 30 ˚C. PGE$_2$ (10 µM) was used as a positive control for receptor binding. Binding reactions were terminated and radioactivity was quantified as previously described[262].

CRE/LacZ Reporter Assay. LVIP2.0Zc cells in 96-well plates stably expressing the HAmEP3γ receptor were incubated with sulprostone (1 pM – 0.1 µM) and DG-041 (0.1 nM – 10 nM) in Opti-MEM containing 5 mM sodium butyrate and 20 µM indomethacin.

After cells were stimulated for 6 hours, media was aspirated and cells were washed with PBS. Cells were incubated for 10 minutes at room temperature in 25 μL of lysis buffer (10 mM sodium phosphate, 0.2 mM $MgSO_4$, and 10 μM $MnCl_2$, pH 8.0). Assay plates were developed as described[261]. Concentration response curves to sulprostone in the presence of varying amounts of DG-041 were determined by measuring relative enzyme activity as absorbance at 570 nm on Multiskan Ascent plate reader (Thermo Labsystems, Waltham, MA). Data were analyzed in the method of Schild[281].

Calcium FLEXstation assay. FLEXstation-based calcium mobilization assays were performed as described in Chapter III.

In vitro metabolite identification. Solutions of DG-041 (20 μM), NADPH (2 mM), $MgCl_2$ (3 mM), and hepatic microsomal protein (1 mg/mL) in potassium phosphate buffer (pH 7.4, 0.1 M) were incubated for 1 hour at 37 °C. Reactions to monitor potential production of reactive intermediates were assembled by including glutathione (GSH; 2 mM). Reactions to control for metabolism not due to Phase I or Phase II enzymes were assembled by assembling solutions replacing NADPH with more buffer. After 1 hour, reactions were quenched by precipitation with 1 mL of ice-cold acetonitrile. Samples were centrifuged at 3700 rpm at 4 °C for 10 minutes. Samples were incubated on ice for 5 minutes until organic-aqueous phase interface was apparent. An aliquot of the organic phase (750 μL) was transferred to a clean tube, dried at 30 °C under nitrogen, and reconstituted in 85:15 water:acetonitrile (125 μL). A "neat" sample of the test compound

was prepared by making a 20 µM solution of compound in 85:15 water:acetonitrile. Samples were analyzed by HPLC/MS.

In vivo pharmacokinetics. Male C57B/6J mice were administered 30 mg/kg DG-041 in corn oil (200 µL) by mouth (PO) via gavage at time $t = 0$. At time points out to 24 hours (20 min, 45 min, 90 min, 3, 6, 12, and 24 hours) mice were sacrificed in pairs by Isoflurane overdose. Blood was collected by cardiac puncture into syringes containing 3.8 % sodium citrate.

Plasma was isolated by centrifugation at room temperature at 5000 rpm for 15 minutes. Plasma was stored at -80 °C until HPLC/MS/MS analysis. Analyte was extracted by precipitation with an ice-cold solution of internal standard in acetonitrile. Mixtures were centrifuged at 3700 rpm at 4 °C for 10 minutes. Samples were incubated on ice for 5 minutes until organic-aqueous phase interface was apparent. An aliquot of the organic phase (750 µL) was transferred to a clean tube, dried at 30 °C under nitrogen, and reconstituted in 85:15 water:acetonitrile (125 µL). Samples were analyzed by HPLC/MS/MS. Test compound plasma concentrations were calculated by comparing the ratio of analyte mass spectrometer response AUC to internal standard mass spectrometer response AUC to a calibration curve of known analyte concentration analyte AUC:standard AUC values.

HPLC/MS and HPLC/MS/MS analysis. HPLC/MS analysis of metabolite identification samples was performed as described in Chapter III. Analysis of samples collected from the in vivo pharmacokinetics experiment was performed as follows. Liquid

chromatographic separation was carried out on a Luna ODS column (5 μm, 2.1 mm x 5 cm) at a flow rate of 0.3 mL/min. The HPLC mobile phase A was 0.1 % formic acid in water and mobile phase B was 0.1 % formic acid in acetonitrile. The initial mobile phase was 20 % B and was held for 1 minute, linearly increased to 100 % B over 4 minutes, and held at 100 % B for 1 minute. HPLC eluates were ionized by ESI and introduced into a ThermoFinnigan TSQ Quantum Ultra triple quadrapole mass spectrometer operating in positive ion mode. Xcalibur (version 2.0) software was used to control the instrument and collect data. The ESI source was fitted with a stainless steel capillary (100 μm internal diameter). Ultra-pure nitrogen gas was used as both the sheath and auxiliary gases. The ion transfer capillary was set at 300 °C. Spray voltage, tube lens voltage, sheath and auxiliary gas pressures were optimized to achieve optimal response from the test compound.

Intracarotid blood pressure measurement. MAP was measured as described in Chapter III.

Results

Synthesis and characterization of DG-041. DG-041, a potent and selective EP3 receptor antagonist, was synthesized by the Vanderbilt Institute for Chemical Biology Synthesis Core as previously described[224]. Briefly, the trihalogenated aniline **1** was alkylated by allyl bromide with potassium *t*-butoxide (KOtBu) in THF. Compound **2** was subjected to

one-pot, tandem Heck reactions: first an intramolecular Heck reaction to close the ring and form an indole; and second with acrylic acid to yield **3**. The nitrogen of the indole was alkylated by dichlorobenzyl chloride with KOtBu. DG-041 was prepared by amide bond synthesis by EDC/HOBt with **4** and dichlorothiophene sulfonamide (Figure 1).
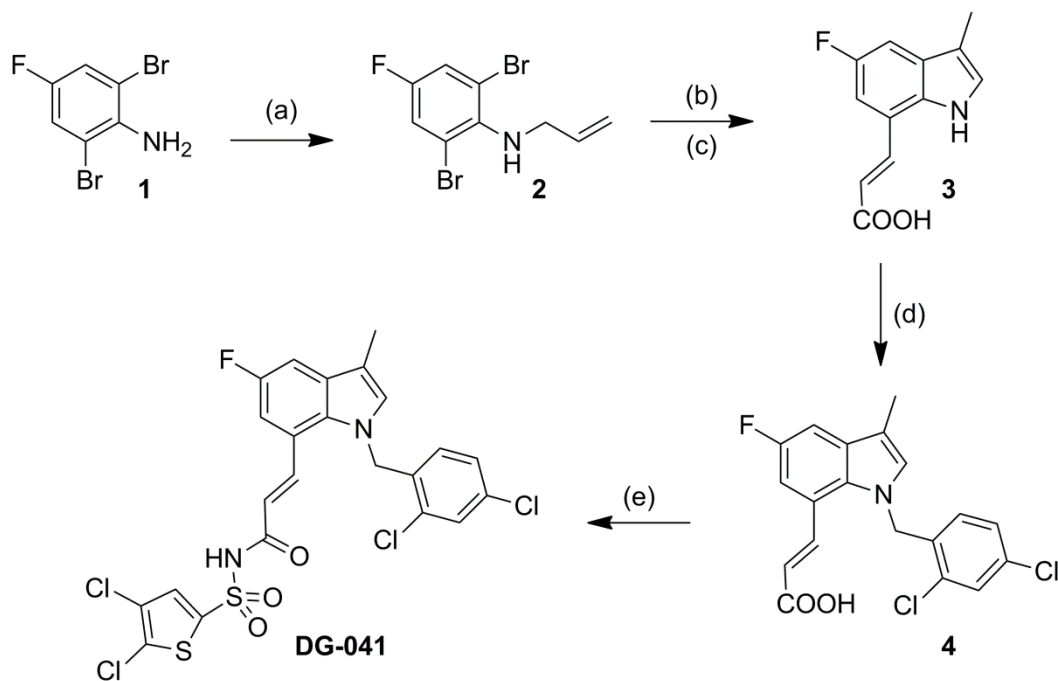
Figure 1 – Synthetic route for DG-041. Reagents: (a) KOtBu/THF, allyl bromide; (b) Pd(OAc)$_2$, P(o-tolyl)$_3$, CH$_3$CN, Et$_3$N, (c) Pd(OAc)$_2$, P(o-tolyl)$_3$, acrylic acid; (d) KOtBu/THF, 2,4-dichlorobenzyl chloride; (e) EDC·HCl, HOBt, DIPEA, 4,5-dichlorothiophene-2-sulfonamide, CH$_2$Cl$_2$

DG-041 was confirmed to be a high affinity ligand of the mouse EP3 receptor (pK$_i$ = 9.16 ± 0.12; Figure 2). However, it was later appreciated that the kinetics of DG-041 binding to human EP3 receptor is characterized by slow, tight binding[226,289]. On the time scale of these in vitro binding assays (a few hours), DG-041 is a pseudo-irreversible ligand of the

EP3 receptor, thereby violating one of the assumptions of the radioligand binding assays described above. What can be said is that should DG-041 be an antagonist of the mouse EP3 receptor, one would expect it to very effectively block the receptor as the dissociation kinetics of DG-041 at EP3 are so slow.
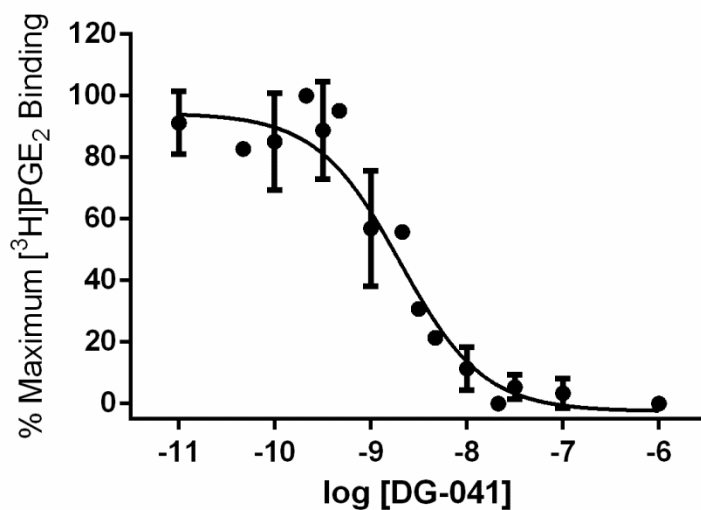
Figure 2 – Competition binding curve for DG-041 against 5 nM [^{3}H]PGE$_2$ at the mouse EP3γ receptor. Data are averages of three independent determinations.

Interestingly, in the LVIP2.0Zc-based CRE/LacZ assay mEP3γ behaves as a classical G$_i$-coupled receptor, as opposed to its behavior in the CRE assay employing transiently pCRE/LacZ-transfected HEK293 cells. In LVIP2.0Zc cells, [cAMP]$_i$ must first be artificially elevated, either by forskolin or activation of a G$_s$-coupled receptor such as β$_2$AR, to raise the β-galactosidase (β-gal) reporter. In this context, activation of mEP3γ potently suppresses expression of the β-gal reporter and therefore [cAMP]$_i$.

112
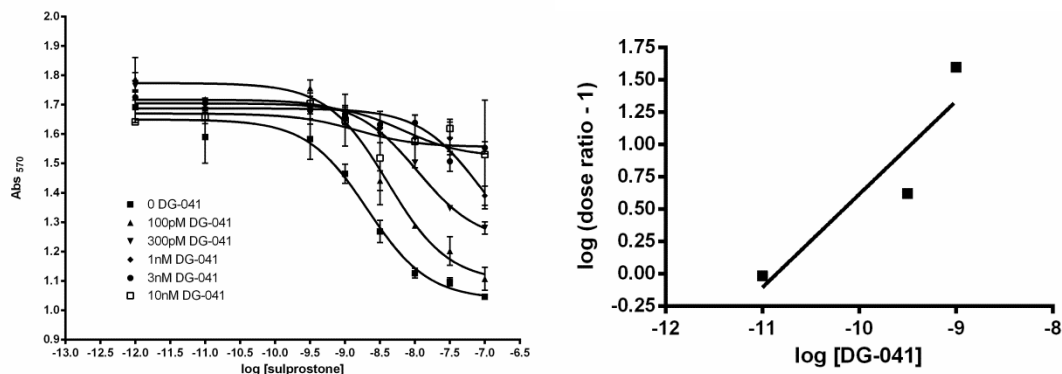
Figure 3 – Schild analysis of DG-041 at HAmEP3γ in LVIP2.0Zc cells. (left) Concentration response curves to sulprostone in the presence of a range of concentrations of DG-041. Each point was determined in duplicate. (right) Schild regression of concentration response data.

Using this assay, DG-041 was characterized at the mouse EP3γ receptor using the method of Schild[281]. HAmEP3γ-expressing LVIP2.0Zc cells were incubated with a range of concentrations of agonist sulprostone in the presence of different concentrations of DG-041. Picomolar concentrations of DG-041 right-shifted the concentration response curve to sulprostone and DG-041 completely suppressed signaling through the EP3 receptor at low nanomolar concentrations (Figure 3, left). DG-041 was found to be a high-affinity, functional antagonist of the mouse EP3γ receptor (pK_D = 10.85, m = 0.72; Figure 3, right). DG-041 has pseudo-irreversible binding kinetics in experiments on this time scale and these analyses require the system to be at equilibrium. Interpretation of these data should be conservative in light of these violations. Qualitatively, very low concentrations of DG-041 would be required to block signaling through EP3 receptors.

With the goal of introducing DG-041 into mice to evaluate the role of the EP3 receptor in the pathophysiology of kidney disease, we characterized the pharmacokinetic properties of DG-041 in mice. Mice were dosed by mouth with 30 mg/kg DG-041 suspended in corn oil. At time points out to 24 hours, pairs of mice were sacrificed and blood was collected by cardiac puncture to determine the plasma concentration of DG-041 at those time points. The results of the HPLC/MS analysis are shown in Figure 4.
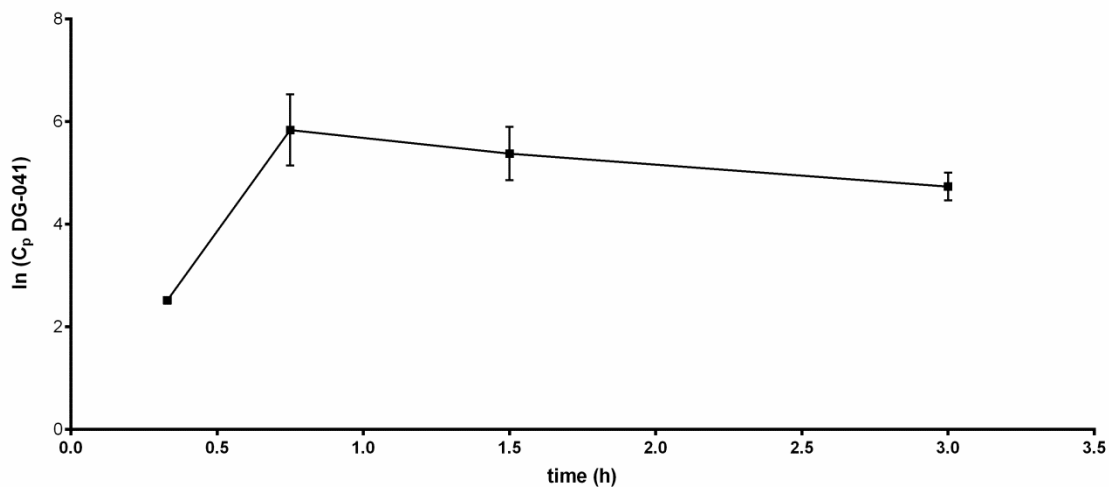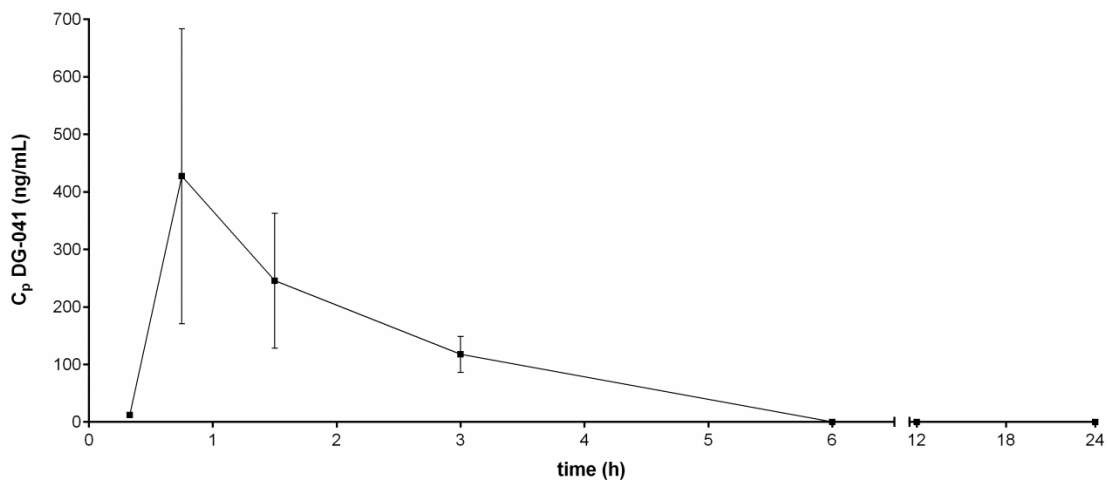
Figure 4 - Plasma concentration-time profile of DG-041 following oral administration. (top) Linear-linear plot of plasma concentration-time profile out to 24 hours. (bottom) Semi-log plot of plasma concentration-time profile to 3 hours.

DG-041 was rapidly eliminated from the mouse; plasma concentrations of DG-041 dropped below the lower limit of detection after 3 hours (Figure 4, top). DG-041 reached a maximum plasma concentration of 722 nM by 45 minutes after administration. Noncompartmental analysis of the plasma concentration-time profile revealed $t_{1/2}$ for

DG-041 in mice of 1.23 hours (Figure 4, bottom). These data indicate DG-041 would have to be administered frequently or more practically from a SC osmotic minipump or pellet to maintain plasma exposure.

A strategy for improving the pharmacokinetic properties of a molecule is to identify the mode of elimination for the compound and block it using principles of medicinal chemistry. The data do not definitely prove DG-041 is eliminated by hepatic metabolism; however this was the initial hypothesis. To identify the sites of hepatic metabolism on DG-041, a metabolite identification experiment was conducted. DG-041 was incubated in vitro with mouse hepatic microsomes. A separate sample was prepared using the same conditions but also including GSH to trap any potential reactive metabolites of DG-041.
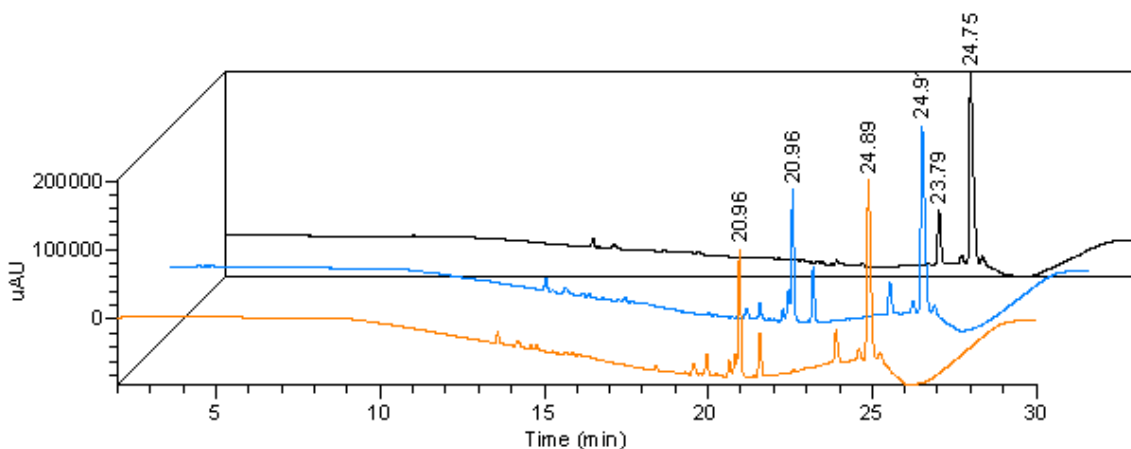
Figure 5 – Three dimensional stack presentation of UV chromatograms for DG-041 incubated with microsomes in the absence of NADPH (black), DG-041 + microsomes + NADPH (blue), DG-041 + microsomes + NADPH + GSH (orange)

116

The HPLC/UV traces revealed DG-041 has a retention time of 25 minutes (Figure 5). No cytochrome P450-independent metabolites of DG-041were identified, as determined by a lack of new chemical species in the sample lacking NADPH (Figure 5, black trace). A single metabolite of DG-041 was identified with a retention time of 21 minutes (Figure 5, blue and orange traces). This product corresponded to a single oxygenation of DG-041 as indicated by the more polar retention time and mass spectrum. No reactive metabolites of DG-041 in the experiment containing GSH were trapped (Figure 5, orange trace). In positive ion mode, DG-041 at retention time 24 minutes had a $[M+H]^+$ ion m/z of 589 amu (Figure 6, top). The molecule at retention time 21 minutes had a $[M+H]^+$ ion m/z of 605 amu (Figure 6, bottom), heavier by a single oxygen atom.
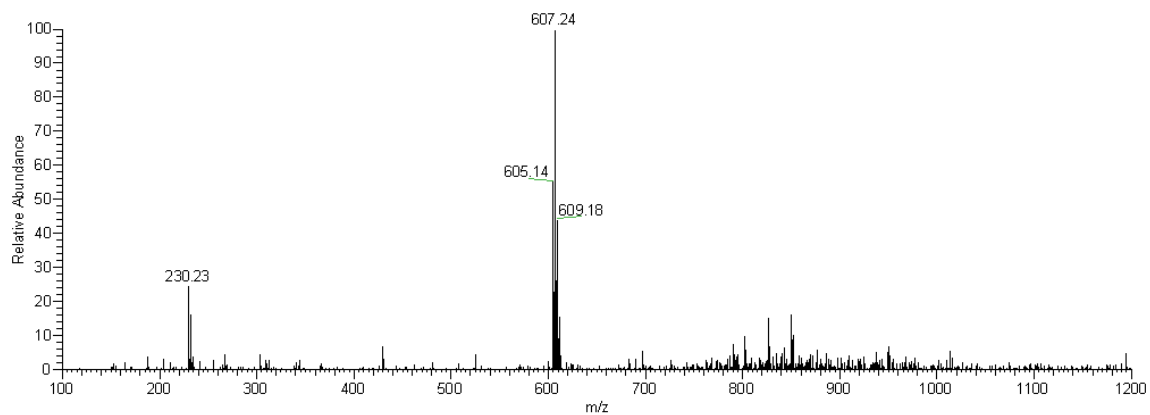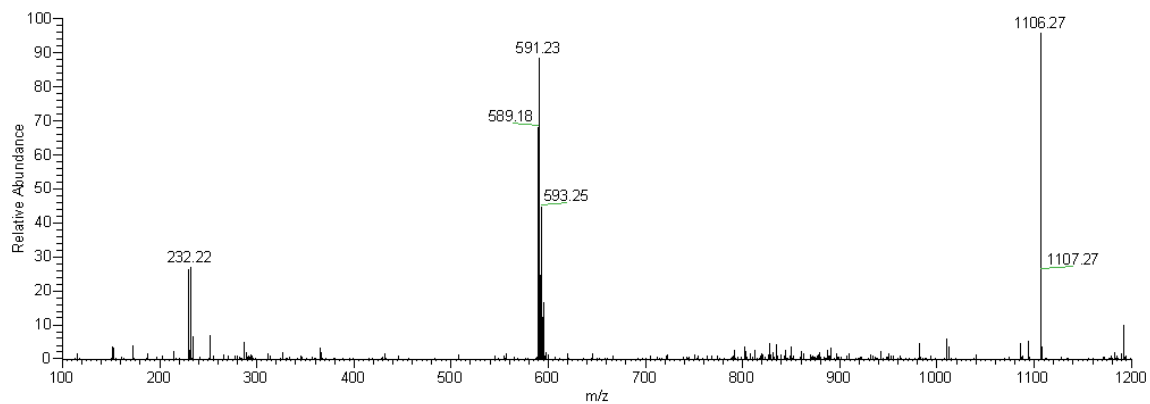
Figure 6 – MS^{1} spectra of (top) retention time 24 minutes and (bottom) retention time 21 minutes.
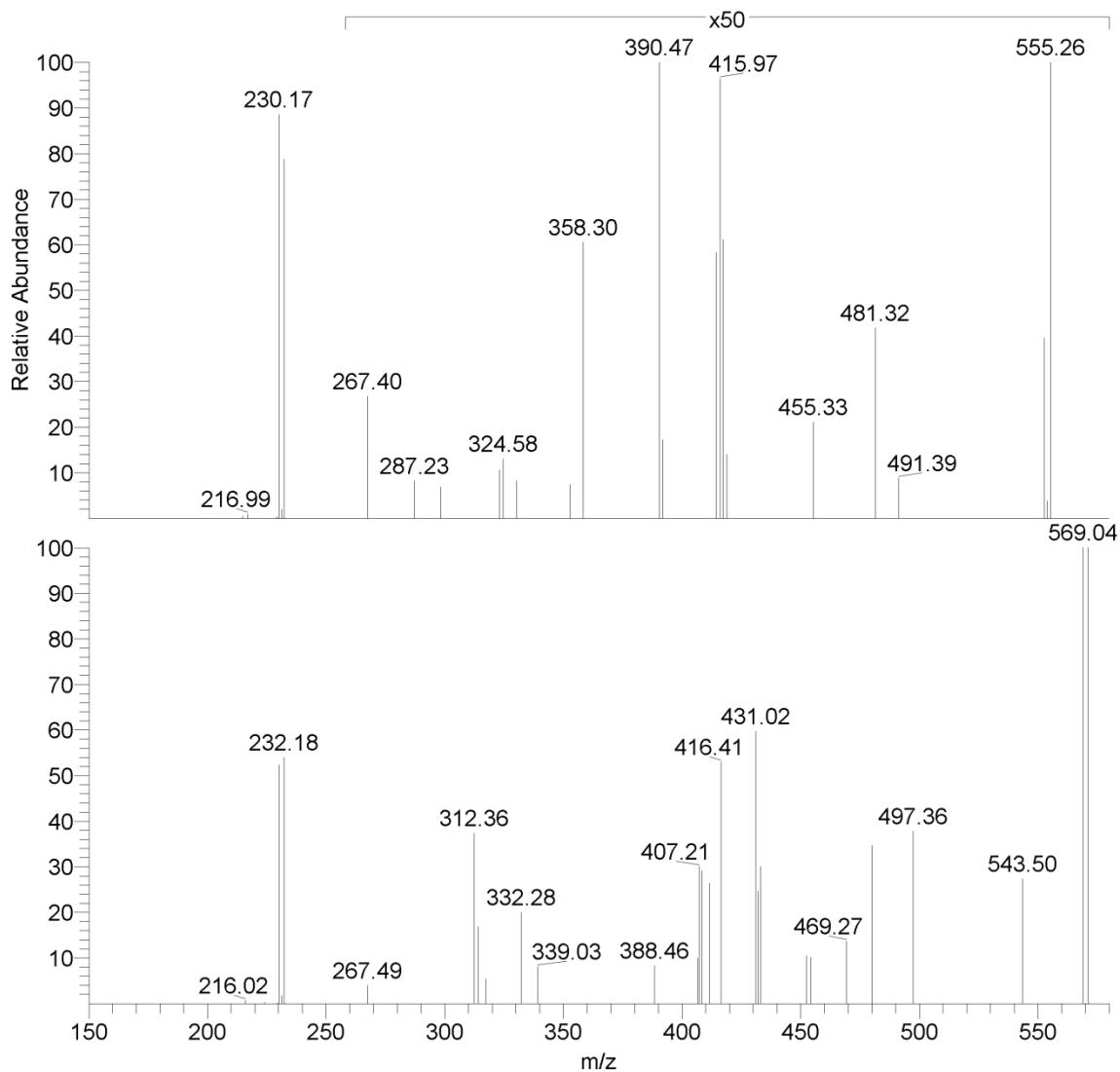
Figure 7 – MS^2 spectra of (top) retention time 24 minutes and (bottom) retention time 21 minutes.

DG-041 fragmented poorly under the mass spectrometric conditions of these experiments. The main fragment that was detected in these experiments is at 230 – 232 amu (Figure 7). This fragment corresponds to the sulfonamide moiety. Because of the poor structural resolution in these experiments, it can be concluded that the oxygen atom

was not added to the sulfonamide portion of the molecule, as both the 21 minute and 24 minute retention time molecules show 230 – 232 amu fragments (Figure 8). These experiments make no indication of relative abundance of compounds; that is, this metabolite of DG-041 may be formed in vivo but at concentrations so low as to be irrelevant to systemic clearance. Further experiments with hepatic S9 fractions to determine Phase II metabolism in vitro have yet to be conducted. It is possible DG-041 is eliminated by a conjugation reaction. Moreover, it is possible the primary route of elimination for DG-041 is not metabolic at all but excretion into the urine. Further experiments will be needed to determine if this is the case and to determine the exact placement of the oxygen in the DG-041 metabolite.
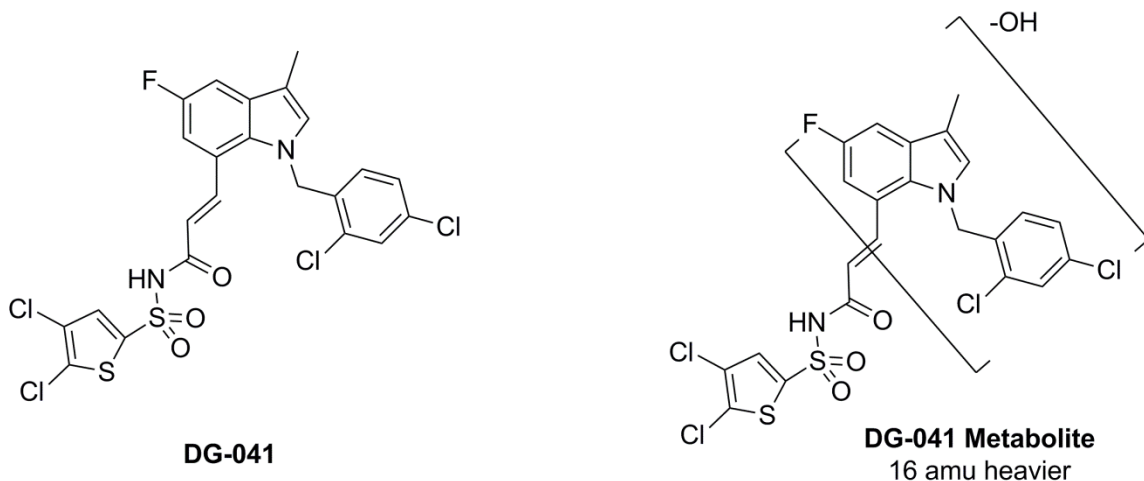
Figure 8 - Structure of DG-041 and proposed structure of the P450 oxidized DG-041 metabolite.

DG-041 is confirmed to be a high-affinity ligand for the mouse EP3 receptor in vitro and to be a functional antagonist, albeit with pseudo-irreversible kinetics. DG-041 was also orally bioavailable, though for a brief window of time possibly due to oxidative metabolism of DG-041. The ability of DG-041 to block acute vasopressor responses to EP3 agonists and other pressor in vivo was evaluated. Sulprostone, an EP1/EP3 agonist, has been shown to cause an acute and transient vasopressor response when injected IV into anesthetized mice[80,120]. Carotid artery and jugular vein catheters were placed into anesthetized mice of different genotypes (wild-type, EP1$^{-/-}$, and EP3$^{-/-}$) and whether pretreatment with DG-041 versus vehicle would block the vasopressor activity of sulprostone in vivo was determined
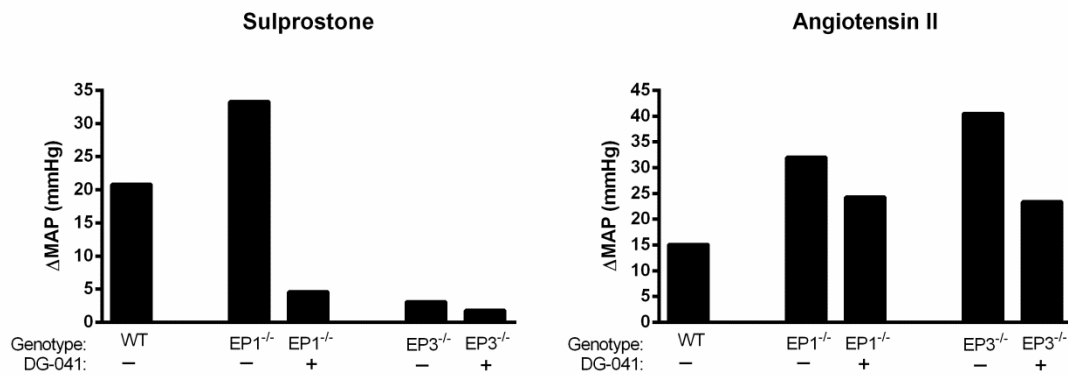
Figure 9 - Direct intracarotid blood pressure measurement in anesthetized mice dosed with sulprostone or angiotensin II after pretreatment with DG-041 or vehicle

Sulprostone injection into a wild-type, vehicle-treated mouse produced an acute and transient vasopressor response on the order of 20 mmHg (Figure 9). Ang II infusion into

121

the same mouse produced a similar response. In an EP1$^{-/-}$ mouse pretreated with vehicle,

sulprostone and angiotensin II produced similar vasopressor responses to vehicle-treated

wild-type mice, suggesting the vasopressor activity of sulprostone is exclusively through

EP3. This is in contrast to the in vitro data that show sulprostone has similar affinities for

EP1 and EP3. Pretreatment of an EP1$^{-/-}$ mouse with DG-041 completely blocked the

vasopressor response to sulprostone, leaving the Ang II vasopressor response intact.

Sulprostone produced no vasopressor response in EP3$^{-/-}$ mice, regardless of vehicle or

DG-041 pretreatment, again suggesting the entire vasopressor phenotype of sulprostone

injection is due to EP3 activation. This small, pilot study demonstrated for the first time

that DG-041 was able to prevent the vasopressor activity of some components of the

PGE$_2$ signaling cascade.
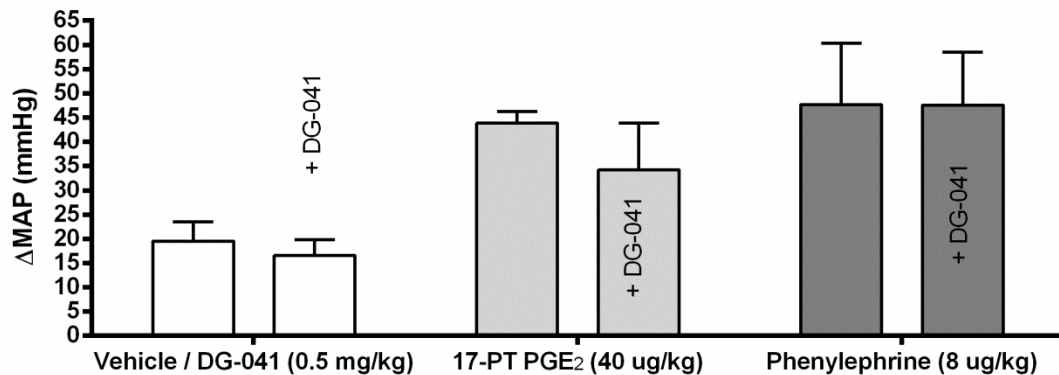
Figure 10 - Direct intracarotid blood pressure measurement in anesthetized mice dosed with 17PTPGE$_2$ with and without DG-041 pretreatment. 17PTPGE$_2$ group, P = 0.3538; Phenylephrine group, P = 0.9951 by two-tailed Student's t test.

A larger study was performed in wild-type mice in which $17PTPGE_2$ was used as the study vasopressor and phenylephrine was the positive control. Blood pressure was measured and compounds were delivered as described in the previous experiment. $17PTPGE_2$ was used as the agonist in this experiment because, like sulprostone, $17PTPGE_2$ is approximately equipotent at EP1 as at EP3 in vitro. Acute infusion of $17PTPGE_2$ caused a transient increase in MAP of about 45 mmHg (Figure 10). Phenylephrine produced a similar response. When mice were pretreated with DG-041, the phenylephrine and $17PTPGE_2$ vasopressor responses were unaffected, though there may be a trend toward reduction for $17PTPGE_2$ activity in DG-041 treated animals. Previous studies have shown about a 50 % reduction in vasopressor activity of $17PTPGE_2$ when the EP1 receptor is genetically deleted[80], suggesting the remaining $17PTPGE_2$ activity is due to the EP3 receptor. However, that same study found a significant effect of EP1 deletion on the vasopressor response to sulprostone, which was not seen in Figure 9. These data would suggest the majority of the vasopressor response to $17PTPGE_2$ is EP1-mediated.

Synthesis and characterization of JD-200. JD-200 was synthesized as previously described[290] with a few modifications (Figure 11). Compound **6** was prepared by heating 3-trifluoromethylphenol with sodium nitrate with sulfuric acid. The phenolic oxygen was protected with methyl chloromethyl ether to yield **7**. The nitro group was reduced by hydrogenation to the aniline **8**. In a separate synthetic route, methoxyfuran was sulfonated by heating with $SO_3 \cdot Py$ in a microwave reactor to yield **9**. The sulfonyl

123

chloride **10** was formed by reacting **9** with thionyl chloride. The aniline **8** was coupled to the thiophene sulfonyl chloride **10** by heating in pyridine to yield **11**. The tertiary sulfonamide was prepared by alkylation with isobutyl iodide. **12** was prepared by deprotecting the phenolic oxygen by heating with HCl. The phenolic oxygen was alkylated with *p*-cyanobenzyl bromide to yield **13**. Finally, JD-200 was prepared by cycloaddition of tributyltin azide with **13** under microwave conditions.
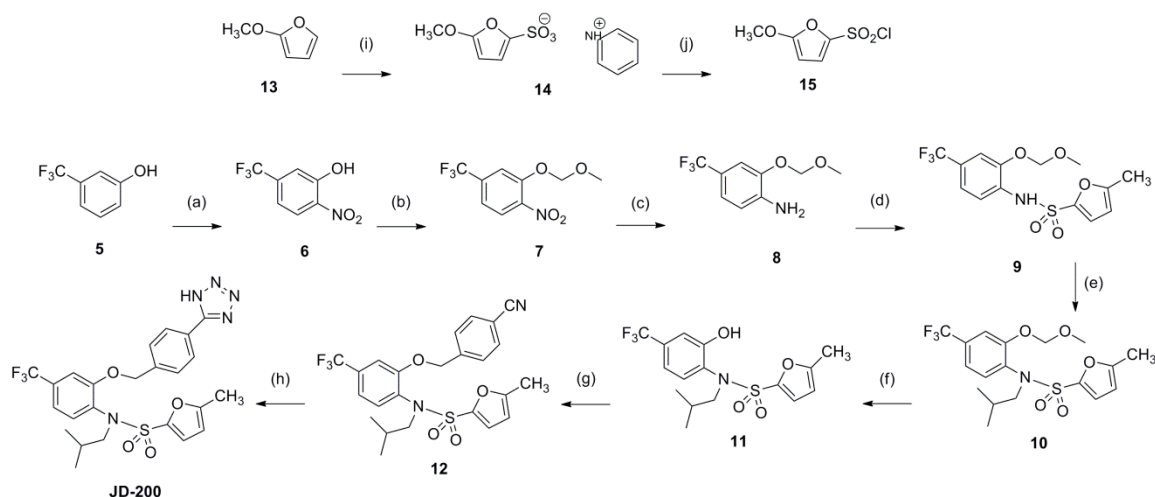
Figure 11 – Synthetic route for JD-200. Reagents: (a) NaNO$_3$, H$_2$SO$_4$, (b) CH$_3$OCH$_2$Cl, DIPEA, CH$_2$Cl$_2$, (c) H$_2$, Pd/C, MeOH, (d) **13**, pyridine, (e) iBuI, K$_2$CO$_3$, DMF, (f) HCl, MeOH, (g) p-cyanobenzyl bromide, K$_2$CO$_3$, DMF, (h) Sn(nBu)$_3$N$_3$, PhMe, μW, (i) SO$_3$·pyridine, CH$_3$CN, μW, (j) SOCl$_2$, DMF

JD-200 was previously reported to have comparable affinity for both the human EP1 and EP3 receptors. JD-200 was synthesized and characterized on the basis of it being a dual selectivity EP1/EP3 antagonist. In radioligand competition binding assays (Figure 12), JD-200 was a high-affinity affinity ligand of the mouse EP3 receptor (K$_I$ = 35.9 nM). JD-200 was confirmed to be a functional antagonist of the mouse EP3 receptor by the

LVIP2.0Zc-based CRE assay (Figure 13, left; pIC_{50} = 7.82). Using a FLEXstation calcium mobilization assay, JD-200 was confirmed to be a functional against of the mouse EP1 receptor (Figure 13, right; pIC_{50} = 7.52). Further studies will be required to determine if JD-200 is selective for EP1 and EP3 over the other prostanoid receptors.
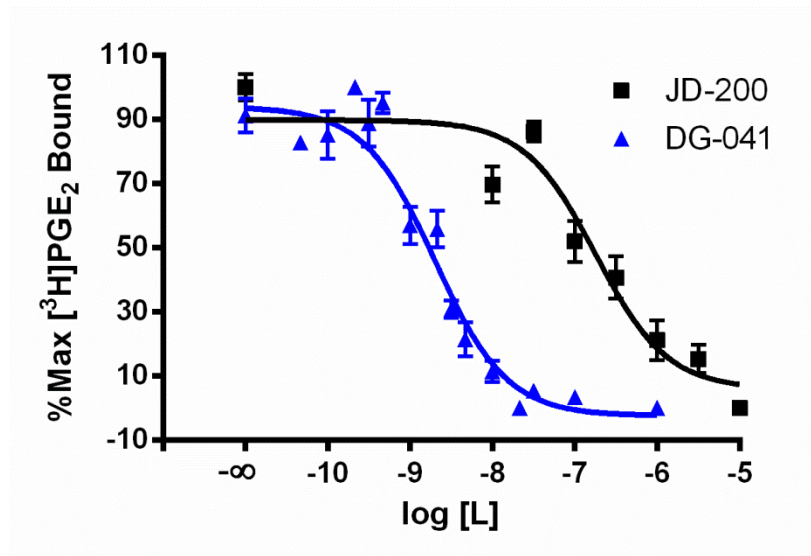
Figure 12 – Competition binding of DG-041 (blue) and JD-200 (black) against 5 nM [^{3}H]PGE$_2$ at the mouse EP3γ receptor expressed in HEK293 cell membranes.
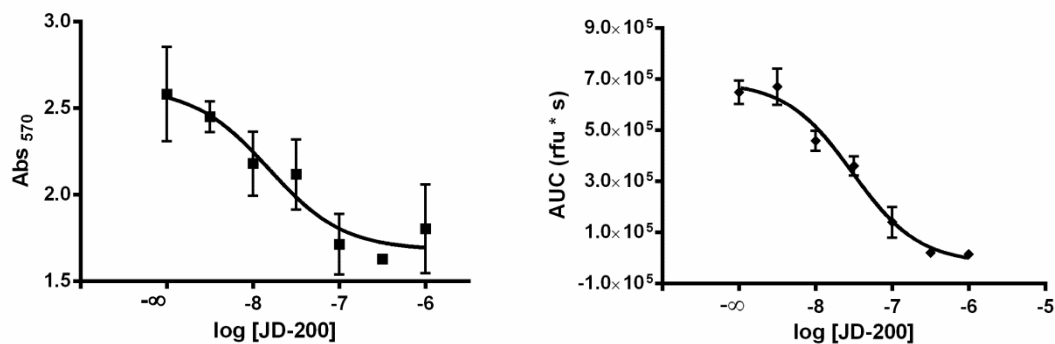
Figure 13 – Concentration response curve of JD-200 against (left) sulprostone in the mEP3γ-expressing LVIP2.0Zc CRE assay and (right) 17PTPGE$_2$ in the FLEXstation-based mEP1 calcium flux assay.

Summary

DG-041. DG-041 is a high-affinity, selective antagonist of the EP3 receptor. The only other prostanoid receptor DG-041 has appreciable affinity for is the DP1 receptor. Whether the subtype selectivity of DG-041 for EP3 is recapitulated in mice is yet to be seen. DG-041 has been shown at the human EP3 receptor to have pseudo-irreversible binding kinetics. Cell membranes expressing human EP3 receptor were incubated with DG-041 and two structural analogues, washed three times, and [^{3}H]PGE$_2$ binding to the membranes was assessed. DG-041 and its analogues completely blocked [^{3}H]PGE$_2$ binding to the membranes whereas pre-incubation with PGE$_2$ only partially reduced subsequent [^{3}H]PGE$_2$ binding compared to pre-incubation in buffer alone[226].

The mouse pharmacokinetic properties of DG-041 were disappointing. An oral dose of 30 mg/kg DG-041 reached a maximum plasma concentration of approximately 0.75 μM. Parallel intravenous dosing of DG-041 was not performed, so exact bioavailability

126

cannot be known. On first inspection c_{max} seems to be low compared to a more drug-like molecule. The high lipophilicity of DG-041 could partially explain this. DG-041 has a predicted *n*-octanol:water partition coefficient of 7.67[289], meaning the predicted ratio of DG-041 in a lipophilic layer versus aqueous layer is approximately 50 billion to 1. DG-041 may passively cross the GI lining, but likely would distribute into adipose tissue; DG-041 likely has a high V_{ss}. Further experiments will be required to confirm these hypotheses.

Orally administered DG-041 was bioavailable to some extent, but systemic DG-041 was rapidly cleared with a $t_{1/2}$ of 1.23 hours. In vitro metabolite identification experiments indicate a single oxygenation event in mouse liver microsomes, which no doubt contributes to the rate of elimination of DG-041. Actual rate of metabolism of DG-041 in mouse liver microsomes will require further experimentation. A common fate for molecules metabolized by Phase I enzymes is subsequent conjugation by Phase II enzymes. It is possible the metabolite of DG-041 is a substrate for glucuronidation, sulfonation, acetylation, or some other Phase II conjugation process. Experiments employing mouse hepatic S9 fractions or mouse hepatocytes, or analysis of plasma from DG-041 treated mice will be required to answer these questions.

DG-041 fragmented poorly in the mass spectrometer in metabolite identification assays. This is a common problem for DG-041 and was seen with both electrospray and chemical ionization techniques on a triple quadrapole mass spectrometer. If possible, the mass spectrometry conditions should be optimized for DG-041 fragmentation to identify the location of hydroxylation on the DG-041 metabolite with better resolution.

DG-041 was able to block sulprostone-induced vasopressor responses in wild-type and EP1$^{-/-}$ mice. These were pilot experiments using a single mouse per data point and will have to be repeated with a larger sample size before too much weight is placed on the data. However, these data would indicate the majority of the pressor response to sulprostone is due to EP3 signaling and not EP1. This was demonstrated with both genetic deletion of EP3 and pharmacological blockade of EP3 with DG-041 in these experiments. The vasopressor responses to Ang II and phenylephrine were intact regardless of genotype or pharmacological treatment. DG-041 did not appear to effectively block 17PTPGE$_2$ vasopressor activity in vivo, though perhaps a larger sample size or larger dose of 17PTPGE$_2$ would have yielded statistically significant data. In any case, it seems the bulk of the vasopressor response to 17PTPGE$_2$ is EP1-mediated.

JD-200 was synthesized as part of an effort to identify single ligands that could simultaneously antagonize the EP1 and EP3 receptors. EP1 and EP3 are involved in the pathophysiology of diabetes, hypertension, and other cardiovascular diseases and at least on the molecular level have some functionally redundant signaling pathways. JD-200 was confirmed in radioligand binding and cell-based signaling assays to antagonize the mouse EP1 and EP3 receptors in vitro. However, the synthesis of this molecule was lengthy and inefficient. These studies add to the toolbox of available ligands to study the EP1 and EP3 receptors in mice and also to the understanding of how EP-selective ligands act on the cardiovascular system in vivo. Future work will involve optimizing the synthetic route to more efficiently yield quantities suitable for in vivo use.

CHAPTER V

DISCUSSION AND FUTURE DIRECTIONS

Structure-function studies of the EP3 receptor

Subsequent to the initiation of the cysteine mutagenesis project described in Chapter II, several GPCR structures have been published[291-295]. The major limitation of the work to optimize mouse EP3 receptor expression in *E. coli* (Chapter II) is the use of *E. coli*. However, heterologous expression of target proteins in *E. coli* is required to isotopically label proteins for NMR-based structural studies. Overexpression of natively folded membrane proteins in *E. coli* is not unprecedented[264,296-299], but more efficient techniques have evolved. One of the most established methods of expressing complex proteins like GPCRs is the baculovirus insect cell expression system. Baculoviruses most commonly infect the larva of moths. A cell line, Sf9, was generated from armyworm ovarian tissue and is used to overexpress heterologous proteins by infecting the insect cells with baculovirus carrying the genetic code for a protein of interest. This system has been used to overexpress a number of proteins, including the COX enzymes and the constructs used to crystallize some of the known structures of GPCRs. Other expression systems have been developed to more effectively overexpress membrane proteins for structural studies. *Pichia pastoris*, a strain of yeast, has been adapted for laboratory use to overexpress membrane proteins[300,301]. Other methods rely on massive culture systems for common laboratory mammalian cell lines. This method has been used to express GPCRs[302] and is

129

commonly used in the biopharmaceutical industry for large scale synthesis (e.g., for antibody production) using bioreactors on the scale of tens of thousands of liters[303].

Work to adapt mEP3γ to these methods of expression has already begun. Previously, attempts have been made to overexpress the β2-adrenergic receptor in mammalian cells in a bioreactor as a proof of concept study. The goal was to demonstrate the method as effective using β2AR and later try overexpressing the EP3 receptor this way. Efforts are currently focused on optimizing expression strategies for EP3 receptor in both *Pichia* and Sf9 expression systems.

Structural determination by X-ray crystallography requires the formation of an ordered lattice of purified, homogenous receptor protein. GPCRs are composed of seven transmembrane alpha helices linked together by loops; these structures are inherently flexible and indeed require this flexibility to switch from inactive and active conformation states. Furthermore, receptors are often post-translationally modified. Extracellular residues of GPCRs are typically heterologously glycosylated and these glycosylations may be required for receptor function, impeding efforts to crystallize the target protein. GPCRs are often lipid modified on the intracellular side of the molecule. However, these modifications are typically homogenous and may not affect protein crystallization.

To circumvent these conformational concerns with crystallizing GPCRs, a number of approaches have been developed. One is to generate chimeric receptor constructs that have another protein (e.g., T4 lysozyme) in one of the intracellular loop domains. These fusion proteins are demonstrated to aid in crystal packing of proteins. Another strategy has been to employ antibodies against the receptor to aid in protein packing. Traditional

130

antibodies against β_2AR were used initially[291]; however, it was appreciated that camelids (e.g., llamas and alpacas) and sharks produce much smaller, single-chain antibodies, so-called "nanobodies." These nanobodies raised against GPCRs have been used to improve the crystal packing of purified receptor protein[304,305].

The cysteine mutagenesis study (Chapter II) mutated each cysteine to an alanine. Future work for this project should involve consideration of different missense mutations than simply conversion to alanine. If a cysteine residue is in a hydrophobic region of the protein, a more lipophilic amino acid such as valine or leucine may be more appropriate and may improve receptor expression. Likewise, if a cysteine is in a solvent-accessible region of the protein, a more hydrophilic amino acid may be more appropriate.

Chapter II identified a pair of cysteine residues absolutely required for proper receptor expression and function. These cysteines correspond to a pair of cysteines absolutely conserved in Family A GPCRs (Chapter II, Figure 1). These cysteines form a disulfide bond that likely provides critical tertiary structure support either while the nascent receptor is folding or maintaining its native fold. Mutation of either of these cysteine residues resulted in a significant decrease in receptor protein presentation at the cell surface, as determined by cell surface ELISA (Chapter II, Figure 4A). It is possible the protein at the cell surface is not the full-length receptor and that mutation of these cysteines to alanines destabilizes the translational machinery, prematurely terminating synthesis of the mutant EP3 receptor. Western blot analysis of membrane fractions of cells expressing these mutant constructs with detection of the N-terminal HA-tag will be performed. Heterologous glycosylation may complicate interpretation of these experiments, so incubation with the glycosidase PNGase F before electrophoretic

131

resolution will also be performed. These experiments will determine the size of the expressed mutant receptors compared to wild-type receptor. Additionally, moving the HA-tag to the C-terminus may provide a handle with which to selectively purify fully translated protein.

What is more likely is that these mutant receptors are misfolded during translation. Detection of misfolded proteins would promote the degradation of these misfolded receptors, reducing surface presentation of the N-terminal HA tag antigen. Protein that did successfully traffic to the cell surface was undetectable by radioligand binding (Chapter II, Figures 3 and 4B). None of the other mutations significantly affected receptor function. Large differences in expression of some constructs were observed, though these data must be interpreted with caution as transiently-transfected HEK293 cells have variable expression levels. It is possible substitution of alternate amino acids into these positions may stabilize receptor structure and/or function. Ott *et al*. generated a mutant of the κ-opioid receptor in which cysteines were mutated to a different amino acid that has some conservation among the opioid receptor family[243]. This strategy will be employed when constructing mutant mEP3γ receptors lacking all but the disulfide cysteines.

It is also possible that mutation of C184 in the second extracellular loop of the mouse EP3 receptor uncouples agonist binding to the receptor from transduction of an intracellular signal. Residues in this region are known to be absolutely conserved among prostanoid receptors. Despite this conservation, mutation of many of these residues including the cysteine did not affect radioligand binding or ligand selectivity, though they have been shown to prevent the signal transduction through the mutant receptor[306]. Separation of the two roles of a GPCR (i.e., agonist binding and stimulation of some

132

intracellular response) is not unprecedented[307] and underlies the concept of functional selectivity. An agonist preferentially shifting the conformation of a receptor toward β-arrestin recruitment independent of G-protein activation, for example, is an example of the same phenomenon but with a more complete description of the system. More proximal measurement of mutant receptor activation using $[^{35}S]GTP\gamma S$ binding in response to PGE_2 or sulprostone will be performed to more closely study the interaction of mutant receptors and their downstream effectors.

This study provides interesting information about the tertiary structure of the mouse EP3 receptor and the role of the many cysteine residues of the receptor in supporting the normal function of the receptor. Combination of several of these mutations into a single construct is likely to maintain at least some native receptor function. Consideration of alternate missense mutations for some sites will likely improve the function and/or expression of these mutants. These data indicate a mutant of the mouse EP3 receptor completely devoid of all cysteine residues is not feasible, but overexpression can still be performed on a protein containing a single pair of cysteine residues that likely require crosslinking for normal receptor expression and function.

<u>Improvement of the pharmacokinetic properties of DG-041</u>

DG-041 is a valuable tool compound with which to study the role of the EP3 receptor in physiology and disease[73,108,147,148]. In Chapter IV, DG-041 was confirmed to be a high-affinity antagonist of the mouse EP3 receptor both in vitro and in vivo. The rapid clearance of the compound (Chapter IV, Figure 4) is not optimal for a pharmacological

133

probe, but could be improved in a number of ways. The molecule itself will be synthetically altered so that hydroxylation cannot occur. Further analytical chemistry will be required to determine precisely where the oxygen is added to DG-041 when incubated in mouse liver microsomes. Bare regions on the indole head group and the phenyl ring, the methyl side chain, and the methylene linker between the indole and phenyl ring are all possible sites of Phase I metabolism. Using an improved mass spectrometric method or NMR analysis, the exact site of modification by P450 enzymes can be identified and then blocked synthetically by substitution with a fluorine atom. Alternatively, each of the modifications can be synthesized in advance and screened for metabolism in mouse liver microsomes. It is also possible that the DG-041 metabolite is subsequently conjugated by Phase II metabolic enzymes. Further studies using mouse hepatic S9 fractions will be performed to determine whether this metabolite is a substrate for conjugation reactions.

DG-041 clearance may be independent of hepatic metabolism and the observed Phase I metabolism may be but a minor mode of clearance. To estimate in vivo CL_H of DG-041 in mice, intrinsic clearance experiments of DG-041 in mouse liver microsomes will be performed. The results of these experiments will predict the extent to which DG-041 is cleared by the liver in vivo.

Urinary excretion of DG-041 was not assessed. It is possible DG-041 is either passively filtered or actively secreted in the kidney into the urine. However, renal clearance is most common with hydrophilic compounds. Indeed, part of the goal of Phase I and II metabolism is to increase the water solubility of a molecule to promote its renal excretion. DG-041 may not be efficiently cleared by the kidney but Phase I or Phase I and II metabolism may increase the hydrophilicity (as observed by the left shift in

retention time for the metabolite in HPLC/metabolite identification experiments; Chapter IV, Figure 5) then becoming susceptible to renal clearance. Mice will be dosed similarly to Chapter IV, Figure 4 and urine will be collected and analyzed for DG-041 excretion. These data will provide a measure of renal clearance (CL_R) which will also indicate passive or active renal excretion of DG-041.

Another important consideration is whether the metabolite is pharmacologically active. On a 600 g/mol molecule, a single oxygenation may be a subtle enough change that the metabolite is still biologically active. The exact structure of the metabolite will be identified and the molecule synthesized. The molecular pharmacology of the metabolite will be determined. If the metabolite is a functional antagonist, further pharmacokinetic experiments will be performed to determine the plasma exposure of the metabolite in addition to the parent compound, as the metabolite would be expected to be biologically active as well.

Whatever the mode of clearance of DG-041, it is not likely to be the case that the DG-041 metabolite is pharmacologically active. DG-041 has been studied in acute blood experiments in mice dosed similarly to the pharmacokinetics experiment for DG-041. Oral administration of DG-041 blocked sulprostone-induced increases in blood pressure with a time course similar to that of the plasma [DG-041]-time profile, indicating no extended "biological half-life" that would be expected in the case of a pharmacologically active metabolite.

An interesting property of DG-041 and closely related molecules is that they display pseudo-irreversible binding as a result of slow, tight binding kinetics. Compounds similar to DG-041 also display a delay in the onset of receptor binding. Jones *et al*. hypothesize

this is due to a slowing of the tissue distribution of DG-041 as it is nonspecifically dissolved into phospholipid bilayers and exchanged back out[289]. Once bound to the EP3 receptor, the off-rate of DG-041 is long enough to appear irreversible on the time scale of a few hours. DG-041 blockade of the EP3 receptor was resistant to three washes over the course of at least four hours[226]. DG-041 pretreatment of adrenal chromaffin cells prevented PGE_2/EP3 mediated attenuation of voltage-dependent calcium currents, and this blockade of EP3 remains despite extensive washing[308]. The possibility of covalent addition of DG-041 to the receptor protein was considered. Michael addition by a nucleophile at the α,β-unsaturated carbonyl moiety was suspected but dismissed after incubation with DTT did not affect DG-041 binding to EP3 and after an analogue of DG-041 lacking the α,β-unsaturation displayed similar slow, tight binding kinetics[226]. More precise experiments will be performed using mass spectrometric detection of protein:DG-041 adducts.

Despite these observations, DG-041 administered to mice consistently shows EP3 antagonism for no more than a few hours (unpublished observations). It is possible some mechanism for dissociating DG-041 and recycling functional EP3 is at play. Chronic agonist stimulation of GPCRs is known to induce internalization, dissociation of the ligand within the endosomal compartment, and recycling of free receptor back to the membrane. Dissociation of DG-041 from EP3 in vivo may employ a similar mechanism to restore EP3 function faster than what is seen in vitro. Further characterization of the discrepancy between the functional half-life of DG-041 in vitro versus in vivo will be performed. Differential centrifugation will be used to separate endosomal from cell-surface receptors. Western blot analysis of subcellular fractions will be used to confirm

receptor internalization and radioligand binding to these fractions will be used to determine DG-041 binding to the receptor. Alternatively, genetic and pharmacological tools are available to prevent endosomal recycling of proteins. These manipulations can be employed against cells expressing mEP3γ and exposed to DG-041 to determine the requirement for recycling in restoration of receptor binding.

Developing a more efficient route for JD-200 synthesis

JD-200 was previously identified to have affinity for the human EP1 and EP3 receptors. JD-200 was confirmed to be an antagonist of the mouse EP1 and EP3 receptors in vitro (Chapter IV, Figures 12 and 13). The synthetic route for JD-200 was prohibitively inefficient to produce quantities required for in vivo use. Minor modifications to the structure of JD-200 will allow completion of the synthesis more efficiently. Synthesis will begin with a 2-bromo-4-trifluoromethylaniline, attaching *p*-cyanobenzyl moiety to the phenyl head group by Suzuki coupling of a benzylboronic acid to the phenyl ring at the bromine or Heck reaction coupling a styrene analogue to the same starting material. These will eliminate the phenolic linker but will also avoid the protection and deprotection steps. Use of a similar, commercially available thiophene sulfonamide will eliminate the thiophene sulfonyl chloride side route. The molecular pharmacology of the product and a series of bioisosteres will be characterized to ensure retention of receptor affinity and selectivity. These works will broaden the chemical scaffolds available for EP1 and/or EP3 antagonist tool compounds.

137

<u>Use of a novel, dual-selectivity EP1/EP3 antagonist to evaluate the role of PGE$_2$</u>

<u>receptors in hypertensive and diabetic kidney diseases</u>

Alternative chemical scaffolds for dual EP1/EP3 antagonists were pursued (Chapter III, Figure 4). Compound **17** is a dual-selectivity mouse EP1/EP3 antagonist. The starting compound upon which the analogues are based (Compound **7**) is an antagonist of the human EP1 receptor and has significant affinity for the human TP receptor and modest affinity for the mouse TP receptor. It also had weak affinity for the mouse EP2 receptor (Chapter III, Table 1). Amide and *N*-acylsulfonamide analogues of the lead compound were generated in an effort to not only block reported glucuronidation of the molecule at the carboxylate, but to improve the selectivity of the compound. Each analogue lost affinity for the mouse TP and EP2 receptors and four (**11**, **17**, **18**, and **21**) gained affinity for the mouse EP3 receptor (Chapter III, Table 3). Future work with these molecules will be to screen their affinity for a large panel of other targets rather beyond the subset of prostanoid receptors reported here. Additionally, many more substitutions of different classes will be evaluated at the same position of the lead molecule (e.g., inverse amides and tetrazoles of varying substitutions). Special focus will be placed on isosteres of **17** that lack the hydrolysable sulfonamide bond (Chapter III, Figure 8).

The highest affinity EP1 selective and EP1/EP3 selective molecules were screened for intrinsic clearance in mouse hepatic microsomes (Chapter III, Table 4). The starting molecule (**7**) displayed moderate predicted CL$_H$ while each of the six compounds subjected to the assay (**8**, **11**, **14**, **17**, **19**, and **21**) had greatly increased CL$_H$, all at values

approaching hepatic blood flow for a mouse (the theoretical maximum for the assay). In vitro metabolite identification experiments for one amide (**11**) and one sulfonamide (**17**) dual-selectivity analogues were performed using mouse hepatic microsomes and mouse hepatic S9 fractions for the in vitro detection of Phase I and Phase II metabolism (Chapter III, Figure 8). The data indicated the amide analogue (**11**) was metabolized into greater than a dozen different low abundance metabolites; whereas, the sulfonamide analogue (**17**) was metabolized into three different major metabolites. In the future, this information can be used to synthesize analogues of this compound that are resistant to these modes of metabolism. The metabolic profile of the amide analogue does not appear to be salvageable. Other amide analogues of the lead compound will be screened in this assay for better metabolic profiles.

One of the metabolites (**M1**) of the lead sulfonamide compound (**17**) is a hydrolysis product back to the starting carboxylic acid (Chapter III, Figure 8). This is notable because when the compound is administered in vivo, **7** will be generated and subsequent blockade of the TP receptor and loss of activity at the EP3 receptor may occur. Blocking hydrolysis at this site will be explored synthetically. **17** is thermally unstable (30 % degradation after four hours at 37 °C) and extensively plasma protein bound (F_u = 0.004), though no more so than the lead carboxylic acid compound **7** (F_u = 0.005).

Administration of **17** SC displayed excellent plasma exposure, amenable to chronic dosing required to study hypertension and diabetes in mice. **17** slowly reached c_{max} and was slowly eliminated from circulation, with the terminal time point (24 hours) remaining above the lower limit of detection for this assay. These pharmacokinetic

properties lend the molecule to chronic administration with a SC osmotic minipump. However, **17** was unstable in mouse plasma at 37 °C. Incubation in chemical stabilizers such as ascorbate or cyclodextrin will be performed to determine if they prevent the thermal breakdown of **17**. Stability of **17** in a pellet will be determined. DOCA is chronically delivered to mice via a SC pellet. **17** will be similarly compounded and keeping the compound out of solution may prolong its integrity.

In an in vivo assay for EP-mediated vasopressor activity (Chapter III, Figures 10 and 11), SC administration of **17** attenuated sulprostone- and 17PTPGE$_2$- stimulated vasopressor activity. **17** will be used as a tool compound to investigate the role of EP1 and EP3 in the pathophysiology of diabetic kidney disease. Lepr$^{db/db}$ eNOS$^{-/-}$ BKS mice are a well-characterized mouse model of T2DM[309]. These mice have endothelial dysfunction and are hypertensive, hyperinsulinemic, hyperglycemic, hyperlipidemic, and progress to overt DN by 24 weeks of age. Chronic administration of **17** through a SC pellet would start at 8 weeks of age. Weight, fasting blood glucose, systolic blood pressure, and urinary albumin-to-creatinine ratio (ACR) will be measured weekly. GFR will be measured by FITC-inulin clearance immediately prior to **17** pellet implantation and at the end of the study. When the DN phenotype is severe ($28 - 36$ weeks of age, will require determination by a preceding pilot study), a cohort of mice in each treatment group will have MAP determined by direct carotid catheterization. Periodic-Schiff and Masson's trichrome stains of kidney sections from each treatment group will be collected.

The untreated diabetic mice are expected to be hypertensive and hyperglycemic, to have significantly increased ACR and possibly reduced GFR. Histology should reveal

wide-spread glomerulosclerosis, tubulointerstitial fibrosis, and tubular proteinaceous casts in the kidneys of untreated diabetic mice. Chronic administration of the dual-selectivity EP1/EP3 antagonist **17** is expected to significantly attenuate each of these markers of DN. Of additional interest is whether starting administration of **17** after development of disease (20 -24 weeks of age) will improve the outcome of the mice with DN.

Determination of the tissue distribution of 17PTPGE$_2$ and sulprostone

The tissue compartments where sulprostone, 17PTPGE$_2$, and PGE$_2$ elicit their vasoactive responses will be more closely studied. In radioligand competition binding assays in cell membranes and cell-based functional assays, 17PTPGE$_2$ and sulprostone are agonists for EP1 and EP3 and both agonists have higher affinity for the mouse EP3 receptor than the mouse EP1 receptor[280]. The simplest explanation is a difference in intrinsic efficacies of the two agonists for EP1 versus EP3; that is, 17PTPGE$_2$ may have a higher intrinsic efficacy for EP1 and negligible for EP3 and the reverse for sulprostone. However, this is not likely the case. Earlier studies characterizing the mouse EP1 receptor in vitro successfully used sulprostone to study the calcium flux response to activation of EP1 in vitro[152]. Using a CHO cell-based calcium mobilization assay for the mouse EP3 receptor, sulprostone, PGE$_2$, and 17PTPGE$_2$ were each shown to be full agonists for the mouse EP3 receptor (Figure 1).
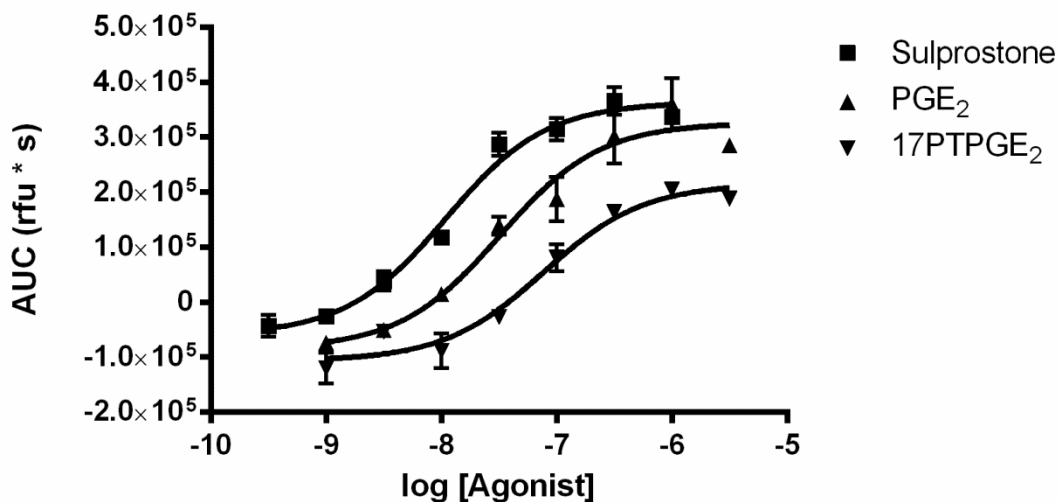
Figure 1 – FLEXstation calcium mobilization concentration response curves for sulprostone, PGE_2, and $17PTPGE_2$ at the mouse EP3γ receptor expressed in CHOk1 cells.

These in vitro data drive the hypothesis that it is not a difference in ligand binding and activation of EP1 versus EP3 receptors, but a difference in delivery of the ligand to the necessary tissue compartment to elicit its activity in vivo. The in vivo pharmacokinetic properties of sulprostone and $17PTPGE_2$ are unknown. Ionization in solution (reported as pK_a) is a physiochemical property that can determine passive diffusion across a lipid membrane, as an ionized molecule cannot passively cross a membrane. However, sulprostone, a *N*-acylsulfonamide, and $17PTPGE_2$, a carboxylic acid, are predicted to have very similar pK_as[310,311]. The ratio of ionized to unionized sulprostone or $17PTPGE_2$ could be as high as 1000:1 (plasma pH 7.4; pK_a ~4.5[310]), so these molecules are unlikely to efficiently diffuse across a membrane. Large differences

142

in lipophilicity between the two molecules are not expected. Metabolism to a compound that prefers one of the two receptors is a possibility; for example, 17PTPGE$_2$ may be a substrate for Phase I metabolism, converting the EP1 and EP3 agonist to an EP1 preferring agonist. Future experiments on the metabolism and disposition of these two molecules will be performed in an effort to explain the mechanism by which these ligands transduce their vasopressor responses through EP1 and EP3.

EP3, and not EP1, is known to mediate a vasopressor response when selective agonists are infused ICV[66]. It is possible sulprostone is a substrate for an organic anion influx transporter on the blood brain barrier and 17PTPGE$_2$ is not. This would preferentially transport sulprostone into the CNS while excluding 17PTPGE$_2$. If the EP3 vasopressor response is mediated predominately by central EP3 receptors, this may explain why the vasopressor response to sulprostone appears to be chiefly EP3-mediated and the vasopressor response to 17PTPGE$_2$ seems to almost completely EP1-mediated. Cell-based, transwell transporter assays will be performed with cultured endothelial cells and Caco-2 cells expressing blood-brain barrier transporters. Transport of 17PTPGE$_2$ or sulprostone across these monolayers will be assessed as a surrogate for transport across the blood-brain barrier. Also, in vivo brain penetrance experiments will be performed in which mice are administered an IV dose of 17PTPGE$_2$ or sulprostone and the concentration of the analyte in brain homogenates will be determined at various time points after administration.

Summary

In closing, these studies provide novel information on the relationships between structure and function of the mouse EP3 receptor. Additionally, these studies add more evidence in support of the hypothesis that simultaneous blockade of EP1 and EP3 in vivo is beneficial beyond blockade of either receptor alone. These two subtypes of PGE_2 receptors have been shown to be deleterious in chronic kidney diseases and selectively targeting them may be of greater therapeutic value with fewer side effects than inhibiting the molecular targets upstream of these receptors (e.g., mPGES-1 or COX-1/2). Further studies will provide structural information for the mouse EP3 receptor, preliminary data to test this hypothesis, develop better tool compounds for in vivo study of EP1 and EP3, and explain the conflicting in vitro and in vivo pharmacodynamics of EP ligands.

REFERENCES

1.   Mackowiak PA. Brief History of Antipyretic Therapy. *Clinical Infectious Diseases.* October 01 2000;31(Supplement 5):S154.

2.   Read J. *From Alchemy to Chemistry.* Mineola, NY: Courier Dover Publications; 1995.

3.   Arroo R, Androutsopoulos V, Patel A, Surichan S, Wilsher N, Potter G. Phytoestrogens as natural prodrugs in cancer prevention: a novel concept. *Phytochemistry Reviews.* 2008;7(3):431-443.

4.   Goodman LS, Gilman A, Brunton LL, Lazo JS, Parker KL. *Goodman & Gilman's the pharmacological basis of therapeutics.* 11th ed. New York: McGraw-Hill; 2006.

5.   Jack DB. One hundred years of aspirin. *Lancet.* Aug 1997;350(9075):437-439.

6.   Mehta A. Top Pharmaceuticals: Aspirin. *Chemical & Engineering News.* 2005;83(25).

7.   Nobelstiftelsen. *Nobel Lectures in Physiology Medicine, 1963-1970.* Elsevier; 1973.

8.   von Euler US. On the specific vaso-dilating and plain muscle stimulating substances from accessory genital glands in man and certain animals (prostaglandin and vesiglandin). *The Journal of Physiology.* 1936;88(2):213-234.

9.   Curtis-Prior P. *The Eicosanoids.* John Wiley & Sons; 2004.

10. Flower RJ. Prostaglandins, bioassay and inflammation. *British journal of pharmacology.* 01/ 2006;147 Suppl 1:S182-192.

11. McCracken JA. Prostaglandins and Leukotrienes Endocrinology. In: Melmed S, Conn PM, eds: Humana Press; 2005:93-111.

12. Horton EW. Review Lecture: The Prostaglandins. *Proceedings of the Royal Society of London. Series B, Biological Sciences.* 1972;182(1069):411-426.

13. Bergström S, Sjövall J. The Isolation of Prostaglandin F from Sheep Prostate Glands. *Acta Chem. Scand.* 1960;14:1693-1700.

14. Bergström S, Sjövall J. The Isolation of Prostaglandin E from Sheep Prostate Glands. *Acta Chem. Scand.* 1960;14:1701-1705.

15. Bergström S, Danielsson H, Samuelsson B. THE ENZYMATIC FORMATION OF PROSTAGLANDIN E2 FROM ARACHIDONIC ACID PROSTAGLANDINS AND RELATED FACTORS 32. *Biochimica et biophysica acta.* 07/ 1964;90:207-210.

16. van Dorp D, Beerthuis RK, Nugteren DH, Vonkeman H. THE BIOSYNTHEIS OF PROSTAGLANDINS. *Biochimica et biophysica acta.* 07/ 1964;90:204-207.

17. Samuelsson B. On the incorporation of oxygen in the conversion of 8, 11, 14-eicosatrienoic acid to prostaglandin E1. *J Am Chem Soc.* Jul 1965;87:3011-3013.

18. Hamberg M, Samuelsson B. Detection and isolation of an endoperoxide intermediate in prostaglandin biosynthesis. *Proceedings of the National Academy of Sciences of the United States of America.* 03/ 1973;70(3):899-903.

19.   Vane JR. Inhibition of Prostaglandin Synthesis as a Mechanism of Action for Aspirin-like Drugs. *Nature.* 1971-06-23 1971;231(25):232-235.

20.   Moncada S. Sir John Robert Vane. 29 March 1927 — 19 November 2004. 2006-12-01 2006.

21.   Johnson AG, Nguyen TV, Day RO. Do Nonsteroidal Anti-inflammatory Drugs Affect Blood Pressure? A Meta-Analysis. *Annals of Internal Medicine.* 1994;121(4):289-300.

22.   Pope J, JJ A, DT F. A meta-analysis of the effects of nonsteroidal anti-inflammatory drugs on blood pressure. *Archives of Internal Medicine.* 1993;153(4):477-484.

23.   Cinquegrani MP, Liang CS. Indomethacin attenuates the hypotensive action of hydralazine. *Clin Pharmacol Ther.* May 1986;39(5):564-570.

24.   Patak RV, Mookerjee BK, Bentzel CJ, Hysert PE, Babej M, Lee JB. Antagonism of the effects of furosemide by indomethacin in normal and hypertensive man. *Prostaglandins.* Oct 1975;10(4):649-659.

25.   Lopez-Ovejero JA, Weber MA, Drayer JI, Sealey JE, Laragh JH. Effects of indomethacin alone and during diuretic or beta-adrenoreceptor-blockade therapy on blood pressure and the renin system in essential hypertension. *Clin Sci Mol Med Suppl.* Dec 1978;4:203s-205s.

26.   Watkins J, Abbott EC, Hensby CN, Webster J, Dollery CT. Attenuation of hypotensive effect of propranolol and thiazide diuretics by indomethacin. *Br Med J.* Sep 1980;281(6242):702-705.

27.   Das UN. Modification of anti-hypertensive action of verapamil by inhibition of endogenous prostaglandin synthesis. *Prostaglandins Leukot Med.* Aug 1982;9(2):167-169.

28.   Moore TJ, Crantz FR, Hollenberg NK, et al. Contribution of prostaglandins to the antihypertensive action of captopril in essential hypertension. *Hypertension.* 1981 Mar-Apr 1981;3(2):168-173.

29.   Salvetti A, Pedrinelli R, Sassano P, Arzilli F, Turini F. Effects of prostaglandins inhibition on changes in active and inactive renin induced by antihypertensive drugs. *Clin Exp Hypertens A.* 1982;4(11-12):2435-2448.

30.   Witzgall H, Hirsch F, Scherer B, Weber PC. Acute haemodynamic and hormonal effects of captopril are diminished by indomethacin. *Clin Sci (Lond).* Jun 1982;62(6):611-615.

31.   Hawkins MM, Seelig CB. A case of acute renal failure induced by the co-administration of NSAIDs and captopril. *N C Med J.* Jun 1990;51(6):291-292.

32.   Seelig CB, Maloley PA, Campbell JR. Nephrotoxicity associated with concomitant ACE inhibitor and NSAID therapy. *South Med J.* Oct 1990;83(10):1144-1148.

33.   de Leeuw PW. Nonsteroidal Anti-Inflammatory Drugs and Hypertension: The Risks in Perspective. *Drugs.* 1996;51(2).

34.   Murray MD, Greene PK, Brater DC, Manatunga AK, Hall SD. Effects of flurbiprofen on renal function in patients with moderate renal insufficiency. *British Journal of Clinical Pharmacology.* 1992;33(4):385-393.

35. Vinci JM, Horwitz D, Zusman RM, Pisano JJ, Catt KJ, Keiser HR. The effect of converting enzyme inhibition with SQ20,881 on plasma and urinary kinins, prostaglandin E, and angiotensin II in hypertensive man. *Hypertension.* 1979 Jul-Aug 1979;1(4):416-426.

36. Swartz SL, Williams GH, Hollenberg NK, Levine L, Dluhy RG, Moore TJ. Captopril-induced changes in prostaglandin production: relationship to vascular responses in normal man. *J Clin Invest.* Jun 1980;65(6):1257-1264.

37. Smith SR, Coffman TM, Svetkey LP. Effect of low-dose aspirin on thromboxane production and the antihypertensive effect of captopril. *Journal of the American Society of Nephrology.* 1993;4(5):1133-1139.

38. Roth SH. NSAID gastropathy. A new understanding. *Arch Intern Med.* 1996 Aug 12-26 1996;156(15):1623-1628.

39. Scheiman JM. NSAIDs, gastrointestinal injury, and cytoprotection. *Gastroenterol Clin North Am.* Jun 1996;25(2):279-298.

40. Simmons DL, Levy DB, Yannoni Y, Erikson RL. Identification of a phorbol ester-repressible v-src-inducible gene. *Proceedings of the National Academy of Sciences.* 1989;86(4):1178-1182.

41. Xie WL, Chipman JG, Robertson DL, Erikson RL, Simmons DL. Expression of a mitogen-responsive gene encoding prostaglandin synthase is regulated by mRNA splicing. *Proceedings of the National Academy of Sciences.* 1991;88(7):2692-2696.

42. Varnum BC, Lim RW, Sukhatme VP, Herschman HR. Nucleotide sequence of a cDNA encoding TIS11, a message induced in Swiss 3T3 cells by the tumor promoter tetradecanoyl phorbol acetate. *Oncogene.* Jan 1989;4(1):119-120.

43. Kujubu DA, Fletcher BS, Varnum BC, Lim RW, Herschman HR. TIS10, a phorbol ester tumor promoter-inducible mRNA from Swiss 3T3 cells, encodes a novel prostaglandin synthase/cyclooxygenase homologue. *Journal of Biological Chemistry.* 1991;266(20):12866-12872.

44. Hawkey CJ. COX-2 inhibitors. *The Lancet.* 1/23/ 1999;353(9149):307-314.

45. Van Hecken A, Schwartz JI, Depre M, et al. Comparative inhibitory activity of rofecoxib, meloxicam, diclofenac, ibuprofen, and naproxen on COX-2 versus COX-1 in healthy volunteers. *The Journal of Clinical Pharmacology.* 2000;40(10):1109-1120.

46. Bombardier C, Laine L, Reicin A, et al. Comparison of upper gastrointestinal toxicity of rofecoxib and naproxen in patients with rheumatoid arthritis. VIGOR Study Group. *N Engl J Med.* Nov 2000;343(21):1520-1528, 1522 p following 1528.

47. Bresalier RS, Sandler RS, Quan H, et al. Cardiovascular events associated with rofecoxib in a colorectal adenoma chemoprevention trial. *N Engl J Med.* Mar 2005;352(11):1092-1102.

48. Nussmeier NA, Whelton AA, Brown MT, et al. Complications of the COX-2 inhibitors parecoxib and valdecoxib after cardiac surgery. *N Engl J Med.* Mar 2005;352(11):1081-1091.

49. Solomon SD, Pfeffer MA, McMurray JJ, et al. Effect of celecoxib on cardiovascular events and blood pressure in two trials for the prevention of colorectal adenomas. *Circulation.* Sep 2006;114(10):1028-1035.

50. Rahme E, Pilote L, LeLorier J. Association between naproxen use and protection against acute myocardial infarction. *Archives of internal medicine.* 2002;162(10):1111.

51. Grosser T. The pharmacology of selective inhibition of COX-2. *Thromb Haemost.* Oct 2006;96(4):393-400.

52. Bresalier RS. Prevention of colorectal cancer: tumor progression, chemoprevention, and COX-2 inhibition. *Gastroenterology.* Jul 2000;119(1):267-268.

53. Bresalier RS. Chemoprevention of intestinal polyposis by COX-2 inhibition: from mouse to man. *Gastroenterology.* Jan 2002;122(1):234-236.

54. McAdam BF, Catella-Lawson F, Mardini IA, Kapoor S, Lawson JA, FitzGerald GA. Systemic biosynthesis of prostacyclin by cyclooxygenase (COX)-2: The human pharmacology of a selective inhibitor of COX-2. *Proceedings of the National Academy of Sciences.* 1999;96(1):272-277.

55. Patrono C, Ciabattoni G, Pinca E, et al. Low dose aspirin and inhibition of thromboxane B2 production in healthy subjects. *Thrombosis Research.* // 1980;17(3–4):317-327.

56. Hata A, Breyer R. Pharmacology and signaling of prostaglandin receptors: multiple roles in inflammation and immune modulation. *Pharmacol Ther.* Aug 2004;103(2):147-166.

57. Edwards RM. Effects of prostaglandins on vasoconstrictor action in isolated renal arterioles. *Am J Physiol.* Jun 1985;248(6 Pt 2):F779-784.

58. Armstrong RA, Lawrence RA, Jones RL, Wilson NH, Collier A. Functional and ligand binding studies suggest heterogeneity of platelet prostacyclin receptors. *Br J Pharmacol.* Jul 1989;97(3):657-668.

59. Murata T, Ushikubi F, Matsuoka T, et al. Altered pain perception and inflammatory response in mice lacking prostacyclin receptor. *Nature.* Aug 14 1997;388(6643):678-682.

60. Gresele P, Arnout J, Deckmyn H, Huybrechts E, Pieters G, Vermylen J. Role of proaggregatory and antiaggregatory prostaglandins in hemostasis. Studies with combined thromboxane synthase inhibition and thromboxane receptor antagonism. *J Clin Invest.* Nov 1987;80(5):1435-1445.

61. Mais DE, DeHoll D, Sightler H, Halushka PV. Different pharmacologic activities for 13-azapinane thromboxane A2 analogs in platelets and blood vessels. *Eur J Pharmacol.* Apr 13 1988;148(3):309-315.

62. Coleman RA, Sheldrick RL. Prostanoid-induced contraction of human bronchial smooth muscle is mediated by TP-receptors. *Br J Pharmacol.* Mar 1989;96(3):688-692.

63. Valentin JP, Bessac AM, Maffre M, John GW. Nitric oxide regulation of TP receptor-mediated pulmonary vasoconstriction in the anesthetized, open-chest rat. *Eur J Pharmacol.* Vol 317. Netherlands1996:335-342.

64. Mori A, Saito M, Sakamoto K, Narita M, Nakahara T, Ishii K. Stimulation of prostanoid IP and EP(2) receptors dilates retinal arterioles and increases retinal and choroidal blood flow in rats. *Eur J Pharmacol.* Sep 2007;570(1-3):135-141.

65. Hristovska A-M, Rasmussen LE, Hansen PBL, et al. Prostaglandin E2 Induces Vascular Relaxation by E-Prostanoid 4 Receptor-Mediated Activation of Endothelial Nitric Oxide Synthase. *Hypertension.* 2007;50(3):525-530.

66. Ariumi H, Takano Y, Masumi A, et al. Roles of the central prostaglandin EP3 receptors in cardiovascular regulation in rats. *Neurosci Lett.* May 10 2002;324(1):61-64.

67. Nakayama Y, Omote K, Namiki A. Role of prostaglandin receptor EP1 in the spinal dorsal horn in carrageenan-induced inflammatory pain. *Anesthesiology.* Nov 2002;97(5):1254-1262.

68. Nakayama Y, Omote K, Kawamata T, Namiki A. Role of prostaglandin receptor subtype EP1 in prostaglandin E2-induced nociceptive transmission in the rat spinal dorsal horn. *Brain Res.* Jun 2004;1010(1-2):62-68.

69. Takasaki I, Nojima H, Shiraki K, et al. Involvement of cyclooxygenase-2 and EP3 prostaglandin receptor in acute herpetic but not postherpetic pain in mice. *Neuropharmacology.* Sep 2005;49(3):283-292.

70. Matsumura S, Abe T, Mabuchi T, et al. Rho-kinase mediates spinal nitric oxide formation by prostaglandin E2 via EP3 subtype. *Biochem Biophys Res Commun.* Dec 2005;338(1):550-557.

71. Johansson T, Narumiya S, Zeilhofer HU. Contribution of peripheral versus central EP1 prostaglandin receptors to inflammatory pain. *Neurosci Lett.* May 2011;495(2):98-101.

72. Palazzo E, Guida F, Gatta L, et al. EP1 receptor within the ventrolateral periaqueductal grey controls thermonociception and rostral ventromedial medulla cell activity in healthy and neuropathic rat. *Mol Pain.* 2011;7:82.

73. Singh J, Zeller W, Zhou N, et al. Antagonists of the EP3 receptor for prostaglandin E2 are novel antiplatelet agents that do not prolong bleeding. *ACS Chem Biol.* Feb 2009;4(2):115-126.

74. Schober LJ, Khandoga AL, Penz SM, Siess W. The EP3-agonist sulprostone, but not prostaglandin E2 potentiates platelet aggregation in human blood. *Thromb Haemost.* Jun 2010;103(6):1268-1269.

75. Petrucci G, De Cristofaro R, Rutella S, et al. Prostaglandin E2 differentially modulates human platelet function through the prostanoid EP2 and EP3 receptors. *J Pharmacol Exp Ther.* Feb 2011;336(2):391-402.

76. Iyú D, Glenn JR, White AE, Fox SC, Dovlatova N, Heptinstall S. $P2Y_{12}$ and EP3 antagonists promote the inhibitory effects of natural modulators of platelet aggregation that act via cAMP. *Platelets.* 2011;22(7):504-515.

77. Makino H, Tanaka I, Mukoyama M, et al. Prevention of diabetic nephropathy in rats by prostaglandin E receptor EP1-selective antagonist. *J Am Soc Nephrol.* Jul 2002;13(7):1757-1765.

78. Rutkai I, Feher A, Erdei N, et al. Activation of prostaglandin E2 EP1 receptor increases arteriolar tone and blood pressure in mice with type 2 diabetes. *Cardiovasc Res.* 2009;83(1):148-154.

79. Vennemann A, Gerstner A, Kern N, et al. PTGS-2-PTGER2/4 signaling pathway partially protects from diabetogenic toxicity of streptozotocin in mice. *Diabetes.* Jul 2012;61(7):1879-1887.

80. Guan Y, Zhang Y, Wu J, et al. Antihypertensive effects of selective prostaglandin E2 receptor subtype 1 targeting. *J Clin Invest.* Sep 2007;117(9):2496-2505.

81. Swan CE, Breyer RM. Prostaglandin E2 modulation of blood pressure homeostasis: studies in rodent models. *Prostaglandins Other Lipid Mediat.* Nov 2011;96(1-4):10-13.

82. Chen L, Miao Y, Zhang Y, et al. Inactivation of the E-Prostanoid 3 Receptor Attenuates the Angiotensin II Pressor Response via Decreasing Arterial Contractility. *Arterioscler Thromb Vasc Biol.* Oct 2012.

83. Bartlett CS, Boyd KL, Harris RC, Zent R, Breyer RM. EP1 Disruption Attenuates End-Organ Damage in a Mouse Model of Hypertension. *Hypertension.* Sep 2012.

84. Kajino H, Taniguchi T, Fujieda K, Ushikubi F, Muramatsu I. An EP4 receptor agonist prevents indomethacin-induced closure of rat ductus arteriosus in vivo. *Pediatr Res.* Oct 2004;56(4):586-590.

85. Momma K, Toyoshima K, Takeuchi D, Imamura S, Nakanishi T. In vivo constriction of the fetal and neonatal ductus arteriosus by a prostanoid EP4-receptor antagonist in rats. *Pediatr Res.* Nov 2005;58(5):971-975.

86. Momma K, Toyoshima K, Takeuchi D, Imamura S, Nakanishi T. In vivo reopening of the neonatal ductus arteriosus by a prostanoid EP4-receptor agonist in the rat. *Prostaglandins Other Lipid Mediat.* Dec 2005;78(1-4):117-128.

87. Segi E, Sugimoto Y, Yamasaki A, et al. Patent ductus arteriosus and neonatal death in prostaglandin receptor EP4-deficient mice. *Biochem Biophys Res Commun.* May 1998;246(1):7-12.

88. Amano H, Hayashi I, Endo H, et al. Host prostaglandin E(2)-EP3 signaling regulates tumor-associated angiogenesis and tumor growth. *J Exp Med.* Jan 2003;197(2):221-232.

89. Shoji Y, Takahashi M, Kitamura T, et al. Downregulation of prostaglandin E receptor subtype EP3 during colon cancer development. *Gut.* Aug 2004;53(8):1151-1158.

90. Amano H, Ito Y, Suzuki T, et al. Roles of a prostaglandin E-type receptor, EP3, in upregulation of matrix metalloproteinase-9 and vascular endothelial growth factor during enhancement of tumor metastasis. *Cancer Sci.* Dec 2009;100(12):2318-2324.

91. Robertson FM, Simeone AM, Lucci A, McMurray JS, Ghosh S, Cristofanilli M. Differential regulation of the aggressive phenotype of inflammatory breast cancer cells by prostanoid receptors EP3 and EP4. *Cancer.* Jun 2010;116(11 Suppl):2806-2814.

92. Sakairi Y, Jacobson HR, Noland TD, Breyer MD. Luminal prostaglandin E receptors regulate salt and water transport in rabbit cortical collecting duct. *Am J Physiol.* Aug 1995;269(2 Pt 2):F257-265.

93. Breyer MD, Zhang Y, Guan YF, Hao CM, Hebert RL, Breyer RM. Regulation of renal function by prostaglandin E receptors. *Kidney Int Suppl.* Sep 1998;67:S88-94.

94. USRDS. USRDS Annual Data Report: Atlas of End-Stage Renal Disease in the United States. In: System USRD, Health NIo, Diseases NIoDaDaK, eds. *USRDS Annual Data Report: Atlas of End-Stage Renal Disease in the United States*. Bethesda, MD: National Institutes of Health, National Institute of Diabetes and Digestive and Kidney Diseases; 2011.

95. Shoelson S. Invited comment on W. Ebstein: On the therapy of diabetes mellitus, in particular on the application of sodium salicylate. Oct 01 2002(10):618-619.

96. James R, Macdougall AI, Andrews MM. Aspirin and Diabetes Mellitus. *BMJ.* 1957;2.

97. Robertson RP, Gavareski DJ, Porte D, Bierman EL. Inhibition of in vivo insulin secretion by prostaglandin E1. *J Clin Invest.* Aug 1974;54(2):310-315.

98. Giugliano D, Torella R, Sgambato S, D'Onofrio F. Effects of alpha-and beta-adrenergic inhibition and somatostatin on plasma glucose, free fatty acids, insulin glucagon and growth hormone responses to prostaglandin E1 in man. *J Clin Endocrinol Metab.* Feb 1979;48(2):302-308.

99. Saccà L, Perez G. Influence of prostaglandins on plasma glucagon levels in the rat. *Metabolism.* 2// 1976;25(2):127-130.

100. Ganguli S, Sperling MA, Frame C, Christensen R. Inhibition of glucagon-induced hepatic glucose production by indomethacin. *American Journal of Physiology - Endocrinology And Metabolism.* 1979;236(4):E358.

101. Metz SA, Robertson RP, Fujimoto WY. Inhibition of prostaglandin E synthesis augments glucose-induced insulin secretion is cultured pancreas. *Diabetes.* Jul 1981;30(7):551-557.

102. Robertson RP, Chen M. A role for prostaglandin E in defective insulin secretion and carbohydrate intolerance in diabetes mellitus. *J Clin Invest.* Sep 1977;60(3):747-753.

103. Giugliano D, Sgamboto S, Coppola L, Misso L, Torella R. Impaired insulin secretion in human diabetes mellitus. II. A possible role for prostaglandins. *Prostaglandins Med.* Jan 1981;6(1):41-50.

104. McRae JR, Metz SA, Robertson RP. A role for endogenous prostaglandins in defective glucose potentiation of nonglucose insulin secretagogues in diabetics. *Metabolism.* Vol 30. United States1981:1065-1075.

105. Tran PO, Gleason CE, Poitout V, Robertson RP. Prostaglandin E(2) mediates inhibition of insulin secretion by interleukin-1beta. *J Biol Chem.* Oct 1999;274(44):31245-31248.

106. Tran PO, Gleason CE, Robertson RP. Inhibition of interleukin-1beta-induced COX-2 and EP3 gene expression by sodium salicylate enhances pancreatic islet beta-cell function. *Diabetes.* Jun 2002;51(6):1772-1778.

107. Matsumoto T, Noguchi E, Ishida K, Kobayashi T, Yamada N, Kamata K. Metformin normalizes endothelial function by suppressing vasoconstrictor prostanoids in mesenteric arteries from OLETF rats, a model of type 2 diabetes. *American Journal of Physiology - Heart and Circulatory Physiology.* 2008;295(3):H1165-H1176.

108. Chissoe S, Inventor; SmithKline Beecham Corportation, assignee. Genes Associated with Type II Diabetes Mellitus. 2006.

109. Gurwitz JH, Avorn J, Bohn RL, Glynn RJ, Monane M, Mogun H. Initiation of antihypertensive treatment during nonsteroidal anti-inflammatory drug therapy. *JAMA.* Sep 1994;272(10):781-786.

110. Ruilope L, Robles RG, Barrientos A, et al. The Role of Urinary PGE2 and Renin-Angiotensin-Aldosterone System in the Pathogenesis of Essential Hypertension. *Clinical and Experimental Hypertension.* 1982/01/01 1982;a4(6):989-1000.

111. Lewis EJ, Hunsicker LG, Clarke WR, et al. Renoprotective effect of the angiotensin-receptor antagonist irbesartan in patients with nephropathy due to type 2 diabetes. *N Engl J Med.* Sep 2001;345(12):851-860.

112. Brenner BM, Cooper ME, de Zeeuw D, et al. Effects of losartan on renal and cardiovascular outcomes in patients with type 2 diabetes and nephropathy. *N Engl J Med.* Sep 2001;345(12):861-869.

113. Flack JM. Epidemiology and unmet needs in hypertension. *J Manag Care Pharm.* Oct 2007;13(8 Suppl B):2-8.

114. Schmieder RE. End organ damage in hypertension. *Dtsch Arztebl Int.* Dec 2010;107(49):866-873.

115. Imanishi M, Kawamura M, Akabane S, et al. Aspirin lowers blood pressure in patients with renovascular hypertension. *Hypertension.* Nov 1989;14(5):461-468.

116. Eklund B, Carlson LA. Central and peripheral circulatory effects and metabolic effects of different prostaglandins given I.V. to man. *Prostaglandins.* Aug 1980;20(2):333-347.

117. Ferreira SH, Vane JR. Prostaglandins: Their Disappearance from and Release into the Circulation. *Nature.* 12/02/print 1967;216(5118):868-873.

118. Hockel GM, Cowley AW. Prostaglandin E2-induced hypertension in conscious dogs. *Am J Physiol.* Oct 1979;237(4):H449-454.

119. Audoly LP, Tilley SL, Goulet J, et al. Identification of specific EP receptors responsible for the hemodynamic effects of PGE2. *Am J Physiol.* Sep 1999;277(3 Pt 2):H924-930.

120. Zhang Y, Guan Y, Schneider A, Brandon S, Breyer RM, Breyer MD. Characterization of murine vasopressor and vasodepressor prostaglandin E(2) receptors. *Hypertension.* May 2000;35(5):1129-1134.

121. Jakobsson P-J, Thorén S, Morgenstern R, Samuelsson B. Identification of human prostaglandin E synthase: A microsomal, glutathione-dependent, inducible enzyme, constituting a potential novel drug target. *Proceedings of the National Academy of Sciences.* 1999;96(13):7220-7225.

122. Murakami M, Naraba H, Tanioka T, et al. Regulation of prostaglandin E2 biosynthesis by inducible membrane-associated prostaglandin E2 synthase that acts in concert with cyclooxygenase-2. *J Biol Chem.* Vol 275. United States2000:32783-32792.

123. Murakami M, Nakashima K, Kamei D, et al. Cellular prostaglandin E2 production by membrane-bound prostaglandin E synthase-2 via both cyclooxygenases-1 and -2. *J Biol Chem.* Vol 278. United States2003:37937-37947.

124. Watanabe K, Kurihara K, Suzuki T. Purification and characterization of membrane-bound prostaglandin E synthase from bovine heart. *Biochimica et*

Biophysica Acta (BBA) - Molecular and Cell Biology of Lipids. 8/18/1999;1439(3):406-414.

125. Tanioka T, Nakatani Y, Semmyo N, Murakami M, Kudo I. Molecular identification of cytosolic prostaglandin E2 synthase that is functionally coupled with cyclooxygenase-1 in immediate prostaglandin E2 biosynthesis. *J Biol Chem.* Vol 275. United States2000:32775-32782.

126. Facemire CS, Griffiths R, Audoly LP, Koller BH, Coffman TM. The Impact of Microsomal Prostaglandin E Synthase 1 on Blood Pressure Is Determined by Genetic Background. *Hypertension.* 2010;55(2):531-538.

127. Wang M, Lee E, Song W, et al. Microsomal Prostaglandin E Synthase-1 Deletion Suppresses Oxidative Stress and Angiotensin II–Induced Abdominal Aortic Aneurysm Formation. *Circulation.* 2008;117(10):1302-1309.

128. Quraishi O, Mancini JA, Riendeau D. Inhibition of inducible prostaglandin E(2) synthase by 15-deoxy-Delta(12,14)-prostaglandin J(2) and polyunsaturated fatty acids. *Biochem Pharmacol.* Vol 63. England2002:1183-1189.

129. Riendeau D, Aspiotis R, Ethier D, et al. Inhibitors of the inducible microsomal prostaglandin E2 synthase (mPGES-1) derived from MK-886. *Bioorg Med Chem Lett.* Vol 15. England2005:3352-3355.

130. Cote B, Boulet L, Brideau C, et al. Substituted phenanthrene imidazoles as potent, selective, and orally active mPGES-1 inhibitors. *Bioorg Med Chem Lett.* Vol 17. England2007:6816-6820.

131. Nakano J, Anggård E, Samuelsson B. 15-Hydroxy-prostanoate dehydrogenase. Prostaglandins as substrates and inhibitors. *Eur J Biochem.* Dec 1969;11(2):386-389.

132. Anderson MW, Eling TE. Prostaglandin removal and metabolism by isolated perfused rat lung. *Prostaglandins.* Apr 1976;11(4):645-677.

133. Kanai N, Lu R, Satriano JA, Bao Y, Wolkoff AW, Schuster VL. Identification and Characterization of a Prostaglandin Transporter. *Science.* 1995;268(5212):866-869.

134. Chan BS, Satriano JA, Pucci M, Schuster VL. Mechanism of prostaglandin E2 transport across the plasma membrane of HeLa cells and Xenopus oocytes expressing the prostaglandin transporter "PGT". *J Biol Chem.* Mar 20 1998;273(12):6689-6697.

135. Itoh S, Lu R, Bao Y, Morrow JD, Roberts LJ, Schuster VL. Structural determinants of substrates for the prostaglandin transporter PGT. *Mol Pharmacol.* Oct 1996;50(4):738-742.

136. Chan BS, Bao Y, Schuster VL. Role of Conserved Transmembrane Cationic Amino Acids in the Prostaglandin Transporter PGT†. *Biochemistry.* 2002/07/01 2002;41(29):9215-9221.

137. Bito LZ, Salvador EV. Effects of anti-inflammatory agents and some other drugs on prostaglandin biotransport. *Journal of Pharmacology and Experimental Therapeutics.* 1976;198(2):481-488.

138. Chi Y, Khersonsky SM, Chang Y-T, Schuster VL. Identification of a New Class of Prostaglandin Transporter Inhibitors and Characterization of Their Biological

Effects on Prostaglandin E2 Transport. *Journal of Pharmacology and Experimental Therapeutics.* 2006;316(3):1346-1350.

139. Schuster VL, Chi Y, Chang YT, Min J, Inventors; Albert Einstein College of Medicine or Yeshiva University, assignee. Prostaglandin Transporter Inhibitors. US patent 8,227,466 B2. 07/24/2012, 2012.

140. Änggård E, Samuelsson B. Prostaglandins and Related Factors. *Journal of Biological Chemistry.* 1964;239(12):4097-4102.

141. Ensor CM, Yang JY, Okita RT, Tai HH. Cloning and sequence analysis of the cDNA for human placental NAD(+)-dependent 15-hydroxyprostaglandin dehydrogenase. *Journal of Biological Chemistry.* 1990;265(25):14888-14891.

142. Flower RJ. Drugs Which Inhibit Prostaglandin Biosynthesis. *Pharmacological Reviews.* 1974;26(1):33-67.

143. Berry CN, Hoult JRS, Phillips JA, McCarthy TM, Agback H. Highly potent inhibition of prostaglandin 15-hydroxydehydrogenase in-vitro and of prostaglandin inactivation in perfused lung by the new azobenzene analogue, Ph CL 28A. *Journal of Pharmacy and Pharmacology.* 1985;37(9):622-628.

144. Niesen FH, Schultz L, Jadhav A, et al. High-Affinity Inhibitors of Human NAD$^+$-Dependent 15-Hydroxyprostaglandin Dehydrogenase: Mechanisms of Inhibition and Structure-Activity Relationships. *PLoS ONE.* 2010;5(11):e13719.

145. Xiao C-Y, Yuhki K-i, Hara A, et al. Prostaglandin E2 Protects the Heart From Ischemia-Reperfusion Injury via Its Receptor Subtype EP4. *Circulation.* 2004;109(20):2462-2468.

146. Jiang J, Ganesh T, Du Y, et al. Neuroprotection by selective allosteric potentiators of the EP2 prostaglandin receptor. *Proceedings of the National Academy of Sciences.* 2010;107(5):2307-2312.

147. Ikeda-Matsuo Y, Tanji H, Narumiya S, Sasaki Y. Inhibition of prostaglandin E2 EP3 receptors improves stroke injury via anti-inflammatory and anti-apoptotic mechanisms. *Journal of Neuroimmunology.* 9/15/ 2011;238(1–2):34-43.

148. Ikeda-Matsuo Y, Laboratory of Pharmacology SoPS, Kitasato University, Tokyo, Japan, and, Tanji H, et al. Microsomal prostaglandin E synthase-1 contributes to ischaemic excitotoxicity through prostaglandin E2 EP3 receptors. *British Journal of Pharmacology.* 2012;160(4):847-859.

149. Nakagawa T, Masuda T, Watanabe T, Minami M, Satoh M. Possible involvement of the locus coeruleus in inhibition by prostanoid EP3 receptor-selective agonists of morphine withdrawal syndrome in rats. *European Journal of Pharmacology.* 3/3/ 2000;390(3):257-266.

150. Watabe A, Sugimoto Y, Honda A, et al. Cloning and expression of cDNA for a mouse EP1 subtype of prostaglandin E receptor. *J Biol Chem.* Sep 1993;268(27):20175-20178.

151. Funk CD, Furci L, FitzGerald GA, et al. Cloning and expression of a cDNA for the human prostaglandin E receptor EP1 subtype. *J Biol Chem.* Dec 15 1993;268(35):26767-26772.

152. Katoh H, Watabe A, Sugimoto Y, Ichikawa A, Negishi M. Characterization of the signal transduction of prostaglandin E receptor EP1 subtype in cDNA-transfected Chinese hamster ovary cells. *Biochim Biophys Acta.* May 11 1995;1244(1):41-48.
153. Ji R, Chou C-L, Xu W, Chen X-B, Woodward DF, Regan JW. EP1 Prostanoid Receptor Coupling to Gi/o Up-Regulates the Expression of Hypoxia-Inducible Factor-1α through Activation of a Phosphoinositide-3 Kinase Signaling Pathway. *Molecular Pharmacology.* 2010;77(6):1025-1036.
154. McGraw DW, Mihlbachler KA, Schwarb MR, et al. Airway smooth muscle prostaglandin-EP1 receptors directly modulate β2–adrenergic receptors within a unique heterodimeric complex. *The Journal of Clinical Investigation.* 2006;116(5):1400-1409.
155. Stock JL, Shinjo K, Burkhardt J, et al. The prostaglandin E2 EP1 receptor mediates pain perception and regulates blood pressure. *J Clin Invest.* Feb 2001;107(3):325-331.
156. Capone C, Faraco G, Anrather J, Zhou P, Iadecola C. Cyclooxygenase 1-derived prostaglandin E2 and EP1 receptors are required for the cerebrovascular dysfunction induced by angiotensin II. *Hypertension.* Apr 2010;55(4):911-917.
157. Sanner JH. Antagonism of prostaglandin E2 by 1-acetyl-2-(8-chloro-10, 11-dihydrodibenz (b, f)(1, 4) oxazepine-10-carbonyl) hydrazine (SC-19220). *Archives internationales de pharmacodynamie et de thérapie.* 1969;180(1):46.
158. Hallinan EA, Hagen TJ, Husa RK, et al. N-substituted dibenzoxazepines as analgesic PGE2 antagonists. *J Med Chem.* Oct 29 1993;36(22):3293-3299.
159. Hallinan E, Stapelfeld A, Savage MA, Reichman M. 8-chlorodibenz [b, f][1, 4] oxazepine-10 (11H)-carboxylic acid, 2-[3-[2-(furanylmethyl) thio]-1-oxopropyl] hydrazide (SC-51322): A potent PGE< sub> 2</sub> antagonist and analgesic. *Bioorganic & Medicinal Chemistry Letters.* 1994;4(3):509-514.
160. Coleman RA, Kennedy I, Sheldrick RLG. AH6809, a prostanoid EP1 receptor blocking drug. *Br. J. Pharmacol.* 1985;85:273P.
161. Kawahara H, Sakamoto A, Takeda S, Onodera H, Imaki J, Ogawa R. A prostaglandin E2 receptor subtype EP1 receptor antagonist (ONO-8711) reduces hyperalgesia, allodynia, and c-fos gene expression in rats with chronic nerve constriction. *Anesth Analg.* Oct 2001;93(4):1012-1017.
162. Omote K, Kawamata T, Nakayama Y, Kawamata M, Hazama K, Namiki A. The effects of peripheral administration of a novel selective antagonist for prostaglandin E receptor subtype EP(1), ONO-8711, in a rat model of postoperative pain. *Anesth Analg.* Jan 2001;92(1):233-238.
163. Omote K, Yamamoto H, Kawamata T, Nakayama Y, Namiki A. The effects of intrathecal administration of an antagonist for prostaglandin E receptor subtype EP(1) on mechanical and thermal hyperalgesia in a rat model of postoperative pain. *Anesth Analg.* Dec 2002;95(6):1708-1712, table of contents.
164. Hall A, Atkinson S, Brown SH, et al. Structure–activity relationships of 1,5-biaryl pyrroles as EP1 receptor antagonists. *Bioorg Med Chem Lett.* 7/15/ 2006;16(14):3657-3662.

165. Hall A, Brown SH, Chessell IP, et al. 1,5-Biaryl pyrrole derivatives as EP1 receptor antagonists: Structure–activity relationships of 4- and 5-substituted benzoic acid derivatives. *Bioorg Med Chem Lett.* 2/1/ 2007;17(3):732-735.
166. Hall A, Brown SH, Budd C, et al. Discovery of GSK345931A: An EP1 receptor antagonist with efficacy in preclinical models of inflammatory pain. *Bioorg Med Chem Lett.* 1/15/ 2009;19(2):497-501.
167. Hall A, Billinton A, Bristow AK, et al. Discovery of brain penetrant, soluble, pyrazole amide EP1 receptor antagonists. *Bioorg Med Chem Lett.* 7/15/ 2008;18(14):4027-4032.
168. Hall A, Billinton A, Brown SH, et al. Discovery of sodium 6-[(5-chloro-2-{[(4-chloro-2-fluorophenyl)methyl]oxy}phenyl)methyl]-2-pyridinecarboxylate (GSK269984A) an EP1 receptor antagonist for the treatment of inflammatory pain. *Bioorg Med Chem Lett.* 5/1/ 2009;19(9):2599-2603.
169. McKeown SC, Hall A, Giblin GMP, et al. Identification of novel pyrazole acid antagonists for the EP1 receptor. *Bioorg Med Chem Lett.* 9/15/ 2006;16(18):4767-4771.
170. Allan AC, Billinton A, Brown SH, et al. Discovery of a novel series of nonacidic benzofuran EP1 receptor antagonists. *Bioorg Med Chem Lett.* 7/15/ 2011;21(14):4343-4348.
171. Honda A, Sugimoto Y, Namba T, et al. Cloning and expression of a cDNA for mouse prostaglandin E receptor EP2 subtype. *Journal of Biological Chemistry.* 1993;268(11):7759-7762.
172. Bastien L, Sawyer N, Grygorczyk R, Metters KM, Adam M. Cloning, functional expression, and characterization of the human prostaglandin E2 receptor EP2 subtype. *Journal of Biological Chemistry.* 1994;269(16):11873-11877.
173. Regan JW, Bailey TJ, Pepperl DJ, et al. Cloning of a novel human prostaglandin receptor with characteristics of the pharmacologically defined EP2 subtype. *Molecular Pharmacology.* 1994;46(2):213-220.
174. Nishigaki N, Negishi M, Honda A, et al. Identification of prostaglandin E receptor 'EP2' cloned from mastocytoma cells as EP4 subtype. *FEBS Letters.* 5/15/ 1995;364(3):339-341.
175. Abramovitz M, Adam M, Boie Y, et al. The utilization of recombinant prostanoid receptors to determine the affinities and selectivities of prostaglandins and related analogs. *Biochim Biophys Acta.* Jan 2000;1483(2):285-293.
176. Chun K-S, Lao H-C, Langenbach R. The Prostaglandin E2 Receptor, EP2, Stimulates Keratinocyte Proliferation in Mouse Skin by G Protein-dependent and β-Arrestin1-dependent Signaling Pathways. *Journal of Biological Chemistry.* 2010;285(51):39672-39681.
177. Tilley SL, Audoly LP, Hicks EH, et al. Reproductive failure and reduced blood pressure in mice lacking the EP2 prostaglandin E2 receptor. *J Clin Invest.* Jun 1999;103(11):1539-1545.
178. Kennedy CR, Zhang Y, Brandon S, et al. Salt-sensitive hypertension and reduced fertility in mice lacking the prostaglandin EP2 receptor. *Nat Med.* Feb 1999;5(2):217-220.

179. Gardiner PJ. Characterization of prostanoid relaxant/inhibitory receptors (psi) using a highly selective agonist, TR4979. *Br J Pharmacol.* Jan 1986;87(1):45-56.

180. Tani K, Naganawa A, Ishida A, et al. Development of a highly selective EP2-receptor agonist. Part 1: identification of 16-hydroxy-17,17-trimethylene PGE2 derivatives. *Bioorganic & Medicinal Chemistry.* 4// 2002;10(4):1093-1106.

181. Sugimoto Y, Namba T, Honda A, et al. Cloning and expression of a cDNA for mouse prostaglandin E receptor EP3 subtype. *J Biol Chem.* Apr 1992;267(10):6463-6466.

182. Sugimoto Y, Negishi M, Hayashi Y, et al. Two isoforms of the EP3 receptor with different carboxyl-terminal domains. Identical ligand binding properties and different coupling properties with Gi proteins. *Journal of Biological Chemistry.* 02/05/1993 1993;268(4):2712-2718.

183. Irie A, Sugimoto Y, Namba T, et al. Third isoform of the prostaglandin-E-receptor EP3 subtype with different C-terminal tail coupling to both stimulation and inhibition of adenylate cyclase. *Eur J Biochem.* Oct 1 1993;217(1):313-318.

184. Regan JW, Bailey TJ, Donello JE, et al. Molecular cloning and expression of human EP3 receptors: evidence of three variants with differing carboxyl termini. *Br J Pharmacol.* Jun 1994;112(2):377-385.

185. Yang J, Xia M, Goetzl EJ, An S. Cloning and expression of the EP3-subtype of human receptors for prostaglandin E2. *Biochem Biophys Res Commun.* 1994;198(3):999-1006.

186. Kunapuli SP, Fen Mao G, Bastepe M, et al. Cloning and expression of a prostaglandin E receptor EP3 subtype from human erythroleukaemia cells. *Biochem J.* Mar 1 1994;298 (Pt 2):263-267.

187. Pierce KL, Regan JW. Prostanoid receptor heterogeneity through alternative mRNA splicing. *Life Sci.* 1998;62(17-18):1479-1483.

188. Sugimoto Y, Negishi M, Hayashi Y, et al. Two isoforms of the EP3 receptor with different carboxyl-terminal domains. Identical ligand binding properties and different coupling properties with Gi proteins. *Journal of Biological Chemistry.* 1993;268(4):2712-2718.

189. De Lean A, Stadel JM, Lefkowitz RJ. A ternary complex model explains the agonist-specific binding properties of the adenylate cyclase-coupled beta-adrenergic receptor. *Journal of Biological Chemistry.* 1980;255(15):7108-7117.

190. Negishi M, Sugimoto Y, Irie A, Narumiya S, Ichikawa A. Two isoforms of prostaglandin E receptor EP3 subtype. Different COOH-terminal domains determine sensitivity to agonist-induced desensitization. *Journal of Biological Chemistry.* 1993;268(13):9517-9521.

191. Namba T, Sugimoto Y, Negishi M, et al. Alternative splicing of C-terminal tail of prostaglandin E receptor subtype EP3 determines G-protein specificity. *Nature.* Sep 9 1993;365(6442):166-170.

192. An S, Yang J, So SW, Zeng L, Goetzl EJ. Isoforms of the EP3 subtype of human prostaglandin E2 receptor transduce both intracellular calcium and cAMP signals. *Biochemistry.* Dec 6 1994;33(48):14496-14502.

193. Hasegawa H, Negishi M, Ichikawa A. Two isoforms of the prostaglandin E receptor EP3 subtype different in agonist-independent constitutive activity. *Journal of Biological Chemistry.* 1996;271(4):1857-1860.

194. Negishi M, Hasegawa H, Ichikawa A. Prostaglandin E receptor EP3γ isoform, with mostly full constitutive Gi activity and agonist-dependent Gs activity. *FEBS letters.* 1996;386(2):165-168.

195. Kimura K, Ito M, Amano M, et al. Regulation of Myosin Phosphatase by Rho and Rho-Associated Kinase (Rho-Kinase). *Science.* 1996;273(5272):245-248.

196. Masumoto A, Mohri M, Shimokawa H, Urakami L, Usui M, Takeshita A. Suppression of Coronary Artery Spasm by the Rho-Kinase Inhibitor Fasudil in Patients With Vasospastic Angina. *Circulation.* 2002;105(13):1545-1547.

197. Fukumoto Y, Matoba T, Ito A, et al. Acute vasodilator effects of a Rho-kinase inhibitor, fasudil, in patients with severe pulmonary hypertension. *Heart.* 2005;91(3):391-392.

198. Shibuya M, Hirai S, Seto M, Satoh S, Ohtomo E. Effects of fasudil in acute ischemic stroke: results of a prospective placebo-controlled double-blind trial. *J Neurol Sci.* 2005;238(1-2):31-39.

199. Qian YM, Jones RL, Chan KM, Stock AI, Ho JK. Potent contractile actions of prostanoid EP3-receptor agonists on human isolated pulmonary artery. *Br J Pharmacol.* Oct 1994;113(2):369-374.

200. Jones RL, Qian Y-m, Chan K-m, Yim APC. Characterization of a prostanoid EP3-receptor in guinea-pig aorta: partial agonist action of the non-prostanoid ONO-AP-324. *British Journal of Pharmacology.* 1998;125(6):1288-1296.

201. Jones RL, Chan K-m. Distinction between relaxations induced via prostanoid EP4 and IP1 receptors in pig and rabbit blood vessels. *British Journal of Pharmacology.* 2001;134(2):313-324.

202. Shum WWC, Le G-y, Jones RL, Gurney AM, Sasaki Y. Involvement of Rho-kinase in contraction of guinea-pig aorta induced by prostanoid EP3 receptor agonists. *British Journal of Pharmacology.* 2003;139(8):1449-1461.

203. Narumiya S, Ishizaki T, Watanabe N. Rho effectors and reorganization of actin cytoskeleton. *FEBS Lett.* Vol 410. Netherlands1997:68-72.

204. Grantham JJ, Orloff J. Effect of prostaglandin E1 on the permeability response of the isolated collecting tubule to vasopressin, adenosine 3',5'-monophosphate, and theophylline. *J Clin Invest.* May 1968;47(5):1154-1161.

205. Nadler SP, Hebert SC, Brenner BM. PGE2, forskolin, and cholera toxin interactions in rabbit cortical collecting tubule. *Am J Physiol.* Jan 1986;250(1 Pt 2):F127-135.

206. Tamma G, Wiesner B, Furkert J, et al. The prostaglandin E2 analogue sulprostone antagonizes vasopressin-induced antidiuresis through activation of Rho. *J Cell Sci.* Aug 2003;116(Pt 16):3285-3294.

207. van den Berghe N, Barros LF, van Mackelenbergh MG, Krans HM. Clostridium botulinum C3 exoenzyme stimulates GLUT4-mediated glucose transport, but not glycogen synthesis, in 3T3-L1 adipocytes--a potential role of rho? *Biochem Biophys Res Commun.* Dec 1996;229(2):430-439.

208. PÜSchel GP, Kirchner C, SchrÖDer A, Jungermann K. Glycogenolytic and antiglycogenolytic prostaglandin E2 actions in rat hepatocytes are mediated via different signalling pathways. *European Journal of Biochemistry.* 1993;218(3):1083-1089.

209. Henkel J, Neuschäfer-Rube F, Pathe-Neuschäfer-Rube A, Püschel GP. Aggravation by prostaglandin E2 of interleukin-6-dependent insulin resistance in hepatocytes. *Hepatology.* 2009;50(3):781-790.

210. Ushikubi F, Segi E, Sugimoto Y, et al. Impaired febrile response in mice lacking the prostaglandin E receptor subtype EP3. *Nature.* Sep 17 1998;395(6699):281-284.

211. Yokotani K, Nishihara M, Murakami Y, Hasegawa T, Okuma Y, Osumi Y. Elevation of plasma noradrenaline levels in urethane-anaesthetized rats by activation of central prostanoid EP3 receptors. *British Journal of Pharmacology.* 1995;115(4):672-676.

212. Zhang Z-H, Wei S-G, Francis J, Felder RB. Cardiovascular and renal sympathetic activation by blood-borne TNF-α in rat: the role of central prostaglandins. *American Journal of Physiology - Regulatory, Integrative and Comparative Physiology.* 2003;284(4):R916-R927.

213. Nakagawa T, Minami M, Katsumata S, Ienaga Y, Satoh M. Suppression of naloxone-precipitated withdrawal jumps in morphine-dependent mice by stimulation of prostaglandin EP3 receptor. *British Journal of Pharmacology.* 1995;116(6):2661-2666.

214. Anggadiredja K, Yamaguchi T, Tanaka H, Shoyama Y, Watanabe S, Yamamoto T. Prostaglandin E2 attenuates SR141716A-precipitated withdrawal in tetrahydrocannabinol-dependent mice. *Brain Research.* 3/14/ 2003;966(1):47-53.

215. Nakamura K, Kaneko T, Yamashita Y, Hasegawa H, Katoh H, Negishi M. Immunohistochemical localization of prostaglandin EP3 receptor in the rat nervous system. *The Journal of Comparative Neurology.* 2000;421(4):543-569.

216. Nakamura K, Li YQ, Kaneko T, Katoh H, Negishi M. Prostaglandin EP3 receptor protein in serotonin and catecholamine cell groups: a double immunofluorescence study in the rat brain. *Neuroscience.* 3/21/ 2001;103(3):763-775.

217. Jouvet M. Biogenic amines and the states of sleep. *Science.* 1969.

218. Sara SJ, Devauges V. Idazoxan, an< i> α</i>-2 antagonist, facilitates memory retrieval in the rat. *Behavioral and neural biology.* 1989;51(3):401-411.

219. Fields HL, Heinricher MM, Mason P. Neurotransmitters in nociceptive modulatory circuits. *Annual review of neuroscience.* 1991;14(1):219-245.

220. Ek M, Arias C, Sawchenko P, Ericsson-Dahlstrand A. Distribution of the EP3 prostaglandin E2 receptor subtype in the rat brain: Relationship to sites of interleukin-1–induced cellular responsiveness. *The Journal of comparative neurology.* 2000;428(1):5-20.

221. Molderings GJ, Colling E, Likungu J, Jakschik J, Göthert M. Modulation of noradrenaline release from the sympathetic nerves of the human saphenous vein and pulmonary artery by presynaptic EP3-and DP-receptors. *British journal of pharmacology.* 1994;111(3):733-738.

222. Guyton AC, Hall JE. *Textbook of medical physiology.* 11th ed. Philadelphia: Elsevier Saunders; 2006.

223. Tani K, Asada M, Kobayashi K, Narita M, Ogawa M, Inventors; ONO Pharmaceutical Co., Ltd., assignee. Carboxylic acid derivatives and pharmaceutical agent comprising the same as active ingredient. US patent 7,786,161 B2. 08/31/2010, 2010.

224. Zegar S, Tokar C, Enache LA, et al. Development of a Scalable Process for DG-041, a Potent EP3 Receptor Antagonist, via Tandem Heck Reactions. *Organic Process Research & Development.* 2007/07/01 2007;11(4):747-753.

225. Heptinstall S, Espinosa DI, Manolopoulos P, et al. DG-041 inhibits the EP3 prostanoid receptor—A new target for inhibition of platelet function in atherothrombotic disease. *Platelets.* 2008/01/01 2008;19(8):605-613.

226. Singh J, Zeller W, Zhou N, et al. Structure−Activity Relationship Studies Leading to the Identification of (2E)-3-[l-[(2,4-Dichlorophenyl)methyl]-5-fluoro-3-methyl-lH-indol-7-yl]-N-[(4,5-dichloro-2-thienyl)sulfonyl]-2-propenamide (DG-041), a Potent and Selective Prostanoid EP3 Receptor Antagonist, as a Novel Antiplatelet Agent That Does Not Prolong Bleeding. *Journal of Medicinal Chemistry.* 2010/01/14 2009;53(1):18-36.

227. Juteau H, Gareau Y, Labelle M, et al. Structure–activity relationship of cinnamic acylsulfonamide analogues on the human EP3 prostanoid receptor. *Bioorganic & Medicinal Chemistry.* 8// 2001;9(8):1977-1984.

228. Coleman RA, Grix SP, Head SA, Louttit JB, Mallett A, Sheldrick RLG. A novel inhibitory prostanoid receptor in piglet saphenous vein. *Prostaglandins.* 1994;47(2):151-168.

229. Buchanan FG, Gorden DL, Matta P, Shi Q, Matrisian LM, DuBois RN. Role of beta-arrestin 1 in the metastatic progression of colorectal cancer. *Proc Natl Acad Sci U S A.* Vol 103. United States2006:1492-1497.

230. Kim JI, Lakshmikanthan V, Frilot N, Daaka Y. Prostaglandin E2 Promotes Lung Cancer Cell Migration via EP4-βArrestin1-c-Src Signalsome. *Molecular Cancer Research.* 2010;8(4):569-577.

231. Leduc M, Breton B, Galés C, et al. Functional selectivity of natural and synthetic prostaglandin EP4 receptor ligands. *Journal of Pharmacology and Experimental Therapeutics.* 2009;331(1):297-307.

232. Nguyen M, Camenisch T, Snouwaert JN, et al. The prostaglandin receptor EP4 triggers remodelling of the cardiovascular system at birth. *Nature.* 11/06/print 1997;390(6655):78-81.

233. Brittain RT, Boutal L, Carter MC, et al. AH23848: a thromboxane receptor-blocking drug that can clarify the pathophysiologic role of thromboxane A2. *Circulation.* 1985;72(6):1208-1218.

234. Kabashima K, Saji T, Murata T, et al. The prostaglandin receptor EP4 suppresses colitis, mucosal damage and CD4 cell activation in the gut. *The Journal of Clinical Investigation.* 2002;109(7):883-893.

235. Cushman DW, Ondetti MA. Design of angiotensin converting enzyme inhibitors. *Nat Med.* 10//print 1999;5(10):1110-1112.

236. Hajduk PJ, Greer J. A decade of fragment-based drug design: strategic advances and lessons learned. *Nature Reviews Drug Discovery.* 2007;6(3):211-219.

237. Petros AM, Huth JR, Oost T, et al. Discovery of a potent and selective Bcl-2 inhibitor using SAR by NMR. *Bioorganic & medicinal chemistry letters.* 2010;20(22):6587-6591.

238. Okada T, Sugihara M, Bondar AN, Elstner M, Entel P, Buss V. The retinal conformation and its environment in rhodopsin in light of a new 2.2 A crystal structure. *J Mol Biol.* Vol 342. England2004:571-583.

239. Vauquelin G, Bottari S, Kanarek L, Strosberg AD. Evidence for essential disulfide bonds in beta1-adrenergic receptors of turkey erythrocyte membranes. Inactivation by dithiothreitol. *J Biol Chem.* Jun 10 1979;254(11):4462-4469.

240. Karnik SS, Khorana HG. Assembly of functional rhodopsin requires a disulfide bond between cysteine residues 110 and 187. *J Biol Chem.* Oct 15 1990;265(29):17520-17524.

241. Palczewski K, Kumasaka T, Hori T, et al. Crystal structure of rhodopsin: A G protein-coupled receptor. *Science.* Aug 4 2000;289(5480):739-745.

242. Cherezov V, Rosenbaum DM, Hanson MA, et al. High-resolution crystal structure of an engineered human beta2-adrenergic G protein-coupled receptor. *Science.* Nov 23 2007;318(5854):1258-1265.

243. Ott D, Frischknecht R, Plückthun A. Construction and characterization of a kappa opioid receptor devoid of all free cysteines. *Protein Eng Des Sel.* Jan 2004;17(1):37-48.

244. Cao X, Peterson JR, Wang G, et al. Angiotensin II–Dependent Hypertension Requires Cyclooxygenase 1–Derived Prostaglandin E2 and EP1 Receptor Signaling in the Subfornical Organ of the Brain. *Hypertension.* 2012;59(4):869-876.

245. Jones RL, Qian Y, Chan K, Yim APC. Characterization of a prostanoid EP3-receptor in guinea-pig aorta: partial agonist action of the non-prostanoid ONO-AP-324. *British journal of pharmacology.* 2009;125(6):1288-1296.

246. Audoly L, Breyer RM. Substitution of charged amino acid residues in transmembrane regions 6 and 7 affect ligand binding and signal transduction of the prostaglandin EP3 receptor. *Mol Pharmacol.* Jan 1997;51(1):61-68.

247. Audoly L, Breyer RM. The second extracellular loop of the prostaglandin EP3 receptor is an essential determinant of ligand selectivity. *J Biol Chem.* May 23 1997;272(21):13475-13478.

248. Norel X, de Montpreville V, Brink C. Vasoconstriction induced by activation of EP1 and EP3 receptors in human lung: effects of ONO-AE-248, ONO-DI-004, ONO-8711 or ONO-8713. *Prostaglandins Other Lipid Mediat.* Oct 2004;74(1-4):101-112.

249. Karnik SS, Sakmar TP, Chen HB, Khorana HG. Cysteine residues 110 and 187 are essential for the formation of correct structure in bovine rhodopsin. *Proc Natl Acad Sci U S A.* Nov 1988;85(22):8459-8463.

250. Noda K, Saad Y, Graham RM, Karnik SS. The high affinity state of the beta 2-adrenergic receptor requires unique interaction between conserved and non-

conserved extracellular loop cysteines. *J Biol Chem.* Mar 4 1994;269(9):6743-6752.

251. Qanbar R, Bouvier M. Role of palmitoylation/depalmitoylation reactions in G-protein-coupled receptor function. *Pharmacol Ther.* Jan 2003;97(1):1-33.

252. Hayes JS, Lawler OA, Walsh MT, Kinsella BT. The prostacyclin receptor is isoprenylated. Isoprenylation is required for efficient receptor-effector coupling. *J Biol Chem.* Aug 20 1999;274(34):23707-23718.

253. Stitham J, Arehart EJ, Gleim SR, Douville KL, Hwa J. Human prostacyclin receptor structure and function from naturally-occurring and synthetic mutations. *Prostaglandins Other Lipid Mediat.* Jan 2007;82(1-4):95-108.

254. Karnik SS, Ridge KD, Bhattacharya S, Khorana HG. Palmitoylation of bovine opsin and its cysteine mutants in COS cells. *Proc Natl Acad Sci U S A.* Jan 1 1993;90(1):40-44.

255. Schulein R, Liebenhoff U, Muller H, Birnbaumer M, Rosenthal W. Properties of the human arginine vasopressin V2 receptor after site-directed mutagenesis of its putative palmitoylation site. *Biochem J.* Jan 15 1996;313 (Pt 2):611-616.

256. Fukushima Y, Saitoh T, Anai M, et al. Palmitoylation of the canine histamine H2 receptor occurs at Cys(305) and is important for cell surface targeting. *Biochim Biophys Acta.* Jun 20 2001;1539(3):181-191.

257. O'Dowd BF, Hnatowich M, Caron MG, Lefkowitz RJ, Bouvier M. Palmitoylation of the human beta 2-adrenergic receptor. Mutation of Cys341 in the carboxyl tail leads to an uncoupled nonpalmitoylated form of the receptor. *J Biol Chem.* May 5 1989;264(13):7564-7569.

258. Miggin SM, Lawler OA, Kinsella BT. Palmitoylation of the human prostacyclin receptor. Functional implications of palmitoylation and isoprenylation. *J Biol Chem.* Feb 28 2003;278(9):6947-6958.

259. Ko JK, Ma J. A rapid and efficient PCR-based mutagenesis method applicable to cell physiology study. *Am J Physiol Cell Physiol.* Jun 2005;288(6):C1273-1278.

260. Chen W, Shields TS, Stork PJ, Cone RD. A colorimetric assay for measuring activation of Gs- and Gq-coupled signaling pathways. *Anal Biochem.* Apr 10 1995;226(2):349-354.

261. Audoly LP, Ma L, Feoktistov I, de Foe SK, Breyer MD, Breyer RM. Prostaglandin E-prostanoid-3 receptor activation of cyclic AMP response element-mediated gene transcription. *J Pharmacol Exp Ther.* Apr 1999;289(1):140-148.

262. Breyer RM, Emeson RB, Tarng JL, et al. Alternative splicing generates multiple isoforms of a rabbit prostaglandin E2 receptor. *J Biol Chem.* Feb 25 1994;269(8):6163-6169.

263. Hunke S, Schneider E. A Cys-less variant of the bacterial ATP binding cassette protein MalK is functional in maltose transport and regulation. *FEBS Lett.* Apr 1999;448(1):131-134.

264. Van Horn WD, Kim HJ, Ellis CD, et al. Solution nuclear magnetic resonance structure of membrane-integral diacylglycerol kinase. *Science.* Jun 2009;324(5935):1726-1729.

265. Khorana HG. Rhodopsin, photoreceptor of the rod cell. An emerging pattern for structure and function. *J Biol Chem.* Jan 5 1992;267(1):1-4.

266. Le Gouill C, Parent JL, Rola-Pleszczynski M, Stankova J. Role of the Cys90, Cys95 and Cys173 residues in the structure and function of the human platelet-activating factor receptor. *FEBS Lett.* Feb 3 1997;402(2-3):203-208.

267. Sanders C, Myers J. Disease-related misassembly of membrane proteins. *Annu Rev Biophys Biomol Struct.* 2004;33:25-51.

268. Davidson JS, Assefa D, Pawson A, et al. Irreversible activation of the gonadotropin-releasing hormone receptor by photoaffinity cross-linking: localization of attachment site to Cys residue in N-terminal segment. *Biochemistry.* Oct 21 1997;36(42):12881-12889.

269. Stitham J, Gleim SR, Douville K, Arehart E, Hwa J. Versatility and differential roles of cysteine residues in human prostacyclin receptor structure and function. *J Biol Chem.* Dec 1 2006;281(48):37227-37236.

270. Unal H, Jagannathan R, Bhat MB, Karnik SS. Ligand-specific conformation of extracellular loop-2 in the angiotensin II type 1 receptor. *J Biol Chem.* May 21 2010;285(21):16341-16350.

271. Kennedy ME, Limbird LE. Mutations of the alpha 2A-adrenergic receptor that eliminate detectable palmitoylation do not perturb receptor-G-protein coupling. *J Biol Chem.* Apr 15 1993;268(11):8003-8011.

272. Raso S, Clark P, Haase-Pettingell C, King J, Thomas GJ. Distinct cysteine sulfhydryl environments detected by analysis of Raman S-hh markers of Cys-->Ser mutant proteins. *J Mol Biol.* Mar 2001;307(3):899-911.

273. Baburina I, Moore DJ, Volkov A, Kahyaoglu A, Jordan F, Mendelsohn R. Three of Four Cysteines, Including That Responsible for Substrate Activation, Are Ionized at pH 6.0 in Yeast Pyruvate Decarboxylase: Evidence from Fourier Transform Infrared and Isoelectric Focusing Studies†. *Biochemistry.* 1996;35(32):10249-10255.

274. Ishida K, Matsumoto T, Taguchi K, Kamata K, Kobayashi T. Protein kinase C delta contributes to increase in EP3 agonist-induced contraction in mesenteric arteries from type 2 diabetic Goto-Kakizaki rats. *Pflugers Arch.* Apr 2012;463(4):593-602.

275. Cao X, Peterson JR, Wang G, et al. Angiotensin II-dependent hypertension requires cyclooxygenase 1-derived prostaglandin E2 and EP1 receptor signaling in the subfornical organ of the brain. *Hypertension.* Apr 2012;59(4):869-876.

276. Allan AC, Billinton A, Brown SH, et al. Discovery of a novel series of nonacidic benzofuran EP1 receptor antagonists. *Bioorganic & Medicinal Chemistry Letters.* 7/15/ 2011;21(14):4343-4348.

277. Hall A, Billinton A, Bristow AK, et al. Discovery of brain penetrant, soluble, pyrazole amide EP1 receptor antagonists. *Bioorganic & Medicinal Chemistry Letters.* 7/15/ 2008;18(14):4027-4032.

278. Hall A, Billinton A, Brown SH, et al. Non-acidic pyrazole EP1 receptor antagonists with in vivo analgesic efficacy. *Bioorganic & Medicinal Chemistry Letters.* 6/1/ 2008;18(11):3392-3399.

279. Hall A, Brown SH, Budd C, et al. Discovery of GSK345931A: An EP1 receptor antagonist with efficacy in preclinical models of inflammatory pain. *Bioorganic & Medicinal Chemistry Letters.* 1/15/ 2009;19(2):497-501.
280. Kiriyama M, Ushikubi F, Kobayashi T, Hirata M, Sugimoto Y, Narumiya S. Ligand binding specificities of the eight types and subtypes of the mouse prostanoid receptors expressed in Chinese hamster ovary cells. *Br J Pharmacol.* Sep 1997;122(2):217-224.
281. Schild HO. pA, a new scale for the measurement of drug antagonism. *Br J Pharmacol Chemother.* Sep 1947;2(3):189-206.
282. Ayala JE, Bracy DP, Malabanan C, et al. Hyperinsulinemic-euglycemic Clamps in Conscious, Unrestrained Mice. *J Vis Exp.* 11/16/ 2011(57):e3188.
283. Ostenfeld T, Neurology Discovery Medicine, Beaumont C, et al. Human Microdose Evaluation of the Novel EP1 Receptor Antagonist GSK269984A. *British Journal of Clinical Pharmacology.* 2012.
284. Chakravarty PK, Naylor EM, Chen A, et al. A Highly Potent, Orally Active Imidazo[4,5-b]pyridine Biphenyl Acylsulfonamide (MK-996; L-159,282): A New AT1-Selective Angiotensin II Receptor Antagonist. *Journal of Medicinal Chemistry.* 1994/11/01 1994;37(24):4068-4072.
285. Asada M, Obitsu T, Kinoshita A, et al. Discovery of novel N-acylsulfonamide analogs as potent and selective EP3 receptor antagonists. *Bioorganic & Medicinal Chemistry Letters.* 2010;20(8):2639-2643.
286. Irie A, Segi E, Sugimoto Y, Ichikawa A, Negishi M. Mouse prostaglandin E receptor EP3 subtype mediates calcium signals via Gi in cDNA-transfected Chinese hamster ovary cells. *Biochem Biophys Res Commun.* Oct 1994;204(1):303-309.
287. Sugimoto Y, Narumiya S. Prostaglandin E receptors. *J Biol Chem.* Apr 20 2007;282(16):11613-11617.
288. König M, Mahan LC, Marsg JW, Fink JS, Brownstein MJ. Method for identifying ligands that bind to cloned Gs- or Gi-coupled receptors. *Molecular and Cellular Neuroscience.* 8// 1991;2(4):331-337.
289. Jones RL, Woodward DF, Wang JW, Clark RL. Roles of affinity and lipophilicity in the slow kinetics of prostanoid receptor antagonists on isolated smooth muscle preparations. *British journal of pharmacology.* 2011;162(4):863-879.
290. Asada M, Obitsu T, Kinoshita A, et al. Discovery of novel N-acylsulfonamide analogs as potent and selective EP3 receptor antagonists. *Bioorg Med Chem Lett.* 2010;20(8):2639-2643.
291. Rasmussen SGF, Choi H-J, Rosenbaum DM, et al. Crystal structure of the human [bgr]2 adrenergic G-protein-coupled receptor. *Nature.* 11/15/print 2007;450(7168):383-387.
292. Jaakola VP, Griffith MT, Hanson MA, et al. The 2.6 angstrom crystal structure of a human A2A adenosine receptor bound to an antagonist. *Science.* Vol 322. United States2008:1211-1217.
293. Shimamura T, Shiroishi M, Weyand S, et al. Structure of the human histamine H1 receptor complex with doxepin. *Nature.* 07/07/print 2011;475(7354):65-70.

294. Hanson MA, Roth CB, Jo E, et al. Crystal Structure of a Lipid G Protein–Coupled Receptor. *Science.* 2012;335(6070):851-855.

295. Wu B, Chien EYT, Mol CD, et al. Structures of the CXCR4 Chemokine GPCR with Small-Molecule and Cyclic Peptide Antagonists. *Science.* 2010;330(6007):1066-1071.

296. Breyer RM, Strosberg AD, Guillet JG. Mutational analysis of ligand binding activity of beta 2 adrenergic receptor expressed in Escherichia coli. *The EMBO journal.* 1990;9(9):2679.

297. Bertin B, Freissmuth M, Breyer RM, Schütz W, Strosberg AD, Marullo S. Functional expression of the human serotonin 5-HT1A receptor in Escherichia coli. Ligand binding properties and interaction with recombinant G protein alpha-subunits. *Journal of Biological Chemistry.* 1992;267(12):8200-8206.

298. Sanders CR, Sönnichsen F. Solution NMR of membrane proteins: practice and challenges. *Magnetic Resonance in Chemistry.* 2006;44(S1):S24-S40.

299. Kang C, Tian C, Sönnichsen FD, et al. Structure of KCNE1 and Implications for How It Modulates the KCNQ1 Potassium Channel†‡. *Biochemistry.* 2008/08/01 2008;47(31):7999-8006.

300. Long SB, Campbell EB, MacKinnon R. Crystal structure of a mammalian voltage-dependent Shaker family K+ channel. *Science Signalling.* 2005;309(5736):897.

301. Brohawn SG, del Mármol J, MacKinnon R. Crystal structure of the human K2P TRAAK, a lipid-and mechano-sensitive K+ ion channel. *Science Signalling.* 2012;335(6067):436.

302. Ho L, Greene CL, Schmidt AW, Huang LH. Cultivation of HEK 293 cell line and production of a member of the superfamily of G-protein coupled receptors for drug discovery applications using a highly efficient novel bioreactor. *Cytotechnology.* 2004;45(3):117-123.

303. Steinmeyer DE, McCormick EL. The art of antibody process development. *Drug Discovery Today.* 7// 2008;13(13–14):613-618.

304. Rosenbaum DM, Zhang C, Lyons JA, et al. Structure and function of an irreversible agonist-[bgr] 2 adrenoceptor complex. *Nature.* 2011;469(7329):236-240.

305. Steyaert J, Kobilka BK. Nanobody stabilization of G protein-coupled receptor conformational states. *Current opinion in structural biology.* 2011;21(4):567-572.

306. Natarajan C, Hata AN, Hamm HE, Zent R, Breyer RM. Extracellular Loop II Modulates GTP Sensitivity of the Prostaglandin EP3 Receptor. *Molecular Pharmacology.* 2012.

307. Scarselli M, Li B, Kim S-K, Wess J. Multiple Residues in the Second Extracellular Loop Are Critical for M3 Muscarinic Acetylcholine Receptor Activation. *Journal of Biological Chemistry.* 2007;282(10):7385-7396.

308. Jewell ML, Breyer RM, Currie KPM. Regulation of Calcium Channels and Exocytosis in Mouse Adrenal Chromaffin Cells by Prostaglandin EP3 Receptors. *Molecular Pharmacology.* 2011;79(6):987-996.

309. Zhao HJ, Wang S, Cheng H, et al. Endothelial Nitric Oxide Synthase Deficiency Produces Accelerated Nephropathy in Diabetic Mice. *Journal of the American Society of Nephrology.* 2006;17(10):2664-2669.

310. Schuster VL, Itoh S, Andrews SW, et al. Synthetic Modification of Prostaglandin F2αIndicates Different Structural Determinants for Binding to the Prostaglandin F Receptor Versus the Prostaglandin Transporter. *Molecular Pharmacology.* 2000;58(6):1511-1516.

311. Meanwell NA. Synopsis of Some Recent Tactical Application of Bioisosteres in Drug Design. *Journal of Medicinal Chemistry.* 2011/04/28 2011;54(8):2529-2591.